

University of Southern Queensland
Faculty of Engineering and Surveying

Analysis of rear spoiler on a car model

Computational simulation approach

A dissertation prepared by
Shamith Puthalath

Supervised by
Ahmad Sharifian

in fulfilment of the requirements of
ENG4111 and ENG4112 Research Project

towards the degree of
Bachelor of Engineering (Honours) (Mechanical)

University of Southern Queensland

Faculty of Health, Engineering and Sciences

ENG4111 & ENG4112 Research Project

Limitations of Use

The Council of the University of Southern Queensland, its Faculty of Health, Engineering and Sciences, and the staff of the University of Southern Queensland, do not accept any responsibility for the truth, accuracy or completeness of material contained within or associated with this dissertation.

Persons using all or any part of this material do so at their own risk, and not at the risk of the Council of the University of Southern Queensland, its Faculty of Health, Engineering and Sciences or the staff of the University of Southern Queensland.

This dissertation reports an educational exercise and has no purpose or validity beyond this exercise. The sole purpose of the course pair entitles “Research Project” is to contribute to the overall education within the student’s chosen degree program. This document, the associated hardware, software, drawings, and any other material set out in the associated appendices should not be used for any other purpose: if they are so used, it is entirely at the risk of the user.

Declaration

I certify that the ideas, designs and experimental work, results, analyses, and conclusions set out in this dissertation are entirely my own effort, except where otherwise indicated and acknowledged.

I further certify that the work is original and has not been previously submitted for assessment in any other course or institution, except where specifically stated.

Student name: **Shamith Puthalath**

Student Number: 

Date: 15th October 2023

Acknowledgment

By completing this dissertation my Research Project has concluded. It has been a tremendous journey through various project phases, and the support I have received throughout from individuals, deserve great amount of appreciation. I would like to thank each one of them who has been part of this journey.

Firstly, I take this opportunity to thank my research project supervisor Dr. Ahmad Sharifian for his continued support and advise without which I wouldn't have been able to complete the project successfully. He has always been very approachable and has provided me very valuable feedbacks periodically. This has quite enhanced my project quality as well as my confidence as the project was progressing.

I would like to thank my course examiner Prof. Belal Yousif who has been quite supportive and responsive when in need. I would also like to thank the UniSQ ICT team, especially Mr. Chris Davey, for his support in helping me setting up remote access for HPC connection.

And most importantly, I would like to thank my wife and my two little children for their incredible support and patience, and letting me focus on my studies, when I was supposed to spend time with them.

Contents

List of figures	8
List of tables.....	13
Abstract	14
1. Introduction:	15
1.1. Project aim and objectives.....	16
1.2. Project limitations	16
1.3. Vehicle Aerodynamics	17
1.4. Effects and scope of aerodynamics	19
1.5. Factors affecting the flow field.	20
1.6. Aerodynamic analysis	21
1.7. Key phases of the project	23
2. Literature review:	24
2.1. Spoiler design and use.....	33
3. Research analysis.....	34
3.1. Idea initiation and knowledge gap	34
3.2. Feasibility analysis	37
3.3. Numerical analysis:	37
3.3.1. Reynold's number (Re):.....	38
3.4. Downforce:.....	38
3.5. CFD Analysis	39
4. Methodology.....	41
4.1. Project cases	41
4.2. Equipment and laboratory or workshop facilities	41
4.3. Project breakdown.....	41
4.4. Project version and scenarios	42
4.5. 3D CAD model design and preparation	43

4.6.	Computational Fluid Dynamics	50
5.	Initial CFD simulation	53
5.1.	Geometry preparation in Ansys	53
5.2.	Mesh setup_CFD-v01	56
5.3.	Solver set up process	58
5.4.	Convergence.....	61
5.5.	Analysing results.....	63
5.6.	Verdict on CFD-v01	65
6.	Final CFD simulation	66
6.1.	Geometry preparation in Ansys.....	66
6.1.2.	Enclosure – Domain size preparation.....	68
6.1.2.1.	Domain size for CFD_v03 cases	68
6.1.2.2.	Domain size for CFD_v04 & v05 cases.....	69
6.2.	Mesh setup – Watertight meshing.....	70
6.2.5.	Boundary layer mesh setting.....	75
6.2.6.	Volume meshing	75
6.3.	Solver set up for Final simulation.	78
7.	Results	82
7.1.	Residuals_CFD_v03.....	82
7.2.	Residuals_CFD_v04.....	83
7.3.	Residuals_CFD_v05.....	84
7.5.	Pressure contours.....	85
7.6.	Velocity contours	88
7.7.	y+ (y plus) analysis	93
8.	Analysis on Results	96
8.1.	Residual plots analysis	96
8.2.	Pressure contour analysis	97

8.3.	Velocity contour analysis	99
8.4.	Drag and lift force analysis	100
8.5.	Geometry analysis of the new spoiler	102
8.6.	Domain size change analysis.....	103
8.7.	Mesh sensitivity analysis.....	103
9.	Conclusion.....	104
10.	Future Scope	105
11.	References	106
	Appendix A - Project specification.....	108
	Appendix B – Risk Assessment.....	109
	Appendix C – Project schedule.....	110
	Appendix D - Challenges faced and HPC issues.	111

List of figures

Figure 1-1-Vehicle aerodynamics basics	18
Figure 1-2-Forces acting on Aerofoil (Ipilakyaa et al., 2018)	18
Figure 1-3-Aerodynamics features- Passive and active. (Aktas & Abdallah, 2017)	20
Figure 1-4 - Factors affecting the aerodynamics of car (R. Li, 2017).....	21
Figure 1-5- Flow separation near wake (Cakir, 2012)	21
Figure 1-6-Branches within Computational fluid dynamics (Cakir, 2012)	22
Figure 2-1 -Pressure Contours (Ipilakyaa et al., 2018).....	24
Figure 2-2 - Illustration of rear spoiler and yaw angle (Yuan Cheng et al., 2020).....	25
Figure 2-3-Variation of drag force against velocity. (Ramasamy et al., 2017)	26
Figure 2-4-CD rise against velocity. (Ramasamy et al., 2017).....	27
Figure 2-5-Effect of CD against velocity (Ramasamy et al., 2017)	27
Figure 2-6-Air flow major locations of flow separation (Ramasamy et al., 2017).....	27
Figure 2-7-Roof slop angle vs drag coefficient (Aktas & Abdallah, 2017).....	28
Figure 2-8-Varun's CFD results from ANSYS (R.Varun 2018)	30
Figure 2-9 - 3D model preparation.	31
Figure 2-10 - Meshing -CFD preparation	31
Figure 2-11 - Turbulent Intensity from contours	31
Figure 2-12 - Velocity magnitude profile from vectors.....	31
Figure 2-13-Underbody panels . (Aktas & Abdallah, 2017).....	33
Figure 2-14-Rear spoilers – various types	34
Figure 3-1 - Generic rear spoiler type.....	34
Figure 3-2 - Car model (Cakir, 2012)	35
Figure 3-3 - Lip spoiler	35
Figure 3-4 - Deck-lid spoiler.....	36
Figure 3-5 - Pressure distribution on a surface	37
Figure 3-6- Downforce generated on spoiler.....	39
Figure 3-7-Basic methods problem solving in fluid dynamics (Chaurasiya et al., 2017)	40
Figure 4-1- Base car model - overall dimensions in mm.....	44
Figure 4-2- Case 1 – Car model without a spoiler	45
Figure 4-3 - Side view of the base car model	45

Figure 4-4-Case 2 – Car with generic rear end spoiler	46
Figure 4-5 - Generic spoiler on the car	46
Figure 4-6-Case 3 – Car with new rear end spoiler	47
Figure 4-7-New profiled spoiler design- Case 3	47
Figure 4-8 - Generic spoiler profile (GrabCAD.com)	48
Figure 4-9 - Generic spoiler - Overall dimensions in mm (GrabCAD.com)	48
Figure 4-10-Case 3: New Spoiler design	48
Figure 4-11-Case 3: Cross section details of the new spoiler.....	48
Figure 4-12 - New spoiler profile features.....	49
Figure 4-13 - Both spoilers overlapped for comparison	49
Figure 4-14- Meshing arrangement (Cakir, 2012)	51
Figure 4-15 - Poly-Hexcore meshing (Ansys.com,2020)	52
Figure 4-16-Poly-Hexcore meshing on Formula one wing (Ansys.com,2020).....	52
Figure 5-1-Geometry tab.....	53
Figure 5-2-Domain size allocation_CFD-v01	54
Figure 5-3-Enclosure constructed around the car_ CFD-v01	54
Figure 5-4-Symmetric section_ CFD-v01	55
Figure 5-5 - Boundary conditions for CFD-v01	55
Figure 5-6 - Mesh tab.....	56
Figure 5-7 - Mesh generation for the whole domain_ CFD-v01	56
Figure 5-8 - 25mm Mesh face sizing_ CFD-v01	57
Figure 5-9 - 60mm Face sizing - CFD-v01	57
Figure 5-10 - Mesh refinement detail_ CFD-v01	57
Figure 5-11 - Setup tab	58
Figure 5-12 -Viscous model_ k-epsilon model_ CFD-v01.....	58
Figure 5-13 - Boundary conditions and parameters defined_ CFD-v01.....	59
Figure 5-14 - Reference values defined_ CFD-v01	60
Figure 5-15 - Calculation run_ CFD-v01.....	60
Figure 5-16 - Convergence conditions-CFD-v01	61
Figure 5-17-Case 1 residual plot_ CFD-v01.....	62
Figure 5-18-Case 2 residual plot_ CFD-v01.....	62
Figure 5-19- Case 3 residual plot_ CFD-v01.....	62
Figure 5-20 - Pressure distribution overview -CFD-v01	63
Figure 5-21-Pressure distribution-Case2_ CFD-v01	64

Figure 5-22 - Pressure distribution-Case1_CFD-v01	64
Figure 5-23-Pressure distribution-Case3_CFD-v01	65
Figure 5-24 - Velocity contour - for all three cases_CFD-v01	65
Figure 6-1-Surface preparation comparison	67
Figure 6-2 - boi-1 and boi-2 geometry.....	68
Figure 6-3 – Domain size_CFD-v03.....	68
Figure 6-4-Domain size_CFD-v04 & v05	69
Figure 6-5 - Symmetric form of enclosure and car_CFD-v03.....	69
Figure 6-6 - Boundary conditions.....	70
Figure 6-7 - Fully generated meshing.....	71
Figure 6-8-Body of influence-nearfield	72
Figure 6-9 - Body of influence - farfield	72
Figure 6-10 - Body of curvature – car profile.....	73
Figure 6-11 -Surface mesh generation_CFD_v03	73
Figure 6-12-Surface mesh generation_CFD_v04	74
Figure 6-13-Surface mesh generation_CFD_v05	74
Figure 6-14 - Boundary layer mesh setting.....	75
Figure 6-15 - Volume mesh generation	75
Figure 6-16 - Volume mesh generation fine details.....	76
Figure 6-17 - Mesh diagnostics_CFD_v03_Case 3	76
Figure 6-18-Mesh diagnostics_CFD_v04_Case 3	77
Figure 6-19-Mesh diagnostics_CFD_v05_Case 3	77
Figure 6-20-Viscous model.....	78
Figure 6-21-Inlet boundary parameters	79
Figure 6-22-Outlet boundary conditions for Final simulations	79
Figure 6-23 - Boundary condition - Car	80
Figure 6-24-Boundary condition – Ground	80
Figure 6-25-Boundary condition - Top and side walls	81
Figure 6-26 - Initialization and calculation run	81
Figure 7-1 - Residuals-Case 1_CFD_v03	82
Figure 7-2-Residuals-Case 2_CFD_v03	82
Figure 7-3-Residuals-Case 3_CFD_v03	83
Figure 7-4-Residuals-Case1_CFD_v04	83
Figure 7-5-Residuals-Case2_CFD_v04	83

Figure 7-6-Residuals-Case3_CFD_v04	84
Figure 7-7-Residuals-Case3_CFD_v04	84
Figure 7-8 - Pressure contours – Case1-v03	85
Figure 7-9-Pressure contours – Case 2-v03	85
Figure 7-10-Pressure contours – Case 3-v03	86
Figure 7-11-Pressure contours – Case 1-v04	86
Figure 7-12-Pressure contours – Case 2-v04	87
Figure 7-13-Pressure contours – Case3-v04	87
Figure 7-14-Pressure contours – Case3-v05	88
Figure 7-15-Velocity contour at midplane – Case1-v03	88
Figure 7-16-Velocity contour off centre – Case1-v03	89
Figure 7-17-Velocity contours at midplane– Case2-v03	89
Figure 7-18-Velocity contours at off centre– Case2-v03	89
Figure 7-19-Velocity contours midplane– Case3-v03	90
Figure 7-20-Velocity contours on flange– Case3-v03	90
Figure 7-21-Velocity contours midplane – Case2-v04	90
Figure 7-22-Velocity contours off centre – Case2-v04	91
Figure 7-23-Velocity contours midplane – Case3-v04	91
Figure 7-24-Velocity contours off centre– Case3-v04	91
Figure 7-25-Velocity contours midplane – Case3-v05	92
Figure 7-26-Velocity contours off centre – Case3-v05	92
Figure 7-27-Velocity contours – Case3	93
Figure 7-28--Y-plus_case1-v03	93
Figure 7-29-Y-plus_case2-v03	93
Figure 7-30-Y-plus_case3-v03	94
Figure 7-31-Y-plus_case1-v04	94
Figure 7-32-Y-plus_case2-v04	95
Figure 7-33-Y-plus_case3-v04	95
Figure 7-34-Y-plus_case3-v05	95
Figure 8-1-cd and cl plot-Case3_CFD-v03.....	96
Figure 8-2-Figure 8 2-cd plot- Case2_CFD-v03	96
Figure 8-3-Figure 8 2-cl plot- Case2_CFD-v03	97
Figure 8-4 - Case 1- pressure contour at rear deck region	97
Figure 8-5-Case 2- pressure contour at rear deck region	98

Figure 8-6-Case 3- pressure contour at rear deck region 98

Figure 8-7-Velocity contour at midplane- case comparison..... 99

Figure 8-8-Velocity contour off centre- case comparison 100

Figure 8-9 - Drag and Lift force comparison..... 101

Figure 8-10 - Curved profile of the new spoiler 102

Figure 8-11 - Velocity increase over the spoiler flange curve- case 3..... 102

List of tables

Table 2-1 - Values of CD and CL from the experiment (Kazi et al., 2016).....	25
Table 2-2 - Drag and lift coefficients for three cases (Cakir, 2012)	26
Table 2-3 - Overall CD in different conditions (Qi-Liang et al., 2017).....	29
Table 2-4-Varun's comparison results for existing and modified model (R.Varun, 2018).....	30
Table 2-5-Simulation results (Ansari & Rana, 2017)	31
Table 2-6 - Estimated results from the CFD simulation (Ansari & Rana, 2017)	32
Table 2-7 - Estimated turbulent intensity (Ansari & Rana, 2017).....	32
Table 5-1-Drag and lift coefficients_CFD-v01.....	63
Table 8-2- Drag and Lift force comparison	101
Table 8-3-Figure 8 11-Domain size change analysis.....	103
Table 8-4-Mesh sensitivity analysis.....	103

Abstract

Research on aerodynamics of cars is fairly complex and wide area for exploration. Over the past few decades engineers has invested substantial amount of effort in research and development in the aerodynamics sector and has resulted in significant improvements to the vehicle designs. Thanks to the cost inflation and greenhouse gas emissions concerns which has put even more serious actions in place in terms of improving fuel efficiency.

Newly developed cars are much more safer and fuel efficient compared to the cars more than a decade ago. This has to do with the reduction in aerodynamic forces namely, the drag force, which affects the fuel efficiency and, the lift force, which affects the stability and cornering of the car. These effects are highly dependent on the shape of the car, as well as the speed and environmental factors such as highways, cross winds etc.

This research project is reviewing some literatures and will carry out some investigations and design simulations on a rear spoiler design for cars. This will try to understand if an improved down force cab be achieved without an increase in drag force. The main objective is to design a new and profiled spoiler design.

There will be 3 cases considered for the analysis.

Case 1: A sedan car model. (This car is used in all three cases as a base car)

Case 2: Car with a generic rear end spoiler

Case 3: Car with profiled spoiler with webbed edges (new design)

More details on research gap, spoiler design features and project objectives are provided in section 3 – Research Analysis. The first two cases will be compared with the results obtained from the new spoiler design (third case) in order to determine the effectiveness of the proposed design.

It is to be noted that the first two cases are generic and existing solution and there is no knowledge gap claimed in this report. All 3D models for car and spoilers are developed in Autodesk Inventor and will be exported to Ansys Fluent for CFD analysis.



("Active Aero," 2023)

1. Introduction:

Aerodynamic is the effect of flowing air on a moving object. Aerodynamics aspect is a major factor that all car manufacturers consider along with safety and comfort. Aerodynamic resistance on a vehicle consumes 3% of fuel in urban driving and about 11% of fuel in the highway driving (Das & Riyad, 2017). The modern cars are generally high-performance cars, and excessive amount of speed creates uplift force which can cause accidents. Such uplift force can be limited by the use of aerodynamic spoilers which can control stalling over the wingspan behind the spoiler.

Development of spoilers became a remarkable inclusion in car design to reduce aerodynamic effects. It is now very common to see that most of the car manufacturers include spoiler designs as an integral part or as optional extra to their car models. Most commonly, spoilers are fitted at the rear of the car. The type and design of the spoilers are varying and depends on the use of the car. For high-speed cars, wing type spoilers are suitable to increase the down force and to keep the stability of the car, improved gripping on the road and better control while cornering. While a rear end spoiler, which reduces drag, is good for generic use cars where the fuel efficiency is important. It has been observed that when an increase in down force is achieved, the drag force is decreased, which is not ideal.

A rear spoiler which is fitted to the rear edge modifies the airflow passing over it. Wing spoilers can be designed to reduce the uplift force significantly but can increase the drag. Since the vehicle's body shape are blunted, the aerodynamic forces are due to the domination of pressure components, whereas the skin friction are of a lesser concern. From the safety perspective it is

primarily important to reduce the uplift force and then reducing drag coefficient (CD), which influences the car performance and fuel efficiency.

1.1. Project aim and objectives

The main objective of this research is to understand the aerodynamic effects on cars with rear spoilers. Then identify the scope of improvements in spoiler designs. Develop a new spoiler concept design in order to achieve improved downforce and simultaneously improve drag force. This would improve car stability and performance.

The new concept design will be a profiled rear spoiler with flanged end profiles and notched mid profile as shown in the following images below. This research project will focus on the aerodynamic studies of this spoiler design by conducting computational fluid dynamics in ANSYS Fluent. The proposed design is expected to maintain downforce at its web end profiles while reducing the wake region by letting the air flow through the notched profile in the middle. This would potentially reduce the drag certain degree. This research is trying to analyse the outcome of this proposed design. It is expected to undergo few design improvements depending upon the initial findings from the analysis. It is certain that multiple rounds of analysis and design changes to the spoiler geometry would ultimately result in a reasonably optimised profile to conclude this project.

1.2. Project limitations

CFD analysis in aerodynamics is a very complex process and require a substantial amount of time, high performance computers and top end ANSYS Fluent software license to achieve a highly tangible result. This project has been conducted solo in an 8-month time period between two semesters. The student version of the ANSYS software has been used for most of the analysis work. Analysis were only being carried out with one car model and two spoiler models. It is understood that the accuracy of the results achieved from the analysis would be limited compared to the professional analysis.

The HPC (High Performance Computer) at Uni SQ facility were accessed to perform some of the project analysis during the 6th week of the project. Unfortunately, while performing remote access of HPC, the interface was too slow and uncontrollable and was very inconvenient to use. A significant amount of time became unproductive during the week trying to access the HPC. Hence it was decided to continue with the student version of ANSYS. The IT personnel at UniSQ and the project supervisor was promptly made aware by emails about this scenario.

Overall, based on the available resources this research project has been doing the best possible way to achieve reasonably conclusive results for the successful completion of the project.

1.3. Vehicle Aerodynamics

Aerodynamics is a branch of fluid dynamics studying the motion of fluid when it interacts with a moving object. It is to understand the way air moves around an object which helps in determining the forces and moments acting on the object.

The aerodynamic effects make an object move up or down and fast or slow. These are from the four forces of aerodynamics which are weight, lift, thrust and drag.

1.3.1. Weight:

Every object has weight, and it comes from earth's gravity pulling it down. The weight of the object determines how strong it can be pushed.

1.3.2. Lift force:

Lift is the push that lets the object move upwards and it is opposite of weight. In other words, it is the force generated perpendicular to the direction of travel. For an object to move upward it must have more lift than its weight, for e.g., an aircraft which gets its lift from its wing. The amount of lift produced is measured by using a value called the coefficient of lift (C_L).

1.3.3. Drag force:

When air (fluid) hits on the surface of a moving object it produces drag force. Drag force is generated parallel to the direction of travel and hence it can slow down a moving object. Drag is dependent upon the surface area and shape of the object. More the surface area more the drag. Round objects or narrow objects have less drag than flat objects or wider objects. The amount of drag is generally measured by using a value called the coefficient of drag (C_D). Form drag or pressure drag is formed due to the shape of the object. Skin friction is formed due to the viscous friction between an object's surface and fluid.

1.3.4. Thrust:

Thrust is the opposite of drag. It is the force with which an object can forward, and it must be more than drag. More details on drag force and lift force is given in Numerical Analysis section.

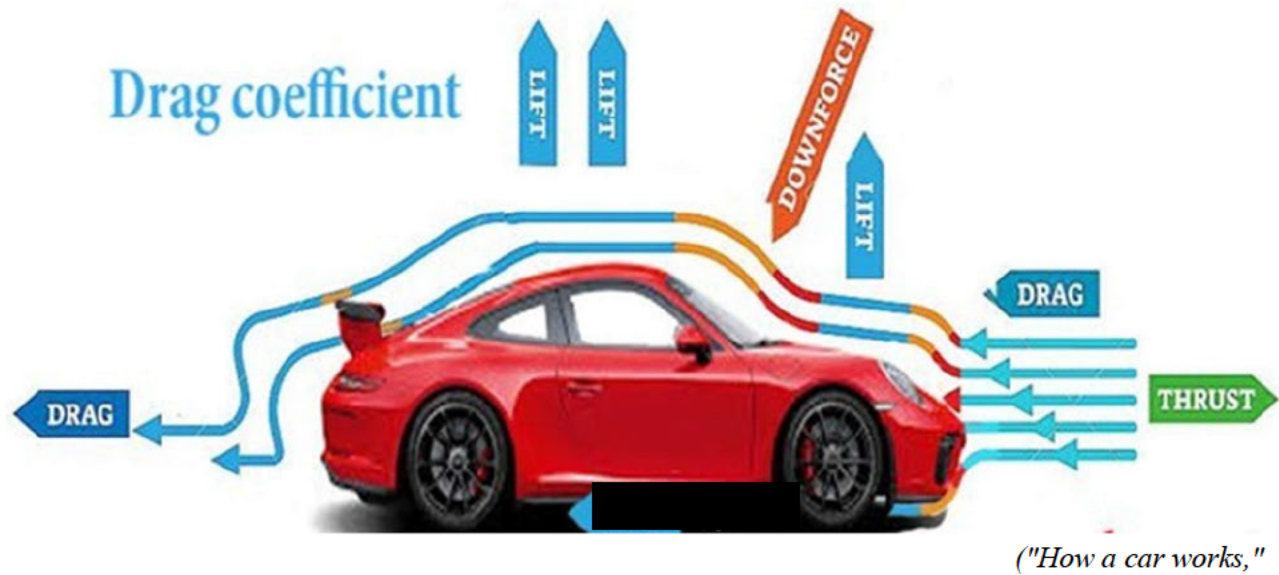


Figure 1-1-Vehicle aerodynamics basics

As per Ipilakyaa, Tuleun, and Kekung (2018), the aerodynamic concepts of drag and lift has been explained comprehensively. The report mentioned that the fluid when moves over a vehicle it exerts pressure forces normal to the surface and shear forces parallel to the surface of the body ("How a car works," 2023). Drag force is the component of the resultant shear and pressure forces and the Lift force is the component of the resultant force that acts normal to the flow direction.

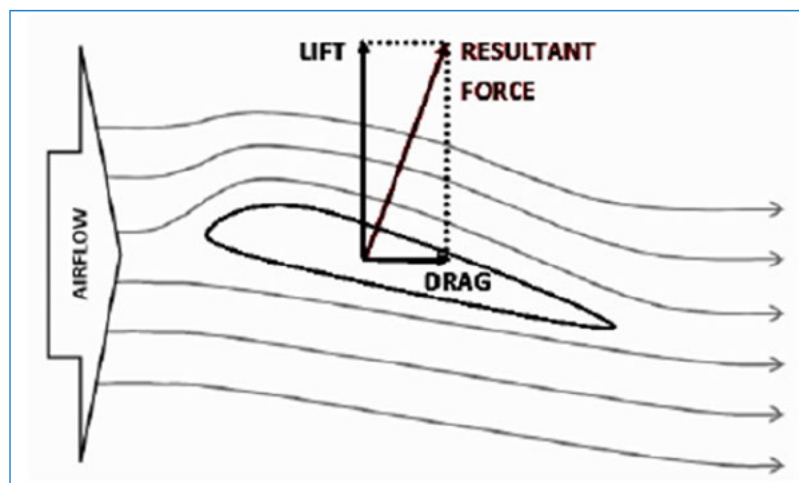


Figure 1-2-Forces acting on Aerofoil (Ipilakyaa et al., 2018)

1.4. Effects and scope of aerodynamics

Air resistance exerted on a vehicle is a significant contribution to the energy consumption of vehicles. (Nabil, Omar, & Mansour, 2020). It is found that the air resistance on cars is around 48% of the total driving resistance on highway speeds. This clearly indicates the direct effect of aerodynamics on cars and how it is influencing the efficiency and motion stability. This indicates that vehicle's travel range can be increased significantly by improving the aerodynamics and reducing the air resistance. The styling of a car is very important as well, not only for its aesthetic looks but also to reflect on the engineering features that are associated with it, such as the aerodynamics (Y. Li & Zhu, 2019).

Many investigations are being carried out to study how the aerodynamics can improve the performance of cars. There are many analyses on the shape of the vehicle, and the factors effecting, such as the drag coefficient. However, there are still huge potential in improving the performance by further investigating and testing.

As per Aktas et al. (Aktas & Abdallah, 2017), 50% of the drag is contributed by the upper body including front and rear end. When it comes to lowering the drag force, it is favourable for fuel consumption, however, too low drag can result in the uplift forces that can lift the rear end of the car which decreases the downforce on the rear tyres (Krzysztof Kurec, 2019). These effects in the sports car are reduced by rear diffusers. For a typical passenger car the reduces downforce is compensated by attaching a rear spoiler or wing. The development in aerodynamics has progressed in such a way that it can now be classified as active and passive aerodynamics. While the passive features are the standard functions on the vehicle, the active ones are which can be enabled when needed, for eg, highway drive etc.

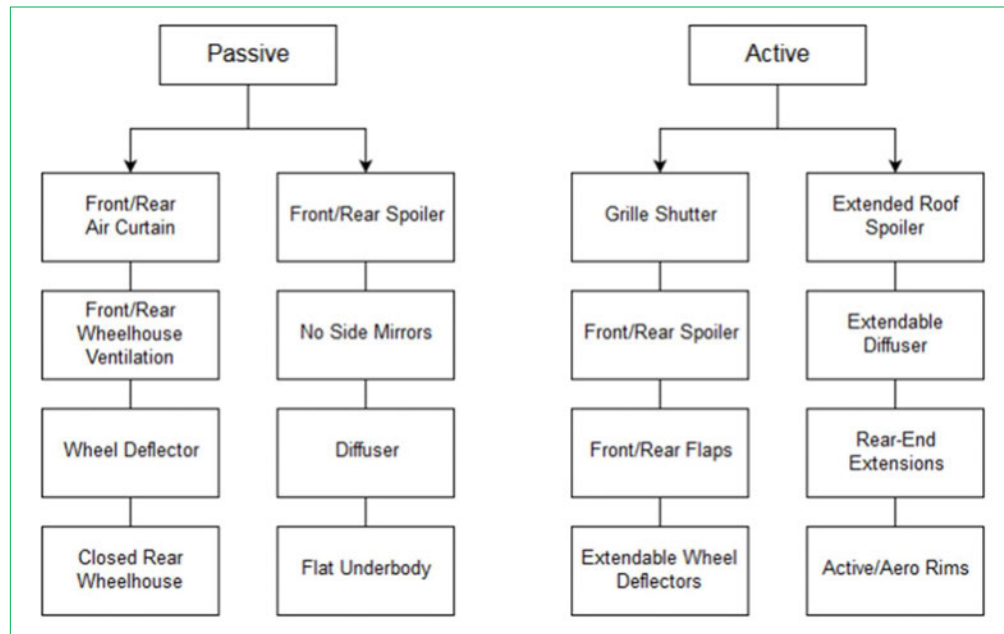


Figure 1-3-Aerodynamics features- Passive and active. (Aktas & Abdallah, 2017)

1.5. Factors affecting the flow field.

- 1.5.1. Boundary layer: It is the thin layer formed around the vehicle due to the viscosity of the air when the vehicle is moving at certain velocity. Outside this layer the air flow is inviscid. This fluid flow imposes pressure on the boundary layer. Within the boundary layer, the fluid is governed by the viscous effect of the fluid.
- 1.5.2. Wake of the vehicle: When the air moving around the vehicle it gets separated at the rear end and leave a large low pressure turbulent region behind the vehicle. This is known as wake and it increases pressure drag, reducing the vehicle performance.
- 1.5.3. Flow separation: when the air is flowing over the vehicle surface at some regions the fluid velocity some to a stall and would even further, start to reverse flow, which mainly occurs at the rear of the vehicle. This separation due to pressure distribution is mainly imposed by the outer layer of the flow. This factor can lead to a larger wake and less pressure at the rear which increases drag.

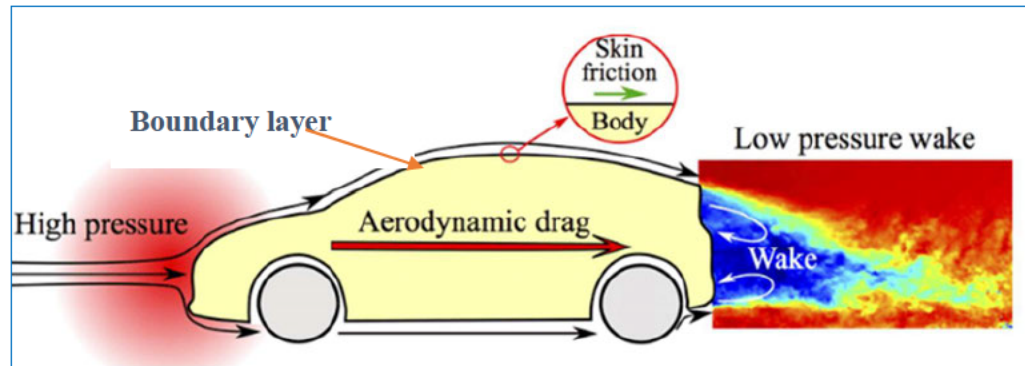


Figure 1-4 - Factors affecting the aerodynamics of car (R. Li, 2017)

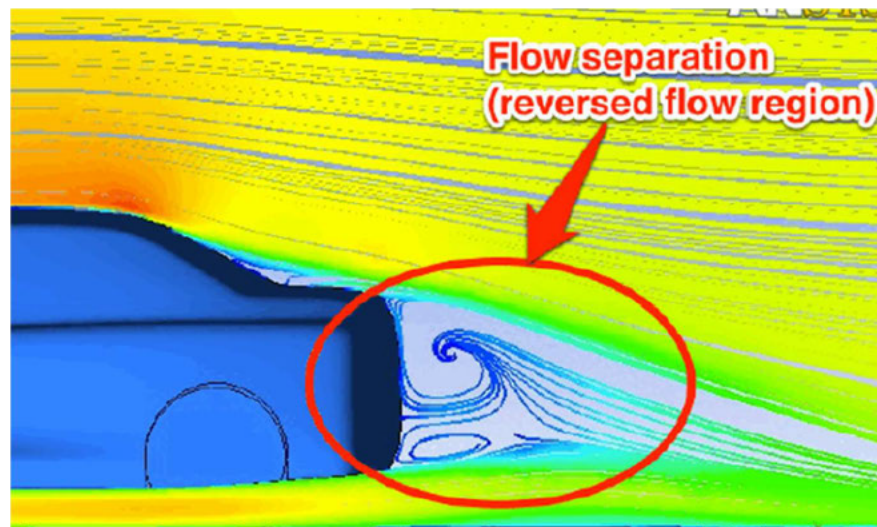


Figure 1-5- Flow separation near wake (Cakir, 2012)

1.6. Aerodynamic analysis

Aerodynamic analysis is a very important factor to determine the stability as well as the efficiency of vehicles. Aerodynamic analysis can be carried out using Computational Fluid Dynamic (CFD) method. In CFD the physical characteristics of the fluid motion can be described through the fundamental mathematical equations in partial differential form and are derived through numerical simulations. This is a very efficient and cost-effective method by simulating the air flow and analysing virtually the effects of airflow over the vehicle. This analysis will help to optimize the design of the spoiler based on the results.

As a result of automotive research over a period of time, the average drag coefficient (C_D) values have improved from 0.7 (for old box shaped cars) to 0.3 for the modern streamlines cars (Singh & Randhawa, 2014). It is observed that aerodynamic drag is mainly due to the flow of air around the vehicle and about 60% of total drag is produced at the rear end of the vehicle (R.Varun, 2018).

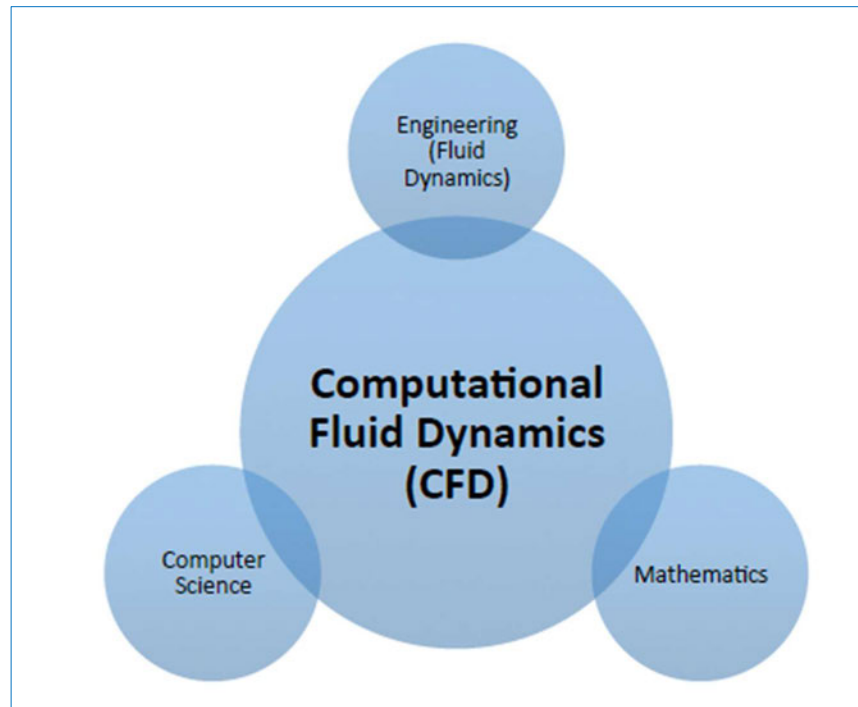


Figure 1-6-Branches within Computational fluid dynamics (Cakir, 2012)

1.7. Key phases of the project

Project phase breakdown	
Phases	Activity
Phase 1	Preperation phase
1A	Project commencement
1B	Discuss with the supervisor
1C	Background research
1D	Update project planning
Phase 2	Resource planning
2A	Request for software
2B	Install software
Phase 3	Litreature review
3A	Collect litreature documents
3B	Prepare litreature reviews
Phase 4	Design phase - 3D modelling
4A	3D modelling
4B	ANSYS simulation training
4C	Discuss with the supervisor
Phase 5	Progress report for semester 1
5A	Prepare progress report
5B	Submit progress report
Phase 6	CFD Simulation phase
6A	ANSYS CFD simulation
6C	Draft the findings
6D	Discuss with the supervisor
Phase 7	Data analysis
7A	More ANSYS simulations
7B	Review the results
7C	Analysis using HPC facility
7D	Discuss with the supervisor
Phase 8	Dissertation
8A	Draft the dissertation
8B	Discuss with the supervisor
8C	Attend the ENG4903 conference
8D	Submit final dissertation

2. Literature review:

CFD analysis done by Ipilakyaa et al. (2018) used two cases. One with a car model without rear spoiler and the second one with a car model with a wing type rear spoiler mounted on the rear deck. In this experiment they are using CAD models of a car and a spoiler and exporting them to Ansys Fluent to perform the CFD analysis. The report explains that with the use of the spoiler the low-pressure region at the trunk of the car, otherwise without a spoiler, is replaced with high pressure region coupled with the downward force developed. Their experiment has proved that an increased downward force (negative lift) is achievable with the wing type spoiler used, however the drag coefficient was increased. Since they put safety first compared to fuel efficiency, their experiment suggests using rear wing spoiler on high-speed sedan cars for better stability, improved cornering and braking performance.

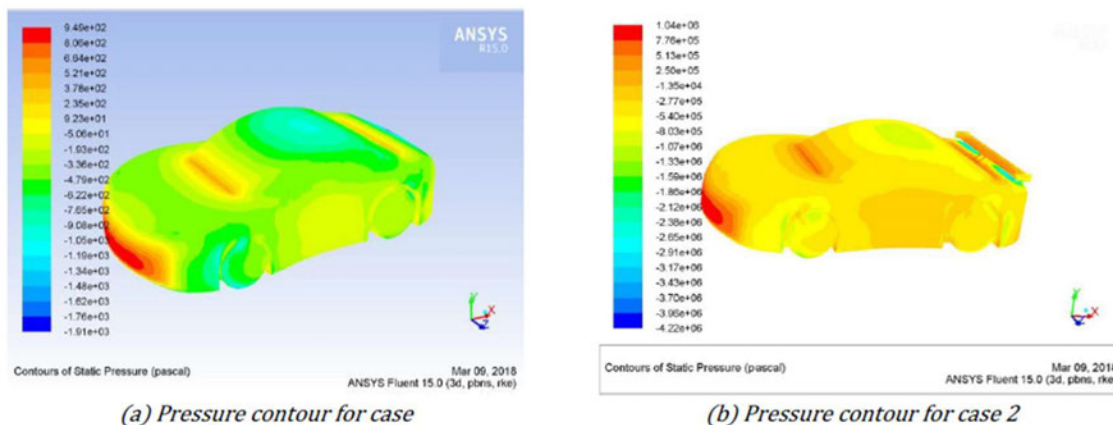


Figure 2-1 -Pressure Contours (Ipilakyaa et al., 2018)

The effect of yaw angle on the aerodynamic performance is also influenced by rear spoiler, especially when cornering (Yuan Cheng, Mansor, Abdullah, & Zakaria, 2020). In the experiment by Yuan Cheng, Ahmed body has been used to replicate a hatch back model and rear spoiler was attached. The analysis indicates that the increase in the yaw angle (Ψ) from zero degrees increases the drag and lift force significantly, which warns the effect of cross winds and turns in the performance of the car. Another experiment shows that by using spoiler on a hatchback car, the C_L is reduced by 59% and C_D is increased by 8.3% (Kazi, Acharya, Patil, & Noraje, 2016).

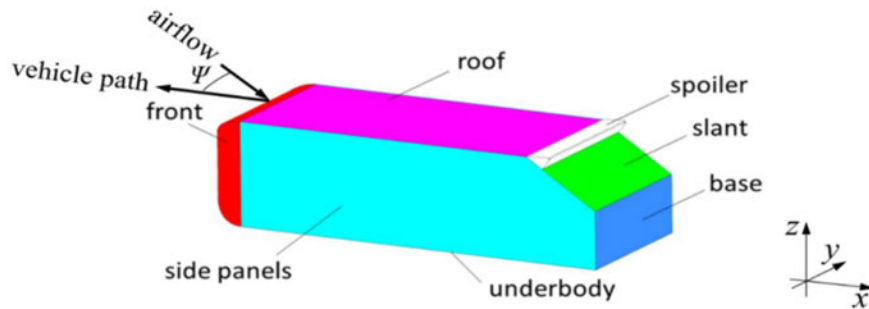


Figure 2-2 - Illustration of rear spoiler and yaw angle (Yuan Cheng et al., 2020)

It is interesting to see, this report has mentioned that when the car was without spoiler, the flow was more attached to the rear end of the car and the wake region was quite smaller, which by introducing the spoiler, the flow was separated and increased the wake region.

Table 2-1 - Values of C_D and C_L from the experiment (Kazi et al., 2016)

Sr. No.	Parameter	Without spoiler	With spoiler	% Change
1	C_D	0.36	0.39	+ 8.33
2	C_L	0.44	0.18	- 59.09

On another report by Cakir (Cakir, 2012), three cases were considered in CFD for the aerodynamic effects of a rear wing. Once case without a rear spoiler and 2nd one with a rear wing spoiler and the 3rd one with a read end spoiler with a generic case a base model. This analysis was performed in ANSYS Fluent by importing the 3D models for the car and spoilers. Modified mesh settings has been used for the analysis with automatic inflation as controlled by the program. It is observed that a volume-controlled mesh sizing has been opted wherever a high-resolution meshing is needed ,is a good method for more accurate results. More localised control volume meshing is required rather than going with one fine mesh across the entire domain. This would take significant amount of time for the analysis. It is of no doubt that the flexibility that the software provides should be utilised to the best way possible.

The report indicated based on the simulation done, that the drag reduction by using a rear wing type spoiler (case 2) at the rear end of the vehicle is very much dependant upon the design or the shape of the spoiler. It is understood in case 3, where the rear end spoiler was used resulted in a lift coefficient (C_L) of -0.268 whereas in case 2 it was only -0.239. However, in case 1 without spoiler the C_L value is -0.222. Resultant values from this report is given below.

Table 2-2 - Drag and lift coefficients for three cases (Cakir, 2012)

Model	C_D	C_L
Case #1 (Vehicle only)	0.232	-0.222
Case #2 (Vehicle + First spoiler)	0.192	-0.239
Case #3 (Vehicle + Second spoiler)	0.217	-0.268

From the above experiment the result indicates that the rear end spoiler improved the downforce but increased the drag compared to a rear wing spoiler. It is to be noted that the author is also emphasising that in terms of safety the reduced lift is more important than reduced drag, which has been mentioned earlier.

In the experiment done by Ramasamy et al. (Ramasamy, Mohanesan, Kadirgama, Noor, & Rahman, 2017), CFD simulation on Proton Iswara car model were done at varying speeds ranging from 40km/hr to 110km/hr were carried out to analyse the coefficient of drag (C_D). The profile of the car has pretty squared edges and less round contours. The findings indicate that the drag increases at 1.2% between 40-80 km/hr, 5% over 90-110km/hr and then gradually decreases after that. High wake region was observed, and the resultant C_D obtained was around 0.326 at 40-110km/hr speed range. The drag to velocity relationship is illustrated in the 3 graphs shown below.

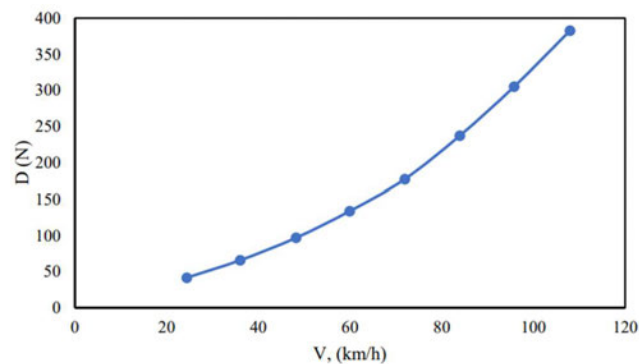


Figure 2-3-Variation of drag force against velocity. (Ramasamy et al., 2017)

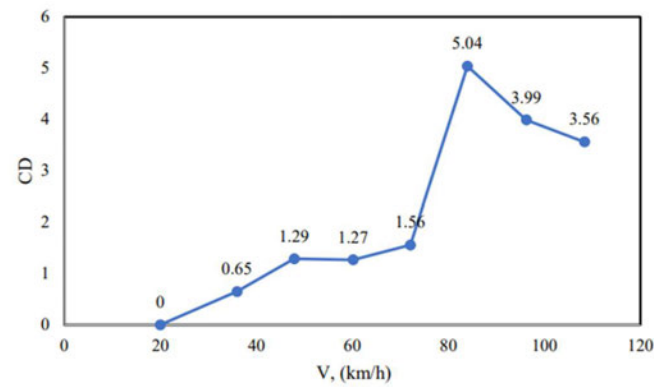


Figure 2-4-CD rise against velocity. (Ramasamy et al., 2017)

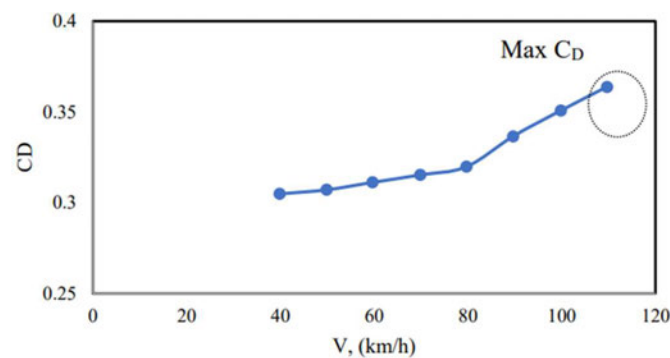


Figure 2-5-Effect of CD against velocity (Ramasamy et al., 2017)

A comprehensive illustration by the author on the air flow separation on the vehicle provides a good guidance on this research.

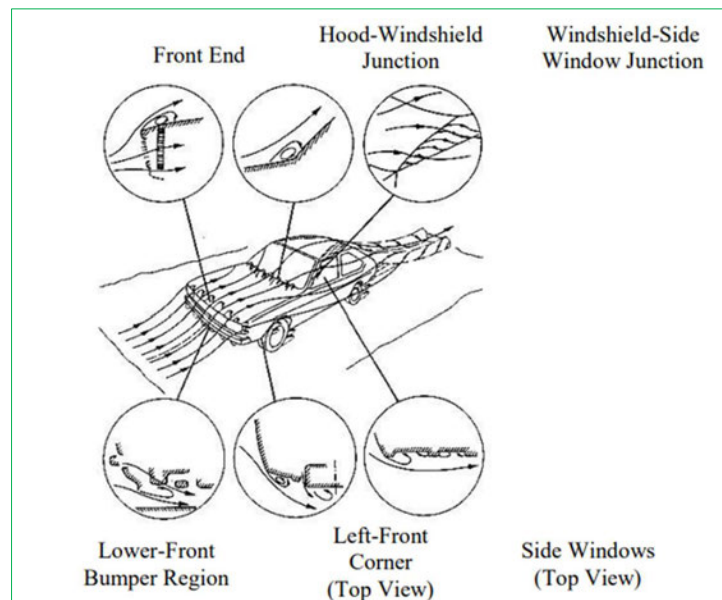


Figure 2-6-Air flow major locations of flow separation (Ramasamy et al., 2017)

Aktas et al. (Aktas & Abdallah, 2017) did a comprehensive review on various aerodynamic features and its importance in reducing the drag coefficient. The paper has reviewed that the front-end spoiler can be used which results in an increased velocity, thus reduced pressure, under the vehicle and a reduced velocity, thus increased pressure, above the vehicle. This would increase the total down force on the vehicle. The paper also suggests that addition of splitter to the front spoiler would reduce the drag. The paper is observing that the at the upper body of the vehicle, optimization of the windshield angle as well as the roof slope angle would significantly reduce the drag. The rear spoilers, roof spoiler or trunk spoiler are used to delay the airflow separation to reduce the wake size as well as the drag.

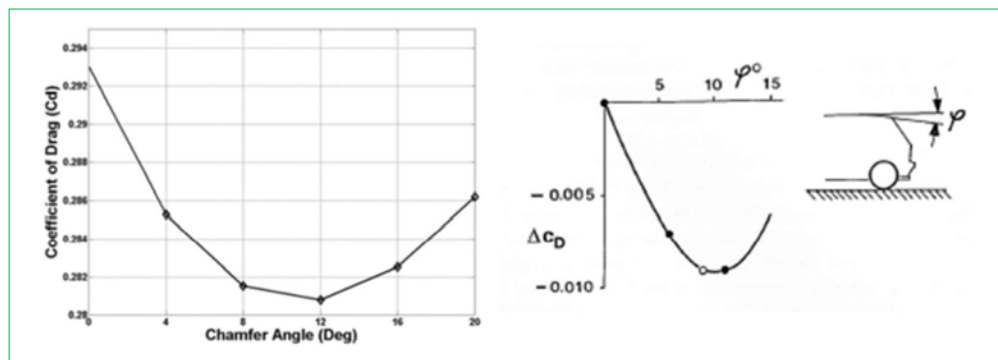


Figure 2-7-Roof slop angle vs drag coefficient (Aktas & Abdallah, 2017)

Qi-Liang (Qi-Liang, Zheng, Xian-Liang, Li-Li, & Zhang, 2017) has performed aerodynamic analysis on Tesla Model S by CFD. The report mentions that the air drag has a significant effect on electric vehicles in the case of high-speed driving. The analysis included various working load conditions as parameters such as ground clearance, rotation of the tyres, tread pattern of the tyres etc. By 3D laser scanner to acquire the model of the car and using STAR-CCM+ software for aerodynamic performance analysis, drag coefficient and local flow field data of the vehicle were simulated. The analysis was carried out with the smallest ground clearance in order to have accelerated air flow and reduced pressure at the bottom of the body, resulting to a reduced aerodynamic lift. The author has analysed the drag (C_D) in different conditions and mentions that the impact of tread pattern of tyres on air drag has a large effect on the C_D .

Table 2-3 - Overall CD in different conditions

(Qi-Liang et al., 2017)

Load and conditions	cd	cl	A(m ²)	cd*A
Half load (Ground-clearance 144mm, Pattern, Rotation)	0.233	0.041	2.405	0.560365
Half load 1 (Ground-clearance 119mm, Pattern, Rotation)	0.232	0.039	2.393	0.555176
No load (Ground-clearance 157mm, Pattern, Rotation)	0.235	0.039	2.418	0.56823
Half load 2 (Ground-clearance 144mm, Pattern, Fixed)	0.242	0.073	2.405	0.58201
Half load 3 (Ground-clearance 144mm, Slicks, Fixed)	0.231	0.058	2.404	0.555324

Liang (Qi-Liang et al., 2017) observed the effect of C_D on different parts of the outer surface and confirms that the face part is the greatest contributing part on air drag and is due to the pressure drag. Laing also observes that the door design, hidden door handles and built-in window frame, reduces the air drag. Additionally, the wiper placed under the trailing edge of the front trunk lid reduces the vortex at the bottom of the front windshield.

Varun (R. Varun, 2018) performed the CFD analysis and compared the results on the existing model and a modified model with a duct added to the roof of a sedan car. His paper aims at reducing the C_D using an air duct fixed at the roof, in order to reduce fuel consumption and increase the performance of the car. He has used Ansys Fluent for CFD analysis and 3D model was created using Catia V5 software. According to Varun's observation, when the vehicle is at certain velocity the viscous effect is mainly on the boundary layer of the car and at the rear end of the car the fluid gets separated. The fluid flow is mainly in two states, laminar flow and turbulent flow. Laminar flow is smooth and predictable whereas turbulent flow is very irregular and three-dimensional flow and hard to predict. These fluid states are represented by Reynold's number (Re). Re depends upon the characteristic length of the body as well as the kinematic viscosity and the velocity of the vehicle. The derivation of Reynold's number is mentioned in section 3.4-Numerical Analysis.

Varun, in his report, has mentioned about wake which is a low-pressure turbulent region created behind the vehicle when the air moving over the vehicle gets separated at the rear end. Wake contributes to the pressure drag and reduces the vehicle performance. His modified version with the duct is aiming to diverge the high-pressure air to flow into the wake area to reduce pressure drag. Varun's results in ANSYS on the standard model shows a C_D value of 1.2 and a pressure difference of 93 Pa is found to be acting opposite to the flow direction. However, the modified car with the added duct (diverging duct) has slightly improved the results with reduce pressure difference and a small value in C_D reduction.

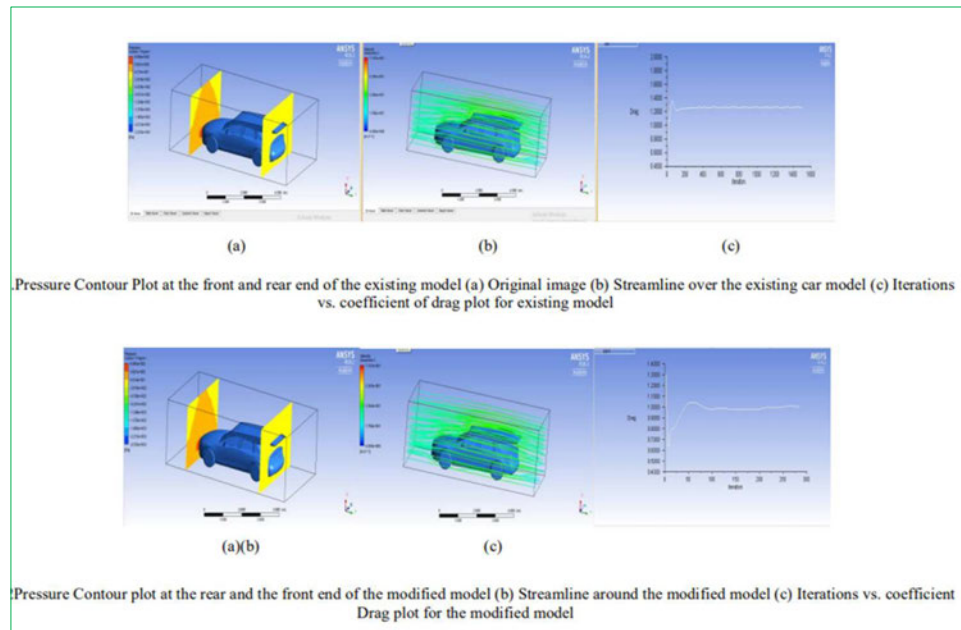


Figure 2-8-Varun's CFD results from ANSYS

(R.Varun 2018)

Table 2-4-Varun's comparison results for existing and modified model (R.Varun, 2018)

Model	Existing	Modified
Drag	1.20	1.10
Pressure at the front end	200 Pa	253 Pa
Pressure at the rear end	107 Pa	197 Pa
Pressure difference	93 Pa	56 Pa

The drag values seems to very high on these analysis. It can be seen that the vehicle has a box shape at the rear end and could be the major contributor for this high drag value. At the rear end of the vehicle a sudden flow separation would occur which would result in a huge wake region for the vortices to develop which could be generate higher drag.

In the paper by Ansari et al. (Ansari & Rana, 2017), they have conducted CFD analysis on a Maruthi Alto model car to find the C_D and F_D . In addition to the 3D modelling and CFD analysis, they have also carried out field test to compare the results. The paper has emphasized the importance of minimizing the lift force to avoid the car to be airborne.

The road test was conducted at varying speeds as given in the table and in North-South direction. The Alto car weight is given as 887kg and area of 1.74sq.m. the results of C_D is given below.

Table 2-5-Simulation results

(Ansari & Rana, 2017)

S.N	Speed km/h	Distance (m)	Time (s)	Drag coefficient C_d
1	20	200	40.16	0.152
2	30	300	59.42	0.324
3	40	330	50.79	1.42
4	50	400	52.96	0.84
5	60	600	60	0.517
6	70	700	78	0.457
7	80	720	82	0.454

The paper also provides the analysis of the ANSYS simulation carried out for the same car model. The 3D model created in Pro/Engineer wildfire 5.0m was imported into ANSYS. With successful meshing and parameters input the authors were able to analyse the results.

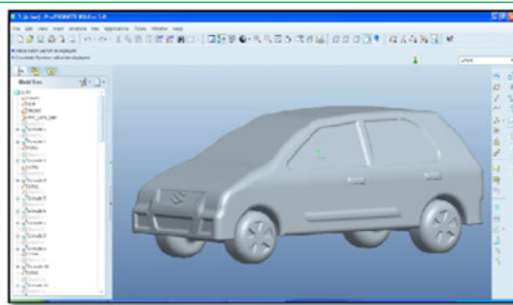


Figure 2-9 - 3D model preparation.

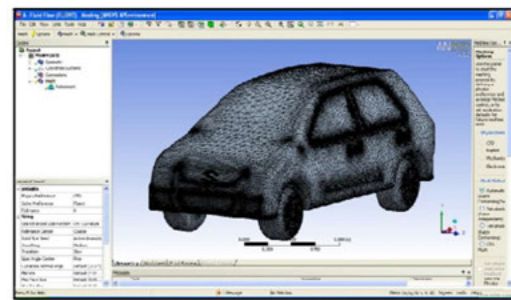


Figure 2-10 - Meshing -CFD preparation

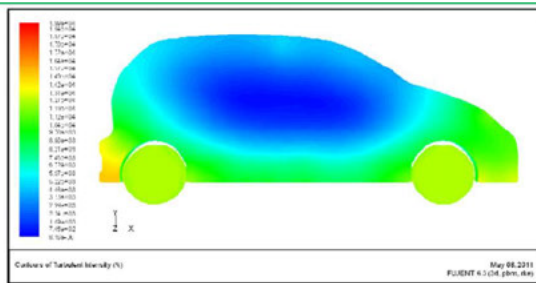


Figure 2-11 - Turbulent Intensity from contours

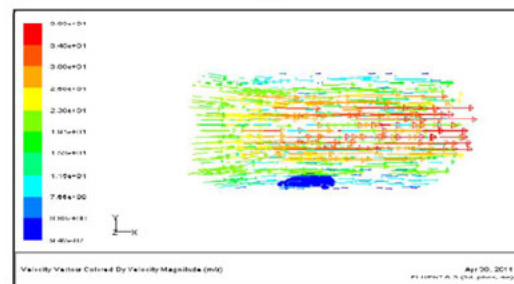


Figure 2-12 - Velocity magnitude profile from vectors

Source:(Ansari & Rana, 2017)

Table 2-6 - Estimated results from the CFD simulation (Ansari & Rana, 2017)

Car	Maximum velocity in m/s	Minimum velocity in m/s	Observed velocity in m/s	Drag coefficient (Cd)
Alto	38.1	7.76	22.3	0.784

Table 2-7 - Estimated turbulent intensity (Ansari & Rana, 2017)

Car	Maximum value in %	Minimum value in %	Mean value in %	Turbulence Intensity $I=u'/U$
Alto	95	34	64.5	1.82 %

From the above results Ansari et al. observe that the turbulence intensity of the car is proportional to the drag coefficient and mentions that the F_D is nil when the speed is less than 25km/hr and as the speed further increases the drag coefficient increases and beyond 60km/hr, C_D becomes constant. At a lower speed the air flow is also at a lower velocity and the flow separation is not abrupt which would reduce the wake region and reduced vortices. This could be the reason for low drag force under 25km/hr. However for speed higher than 65km/hr, C_d being constant, the authors observation may not be fully agreed upon as it could be assumed that the author limits his observation only to the Alto car used for his study. The profile and relatively small size of the car would have resulted in such an observation. The paper concludes that's the results from the theoretical and experimental process only varies in a small value and hence a theoretical value can be much reliable in case of saving time and effort on experimental tests.

The aerodynamic experimental results differ in different conditions such as type of suspension, spring suspension or air suspension, as well as full load/ half load/no-load conditions (Qi-Liang et al., 2017). It is hence important to set the ground clearance to the minimum in half load conditions as well as for high-speed vehicle tests. Such setting would increase the air flow at the bottom and reduces the pressure resulting in a reduced lift force. It is observed that the aerodynamic drag rises to a maximum, around 5.04%, between velocities of 80km/h and 90 km/h (Ramasamy et al., 2017).

Use of underbody panels (Aktas & Abdallah, 2017), including a large front undercover with an aero-optimised convex, a large floor cover with fins and a diffuser with large fins. This increases the air velocity through, under the body, with a reduce air pressure, which reduces drag and lift.

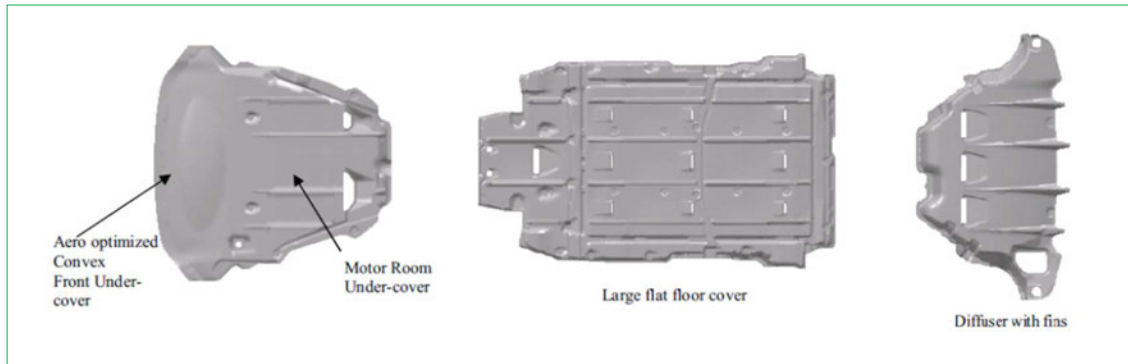


Figure 2-13-Underbody panels

(Aktas & Abdallah, 2017)

In Ramasamy's paper the details on the four geometric zones affected by drag force is given. The front end, rear slant, the base and the side panels, roof and under body. As per Aktas et al. (Aktas & Abdallah, 2017) a diffuser located at the rear end of the car helps in reducing the airflow velocity exiting the underbody and will increase the base pressure at the rear which will reduce the wake size. With an angle of 5° - 8° for a diffuser an optimum angle is reached which reduces the drag.

2.1. Spoiler design and use

Spoilers can be classified as an automotive parts or device which has a specific design function. On a moving vehicle the air flowing over its body is "spoiled" or diverted to certain degree so that the drag forces and lift forces acting on the vehicle are reduced. Most commonly, spoilers are fitted at the rear of the car. Spoilers are of various types and specific types are fitted to specific areas on a car. There are spoilers used for styling purposes as well.

For race cars or high-performance cars, the primary focus is on reducing the lift force, or increase downforce. This is to achieve good gripping and better control on the ground, especially while cornering. However, in normal passenger cars, reducing drag force is given importance. This is to improve fuel efficiency and making it economical.

Rear end spoiler and front spoilers are commonly used for passenger cars. These types significantly reduce drag. Front spoilers are fitted under the bumper and used to decrease the air flow flowing under the car. A rear spoiler which is fitted to the rear delays the air flow separation behind the vehicle. It also increases air pressure in front of the spoiler flange which reduces rear lift (Cakir, 2012).



Figure 2-14-Rear spoilers – various types

(Laha, 2015)

3. Research analysis

3.1. Idea initiation and knowledge gap

While looking at the rear end spoiler, attached to the rear deck without gap, it is suggested that the spoilers would increase downforce but could also increase drag (Cakir, 2012). The design of the rear end used were the generic design spoilers with uniform width as shown below. This design provides increased downforce, which is good for the stability of the car, however it also increases the drag which would reduce the fuel efficiency.

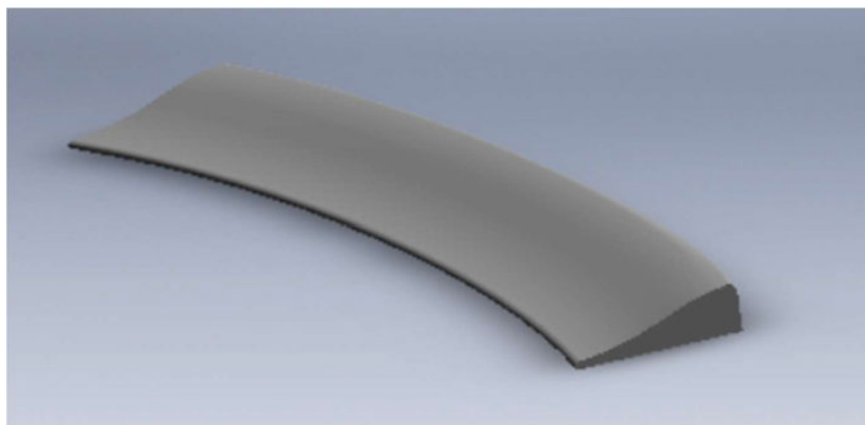
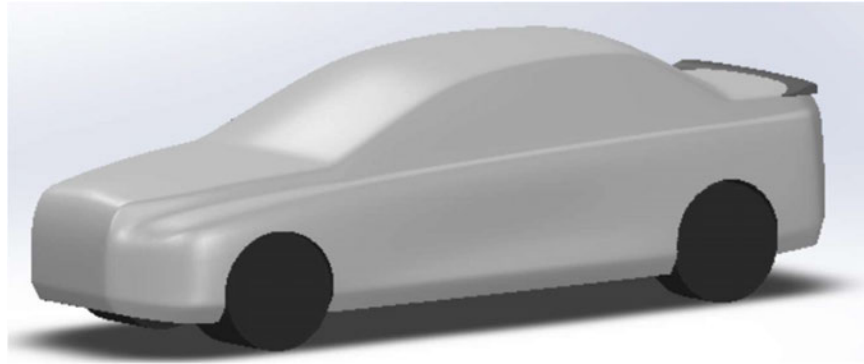


Figure 3-1 - Generic rear spoiler type

*Figure 3-2 - Car model**(Cakir, 2012)*

It has been observed that the literature reviews are discussing on either reducing drag force or reducing lift force. But discussions on simultaneous reduction of both drag and lift forces are less evident. It is understood that simultaneous reduction of these forces is challenging and very limited in terms of achieving consistent or reliable result, this project was aiming to consider this challenge as the research gap and has tried to investigate and determine if simultaneous reduction of both lift force and drag force could be achieved. However, the primary focus was to achieve lift force and not to compromise in the drag force (increasing), if not significantly reducing it.

This research is focussing on passenger car spoiler design and hence the most common type of spoilers used in passenger cars are lip spoilers or deck-lid spoilers. These types are shown in the images below.

*Figure 3-3 - Lip spoiler*



Figure 3-4 - Deck-lid spoiler

The project has developed a new rear spoiler design concept with the above mentioned intend. The new spoiler design has two flanges on either sides and a notch at the centre. As the air flow over the car and the spoiler, these two flanges would gather air and build up pressure on these areas. As the result downforce is generated. Whereas the notch in the middle would let the air pass through it and would reduce the wake region behind the car. This would reduce the drag force as a result.

The ultimate aim of the new concept design is improved stability and fuel efficiency of the car. Hence this research is investigating the aerodynamics effects of rear spoiler design and develop a rear spoiler design in such a way that the drag force can be reduced reasonably while gaining the downforce. The car model considered here is a sedan as a base model for all analysis.

This project performed CFD analysis of rear roof spoiler design on a sedan car model to understand how the airflow is affected by changing the spoiler profile and adding flanges to the end and notch in the middle part. Finding an optimum profile and the flange angle for the achieving such result was determined from performing multiple simulations and optimising the profile dimensions.

3.2. Feasibility analysis

The analysis and methodology intended to do in this research is quite standard and is in line with the analysis mentioned in the literatures. Hence from the feasibility point of view, the process was expected to provide reasonable results. In case of any the design changes were required in order to refine the findings, such geometrical optimizations would have been performed. However, such scenarios did not occur and hence the original concept design was used throughout the project.

For the overall analysis, the scheduled time frame has not been much impacted. The development of the project has been discussed periodically with the project supervisor and valuable inputs were provided at relevant times.

At the final cycle of the analysis access to High Power Computing facility (HPC) at UniSQ has been scheduled to use. This would strengthen the findings and could be a part of the validation process to conclude the project.

3.3. Numerical analysis:

On a moving car the air flows all around the outer surface of the car. This generates velocity distribution and resulting in resistance forces acting on the car. This is a combination of friction and pressure on the geometry of the car. While the shear force acts tangentially on the surface of the car, drag force is generated because of the viscous boundary layer. The pressure force which acts perpendicular to the car surface contributes to the lift force.

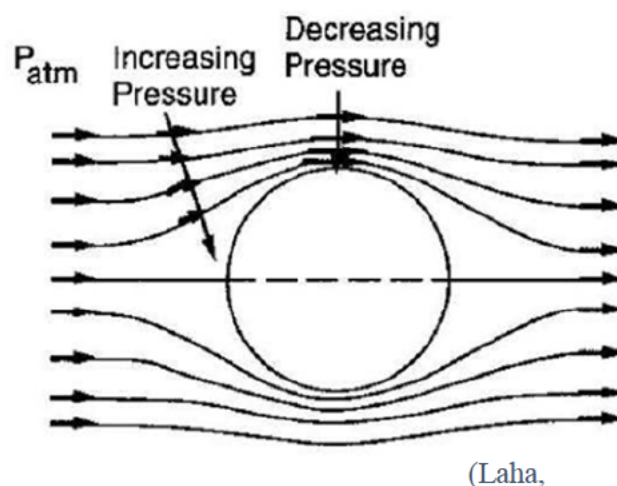


Figure 3-5 - Pressure distribution on a surface

Hence as it is important to streamline the car geometry to reduce these resistance forces and improve the aerodynamics of the car. Hence, the shape of the vehicle needs to optimise and analysed to find the drag coefficient C_D and lift coefficient C_L (Nabil et al., 2020).

Drag and lift coefficient can be derived as:

Drag coefficient

$$C_D = \frac{D}{\frac{1}{2}\rho v_{\infty}^2 A}$$

Lift coefficient

$$C_L = \frac{L}{\frac{1}{2}\rho v_{\infty}^2 A}$$

F_D is the air drag force,

ρ is the density of the air

v is the speed of the car relative to the air

A is the frontal area of the car

C_D is the coefficient of drag, a dimensionless number.

C_L is the coefficient of lift, a dimensionless number.

3.3.1. Reynold's number (Re): is used to determine the flow of the fluid. This is dimensionless and determines whether the fluid flow is laminar, transition or turbulent state.

$$Re = \frac{UL}{\mu}$$

U is the fluid velocity

L is the length of the interaction between the fluid flow and the geometry

μ is the viscosity of the flow.

3.4. Downforce:

Though details on the lift force have been mentioned already, it would be ideal to understand about downforce, which is essentially, the opposite of lift force. The design of the rear spoiler primarily utilizes this aerodynamic property in effectively stabilising a moving car. Downforce is generated when air flows over the car surface and hits on wingspan or on spoiler flange, generating a downward force due to localised high pressure.

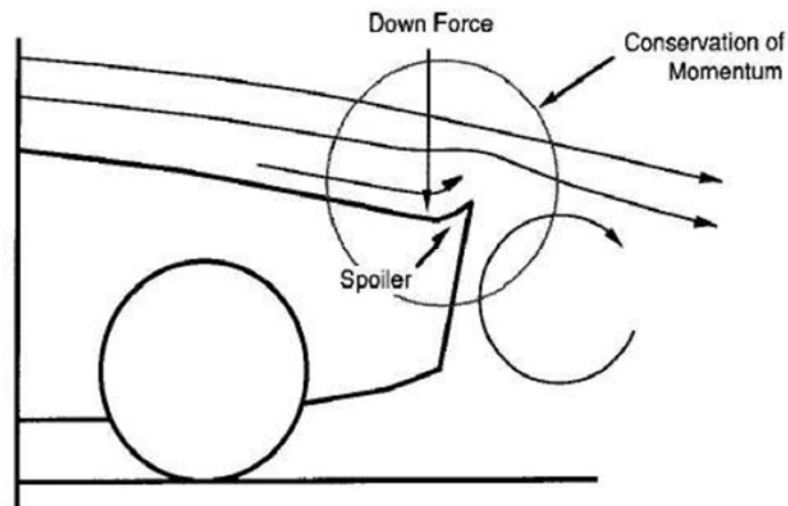


Figure 3-6- Downforce generated on spoiler.

3.5. CFD Analysis

CFD is a process which uses mathematical modelling of a physical phenomenon that involves fluid flow and solving it numerically using computational process (SIMSCALE, 2022). It is a great tool for engineers to perform virtual simulations and provide reasonably accurate results in a very less period of time compared to the numerical analysis. CFD methods used advanced physics models and analyse with the capability of customisation in intuitive space (ANSYS, 2022). CFD is one of the three basic methods used to solve problems in fluid dynamics and heat transfer (Chaurasiya, Kushwaha, & Raees, 2017).

Compared to the traditional experimental based analysis, CFD has lots of advantages such as low cost, efficiency, large amount of results can be produced with no added cost. No tangible damages from experiments are produced which reduces significant cost. The physical characteristics of the fluid motion can be described through fundamental mathematical equations in partial differential form which are the governing equations in CFD. It provides rather detailed pattern of the fluid flow that are generally tedious to predict from traditional experimental methods.

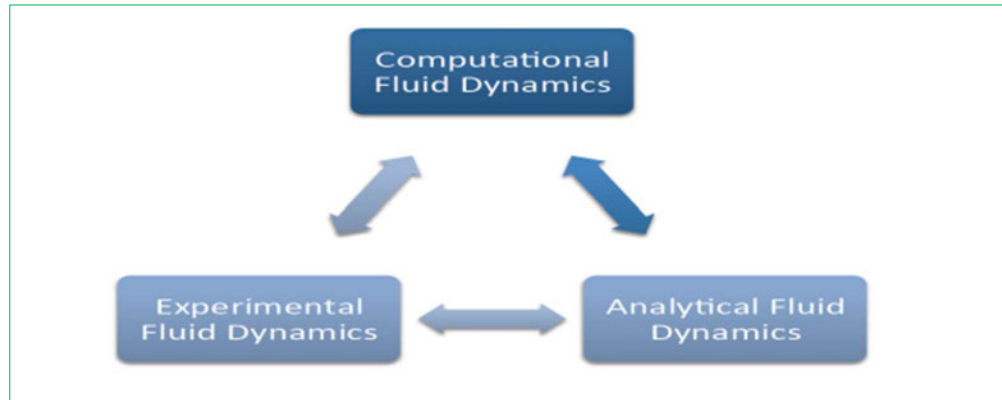


Figure 3-7-Basic methods problem solving in fluid dynamics (Chaurasiya et al., 2017)

CFD packages include user interface, input problem parameters and to examine results. There are three main elements (Chaurasiya et al., 2017).

- **Pre-processor** – used to define the geometry and to generate mesh control volumes for calculations. Fines mesh provides more accurate results but determines the computer hardware and calculation time needed.
- **Solver** – makes the calculations using numerical technique such as finite element, finite difference or spectral methods and equations are solved through iterative methods for solving algebraic equations.
- **Post-processor** – provides visualisation of the results and displays geometry or mesh, creates vector and contour and produce plots in 2D and 3D surfaces. This provides th results from the analysis and can be tracked or manipulated throughout the simulation to achieve the best results.

4. Methodology

4.1. Project cases

This project has conducted CFD analysis on three main cases.

- Case 1 - car without rear spoiler
- Case 2 - car with a generic rear end spoiler
- Case 3 - car with profiled spoiler (new design)

4.2. Equipment and laboratory or workshop facilities

To conduct the analysis the following resources and facilities were utilised.

- 3D modelling CAD Software – Autodesk Inventor 2020
- CFD software:
 - ANSYS Workbench (Fluent) 2023 – Student version
 - ANSYS Workbench HPC access
 - ANSYS Workbench (Fluent) 2023 – UniSQ Academic license package

4.3. Project breakdown

- I. 3D CAD design of base car model
- II. 3D CAD design of generic spoiler
- III. 3D CAD design of new concept spoiler
- IV. Import the 3D CAD models into ANSYS Fluent for CFD analyses.
- V. Create domain parameters.
- VI. Generate mesh geometry.
- VII. Set up boundary conditions and simulation parameters.
- VIII. Performed CFD simulation for case 1
- IX. Performed CFD simulation for case 2
- X. Performed CFD simulation for case 3
- XI. Review results and discuss with supervisor.
- XII. Perform mesh refinement for mesh sensitivity analysis – Limited mesh refinement performed- detailed in the later section named “Challenges Faced”.
- XIII. Investigate domain size adjustments.

- XIV. Review and compare results and discuss with supervisor.
- XV. Perform final CFD simulation at HPC facility – plan aborted *
- XVI. Review results
- XVII. Prepare final report for the thesis.

* Use of HPC facility had to be later aborted due to multiple technical issues which are detailed in the later section named “Challenges Faced”.

4.4. Project version and scenarios

Generally, for most of the analysis process it is important to validate the results by confirming that the results are consistent for the given scenarios or conditions and/or for certain defined parameters. The project was determined to satisfy these criteria, however, due to various unexpected technical hurdles and time constraints as mentioned in the “Challenges faced” section, the project was limited to perform from its originally intended capabilities.

A total of five simulation versions for the three Cases were created in this whole project. These versions are different to each other due to its domain size, mesh setting, mesh sensitivity reasons, and also due to the change in Ansys package license.

Version 03 to 05 were performed in ANSYS Academic version provided by UniSQ. The Ansys academic version was granted by UNISQ when performance issues with the HPC access was identified. While concerned IT staffs were trying to resolve the HPC issues, the academic version helped the project to continue with the analysis run.

Brief details on each of these versions are given below:

1. **CFD-v01 (version 01)** – This is the initial simulation version and it was conducted in Ansys Workbench student version. This is a free student package available from Ansys. However, the package has limitations in terms of its functionality and accuracy. Mesh elements more than 512,000 elements cannot be used for simulation. Due to this reason very coarse mesh elements were used to perform this version of the analysis. More details provided in the Initial Simulation section. The results achieved are not considered in the final conclusion due to discrepancies with the final simulations.
2. **CFD-v02 (version 02)** – This version was created with bigger domain size as version 03 and very fine mesh settings to be able to run in the HPC facility at UniSQ. HPC

access was granted by UniSQ when the project was halfway through. But due to the technical difficulties HPC use had to be aborted. Hence this version has been excluded from the findings section. More details on the HPC issues mentioned in the “Challenges faced” section.

3. **CFD-v03 (version 03) – Large domain** and medium size mesh elements. Specific details on domain size and mesh elements are given in the Final Simulation analysis sections.
4. **CFD-v04 (version 04) – Domain size change.** This version has smaller domain size compared to version 03, but finer mesh elements. The idea behind these changes is to review how the change in domain size has influence on the simulation results.
5. **CFD_v05 (version 05) – For Mesh sensitivity analysis.** This version has same domain size as of version 04 but fine mesh elements. The idea behind these changes is to review how the change in mesh size with same domain size is influencing the simulation results. Please note that due to the time constraints, this version was only performed for Case 3. It is understood that, this single case study would suffice to understand the mesh sensitivity analysis, as the difference between the models in the three cases is only with the spoiler profile change.

More details on each of these versions are explained in the Ansys Geometry preparation, mesh preparation and solution set up sections.

4.5. 3D CAD model design and preparation

One of the initial and crucial preparation for the analysis was developing the 3D models of the car and spoilers. While developing a new design concept, it is important to consider that it should be an easily adaptive solution to most of the common or popular sedan passenger car models. That way the benefits of a successful solution could be widely utilised. With this intention, the first step was to select the base car model as well as the generic spoiler model in order to develop the new concept.

In all the three cases a common base car model needed to be used. Hence the overall dimension of the Honda City sedan car model (2021-year model) has been referred to construct a 3D CAD model for the base car. The suitable generic spoiler CAD model was constructed from a deck-lid spoiler design referring to the dimensions available from GrabCAD.com. Such

a generic spoiler profile would closely match to the physical properties of most of the generic spoiler in that category cars regardless of the manufacturer of the cars.

AUTODESK Inventor 2020 software was used to develop all the 3D CAD models. The CAD files are created in .ipt or .iam file format which are exclusive to inventor file format. These CAD files are then exported to .iges file format (or STEP file format) so that they can be imported into the ANSYS Fluent software for CFD analysis. All the CAD models were dimensioned in 1:1 scale. Please note that these CAD models developed are solely for this research project and the profile and geometric details are approximate only. Most of the fine details of a car model, such as aesthetic profiles, fillets, and the detailed profile characteristics are ignored in these CAD models.

This project had conducted CFD analysis on three cases as listed below. Case 1 and case 2 are generic design models used for analysis comparison to reach a validated conclusion from the findings of the analysis. Case 3 spoiler design has a different profile compared to case 2. More details on Case 3 spoiler are given in the next few sections. This new spoiler design was derived from the generic spoiler model by modifying its profile.

4.5.1. Case 1 - car without rear spoiler

This is a base car model without a spoiler. This base car has been used in all three cases. The overall dimensions given below is inspired from Honda City sedan 2021 passenger car (Carsguide.com).

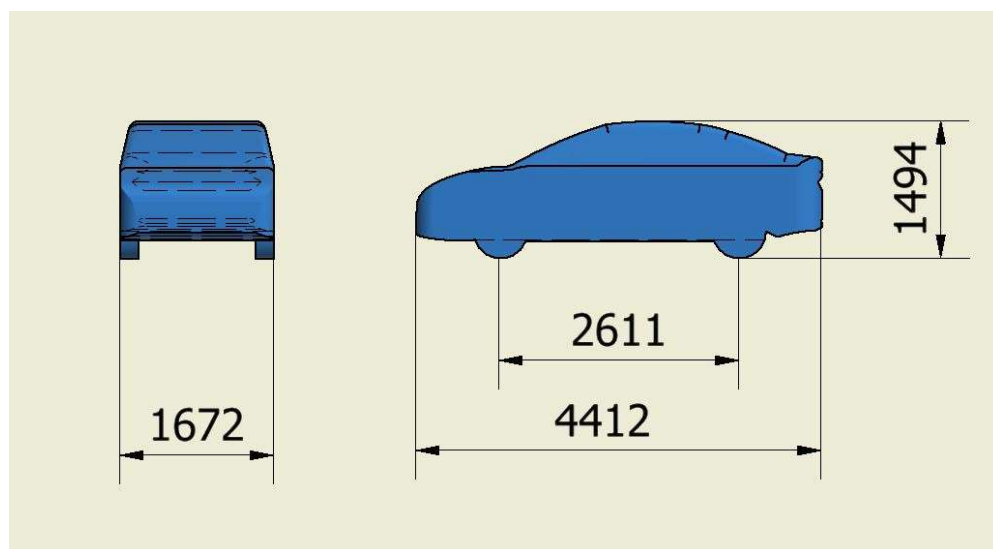


Figure 4-1- Base car model - overall dimensions in mm

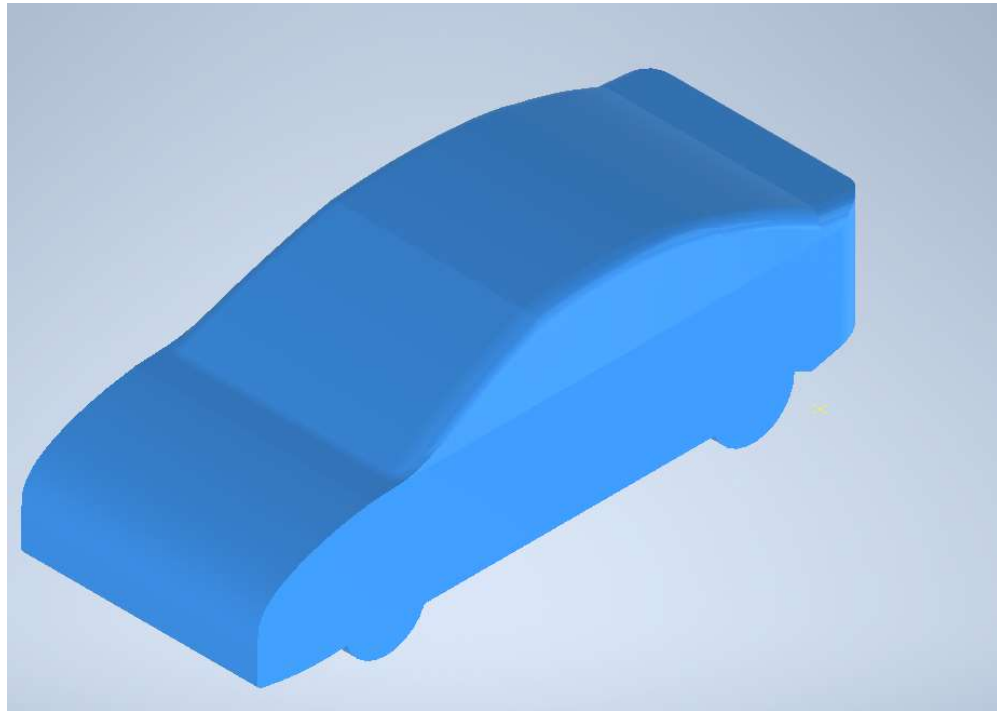


Figure 4-2- Case 1 – Car model without a spoiler

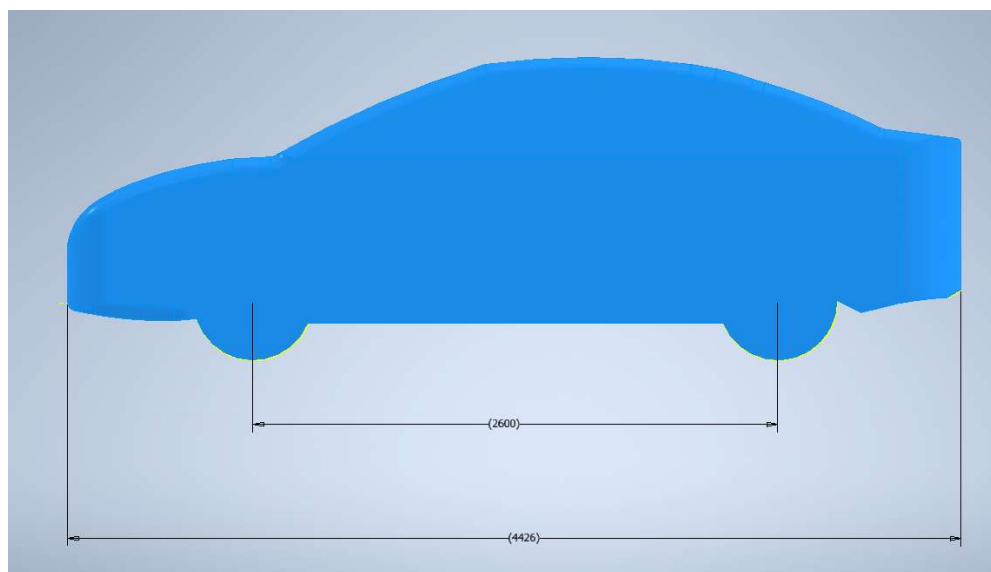


Figure 4-3 - Side view of the base car model

4.5.2. Case 2 - car with a generic rear end spoiler

This case has a base car with a generic rear spoiler. The rear spoiler resembles a common spoiler currently available in the market and any variation on its aerodynamic properties would be quite negligible.

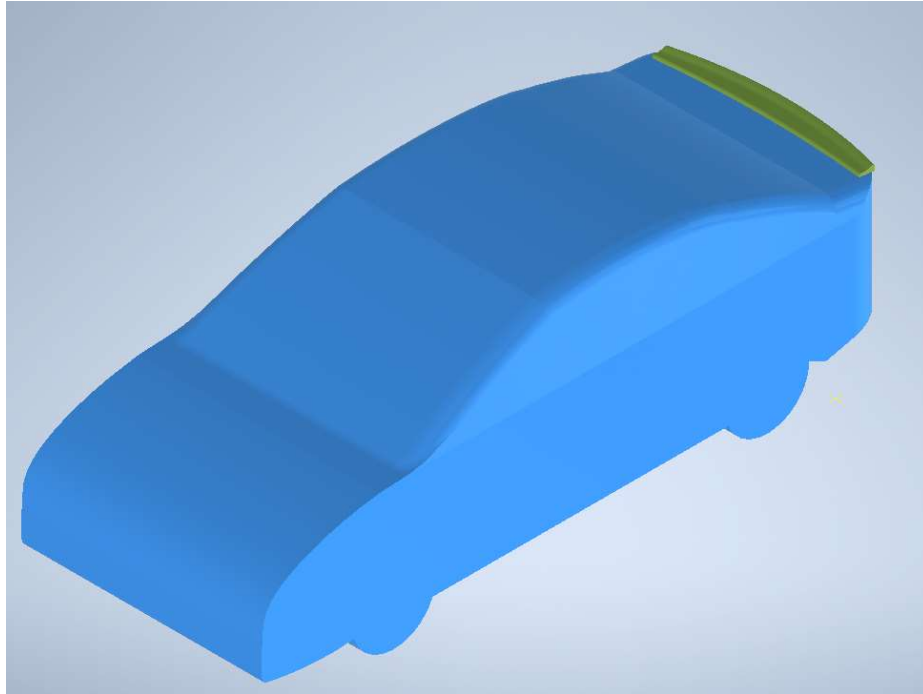


Figure 4-4-Case 2 – Car with generic rear end spoiler

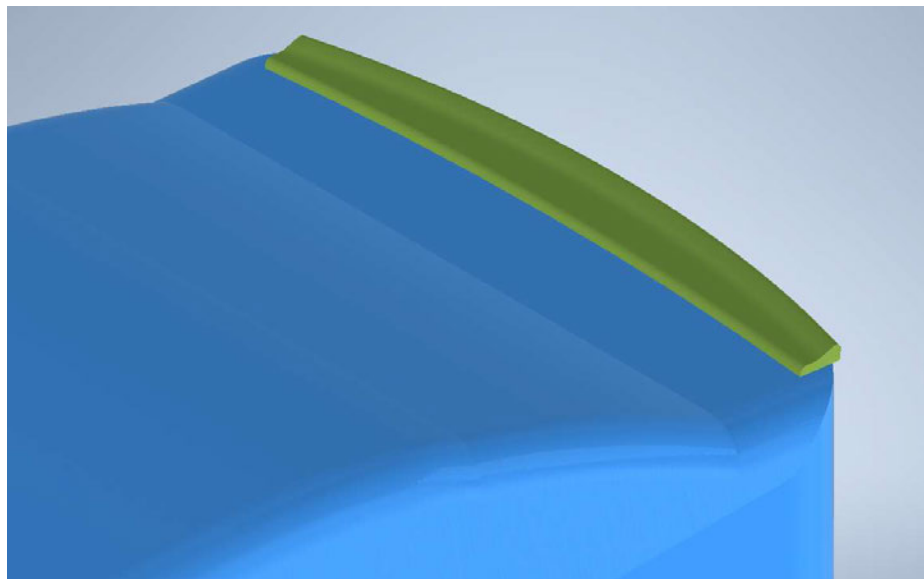


Figure 4-5 - Generic spoiler on the car

4.5.3. Case 3 - car with new spoiler (concept design)

This case has a base car with a new concept design spoiler. This spoiler design is modified from the generic spoiler and the main difference is the extended flanges and a cut-out in the middle part.

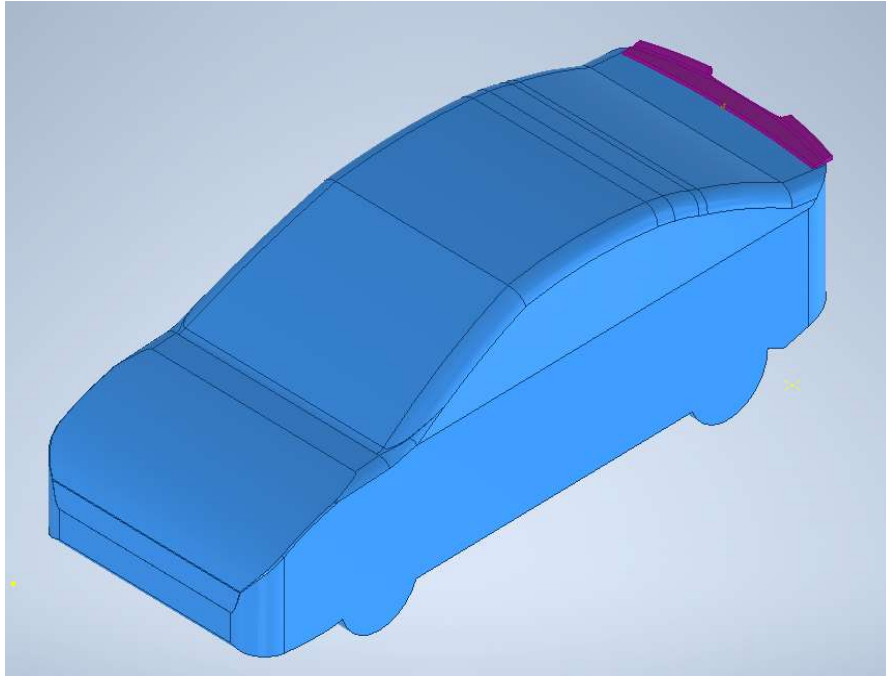


Figure 4-6-Case 3 – Car with new rear end spoiler

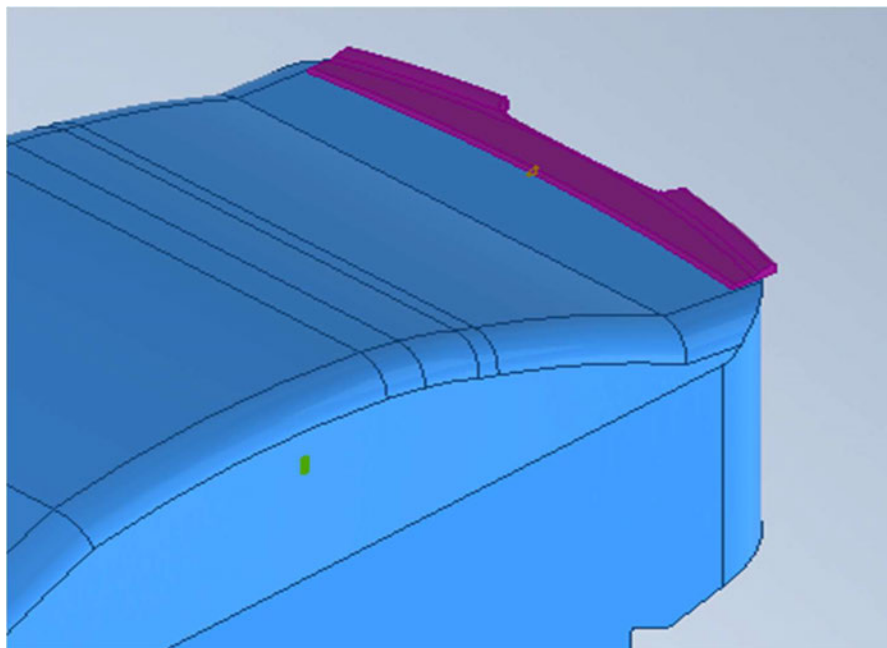


Figure 4-7-New profiled spoiler design- Case 3

4.5.4. Spoiler details

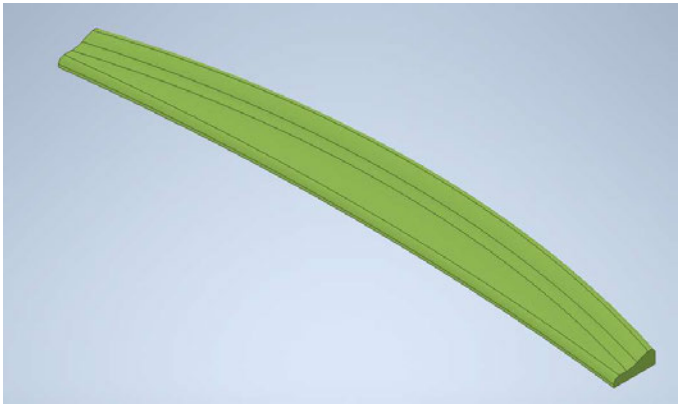


Figure 4-8 - Generic spoiler profile (GrabCAD.com)

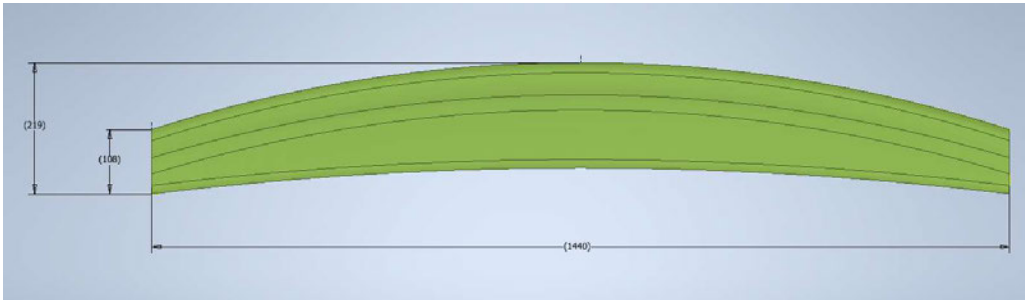


Figure 4-9 - Generic spoiler - Overall dimensions in mm (GrabCAD.com)

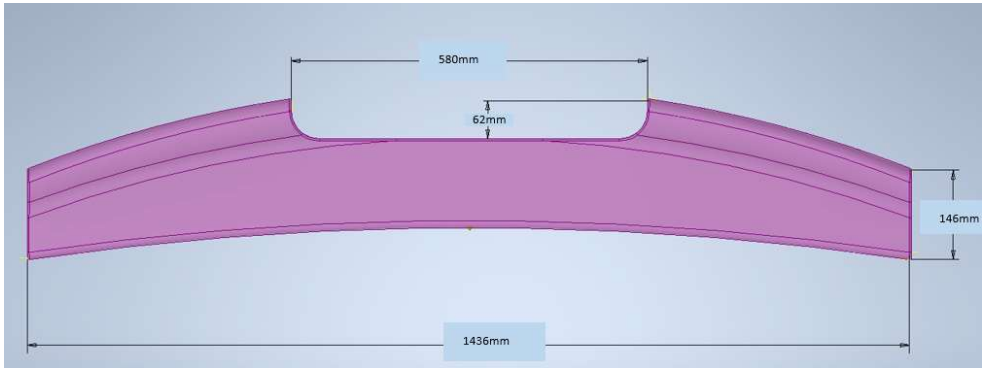


Figure 4-10-Case 3: New Spoiler design

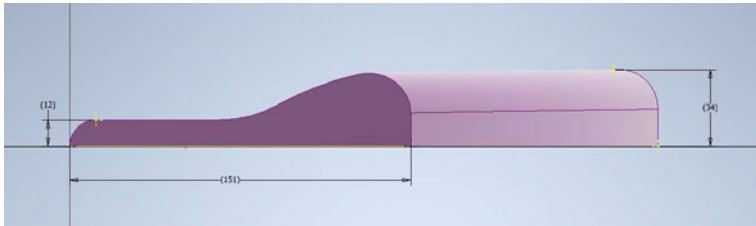


Figure 4-11-Case 3: Cross section details of the new spoiler

4.5.5. New spoiler design intention

The new spoiler concept has a cut-out in the middle and two extended flanges on either side, as seen in the images. As the air flows over the car and the spoiler, more air pressure is developed on those webbed flanges which would create downforce. Meanwhile, at the cut out in the middle area, air would flow through this profile which would reduce the wake region behind the car. This would potentially reduce the drag force on the car. The combined effect would result in an improved downforce and a simultaneous reduction in drag force.

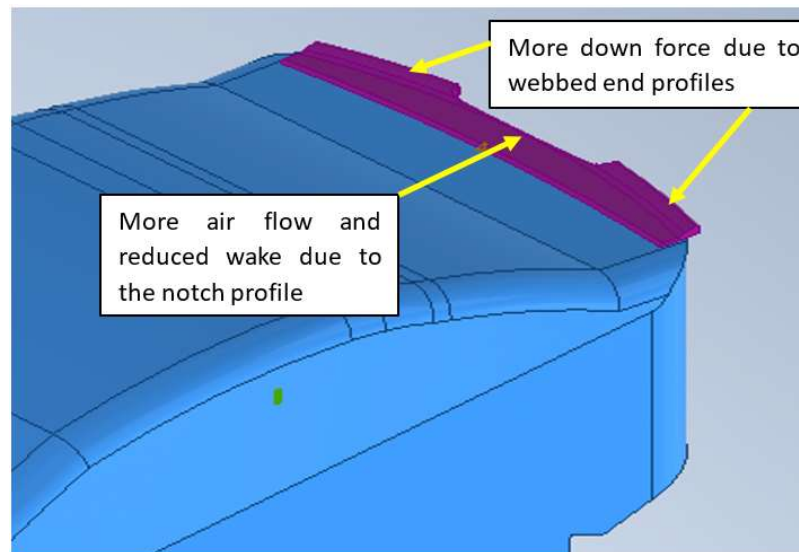


Figure 4-12 - New spoiler profile features

The new spoiler has a wider profile compared to the generic spoiler. To visualise the difference between them the image shown below is showing both spoilers overlapped to one over the other. The major difference between them is around the rear end as seen below.

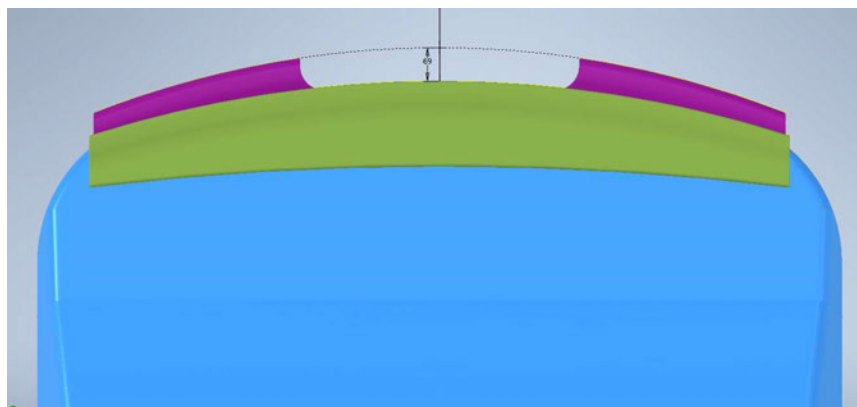


Figure 4-13 - Both spoilers overlapped for comparison

4.6. Computational Fluid Dynamics

Computational Fluid Dynamics (CFD) analysis has a significant role in the engineering sector when it comes to the aerodynamics predictions and calculations. CFD assist in making reasonably accurate predictions about the air behaviour patterns. The general laws of conservation of mass, momentum and energy represented by partial differential equations which governs the fluid behaviour.

CFD is performed by modelling of mathematical equations using partial differential equations and numerical methods and provides qualitative and quantitative predictions of the fluid behaviour.

Multiple methods are integrated into the CFD analysis process. A project file is created in Ansys Workbench as the first step. Following process were carried out for CFD analysis.

- Geometry preparation
- Mesh generation
- Solver set up process
- CFD calculation run (simulation stage)
- Post processing and analysis.

The next few sections will discuss on the above methods in detail, about common methods applied as well as the methods used in all CFD versions.

4.6.1. Geometry preparation

Geometry preparation is the first step involved in an aerodynamic simulation. This defines the control volume where the air would flow and interact with the body of analysis. In all the cases, few basic processes are common in all the versions. However, the methods that are different in each of the versions are discussed in specific versions.

4.6.2. Mesh generation

Mesh generation is very critical process in the CFD simulation analysis. This defines the accuracy of the results. In CFD the domain is subdivided into number of sub-domains which is required to solve the flow of fluid. The fluid flow in each of these sub-domains or cells described are solved numerically and the fluid properties such as pressure, velocity, temperature, and parameters that are of interest can be determined. Hence to obtain more accurate results the size of the mesh or cells should be smaller.

The accuracy is also dependent on the parameters and limitations imposed in the simulation. There are different types of mesh namely, triangular, square, tetrahedral, and

brick types. These types can be set at various sizes according to the domain and the object geometry. In the meshing, self-intersection or any holes should be avoided.

Mesh element distribution is very important as the process is developed in the finite volume. Meshing can be generated automatically, however, the user has the flexibility to change it to required size and types. Mesh can be refined locally to the spaces within the domain according to the accuracy of results required from specific areas. Hence mesh setting is very flexible and effective. Figure 4-14, shows how the mesh element size is bigger around the domain and finer mesh around the car model.

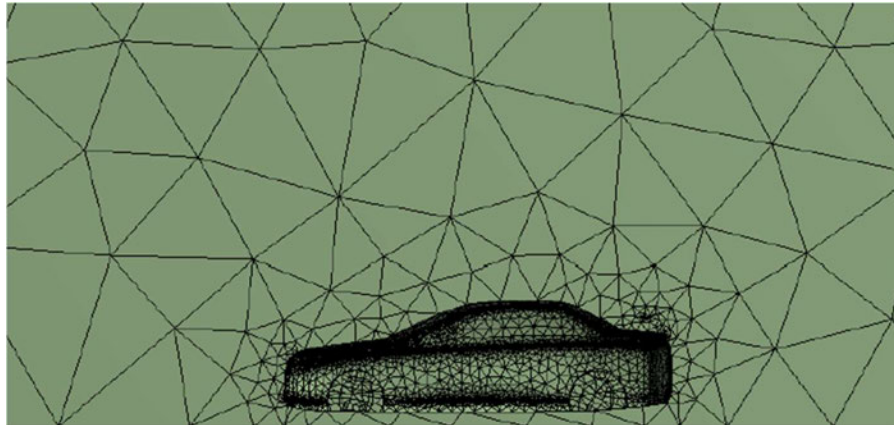


Figure 4-14- Meshing arrangement (Cakir, 2012)

4.6.2.1. Poly-Hexcore meshing

In the final simulation versions, Watertight Geometry Meshing Workflow process in Ansys Fluent is used. Patented by Ansys Mosaic Technology (Ansys.com,2020), Poly-hexcore mesh elements are generated using Watertight Geometry. Hexahedral mesh elements are good with their accuracy and efficiency, while polyhedral elements are well-suited for complex geometries and offer greater efficiency than tetrahedral elements. Ansys has developed a combination of these two mesh elements called Poly-Hexcore mesh type. In this type of meshing the polyhedral meshes are connected to the following element types.

- Surface: triangle, quad, polygon
- Volume: hexahedral, tetrahedral, pyramid, prism

This type of meshing offers flexibility by enabling a customised workflow template which can be used for different geometries. It can generate high quality surface meshes with multiple unique localised sizing ability for precise control of mesh distribution. It can generate volume mesh using poly-hedra, poly-hexcore, hexcore or tetrahedral

meshing algorithms. With parallel meshing application meshing time can be significantly reduced. Ansys claims that the poly-hexcore type meshing provides 46% reduction in mesh size along with improved mesh quality (Ansys.com,2020).

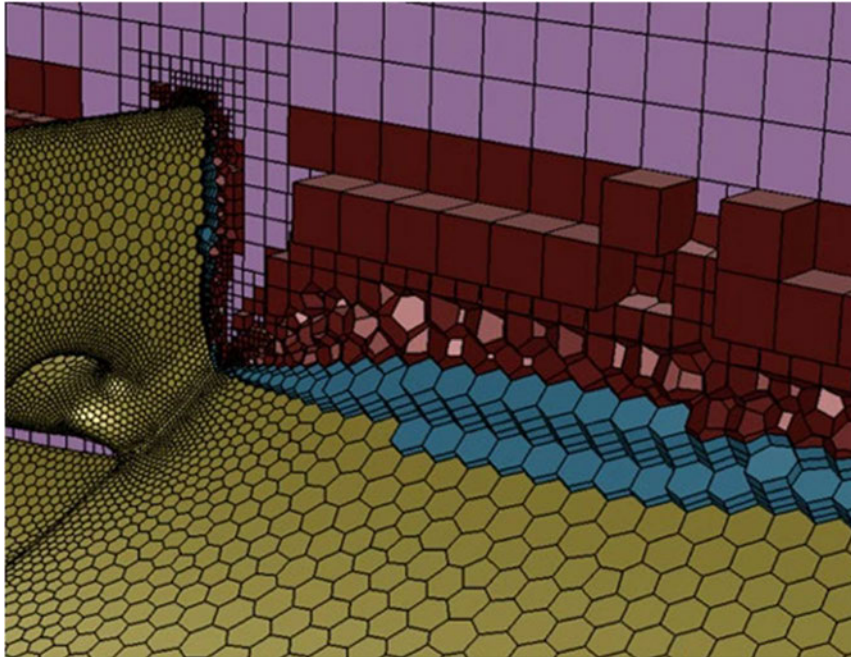


Figure 4-15 - Poly-Hexcore meshing (Ansys.com,2020)

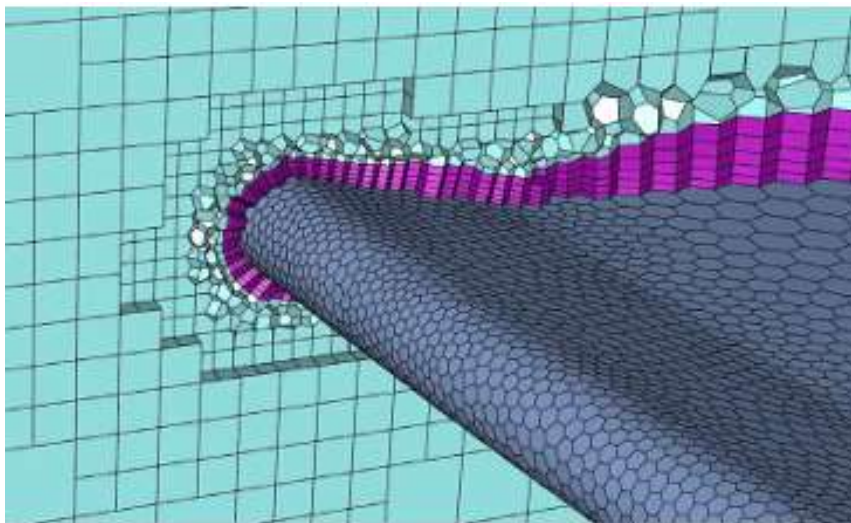


Figure 4-16-Poly-Hexcore meshing on Formula one wing (Ansys.com,2020)

4.6.3. Boundary conditions:

Setting boundary conditions is very important in the analysis set up as they are the constraints that would enable a system to interact with its surroundings. Following are the important boundary conditions that needs to be defined.

- Inlet – Fluid flow inlet conditions into the domain is defined here.
- Outlet – Fluid flow passing out of the domain.
- Symmetries – symmetric face can be defined here.
- Model or vehicle can be defined in the boundary conditions to study drag and lift forces.

5. Initial CFD simulation

This section is discussing simulation set up analysis and results for the Version 01 simulation (CFD-v01). The methods carried out are detailed in step-by-step.

5.1. Geometry preparation in Ansys

In order to prepare the geometry in Ansys the 3D CAD models prepared in Autodesk Inventor are imported into the Ansys Workbench Geometry section in .iges file format to be able to define this control volume. These files are opened in Design Modeler edit mode.



Figure 5-1-Geometry tab

- An enclosure is created to resemble a wind tunnel which defines the domain of the simulation. The size of the domain is very important as it significantly influence the behaviour of the air flow within the domain. To derive the domain size the length of the car is used as a reference length and a relative increment is made to this length.
- Once an enclosure is created around the car, Boolean tool is used, and the 3D profile of the car is subtracted from the enclosure. This leaves a 3D impression of the car model within the enclosure.
- Car model is symmetric along its length hence one symmetric half of the car is enough to perform the CFD simulation. This saves significant number of meshing elements, processing time and ultimately reduces process costs.
- A symmetry feature is used to cut the car and enclosure in half by selecting the mid plane.

- Boundary conditions are defined.
- In this case the domain size is defined as shown below.

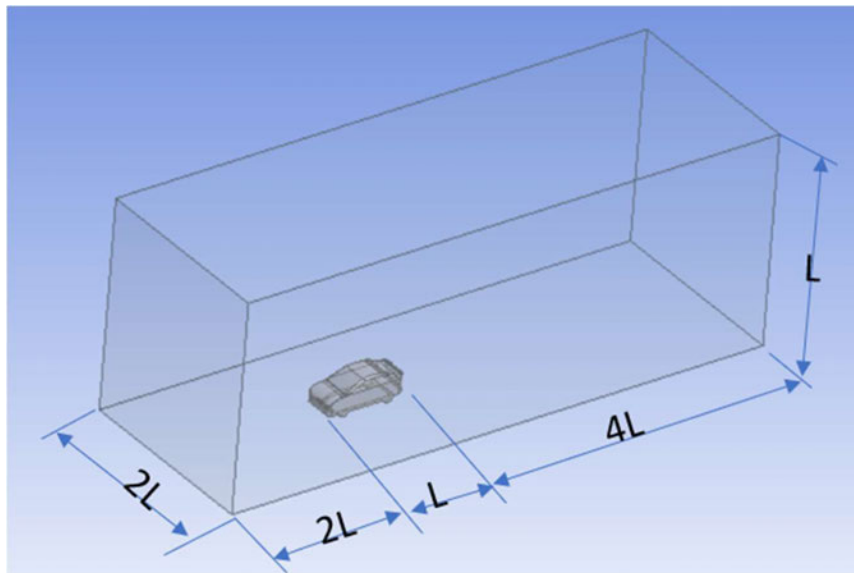


Figure 5-2-Domain size allocation_CFD-v01

Enclosure is created in the geometry and then using Boolean feature the car model is subtracted from the enclosure. This leaves the 3D profile impression of the car constructed in the enclosure.

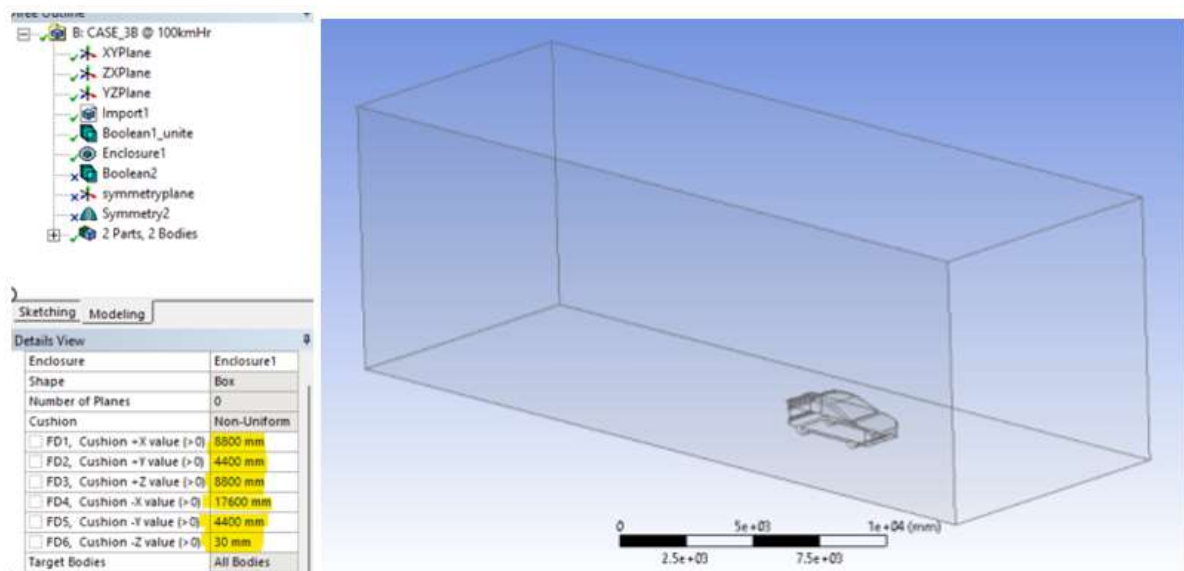


Figure 5-3-Enclosure constructed around the car_CFD-v01

A symmetry feature is used to cut the car and enclosure in half by selecting the mid plane as shown below.

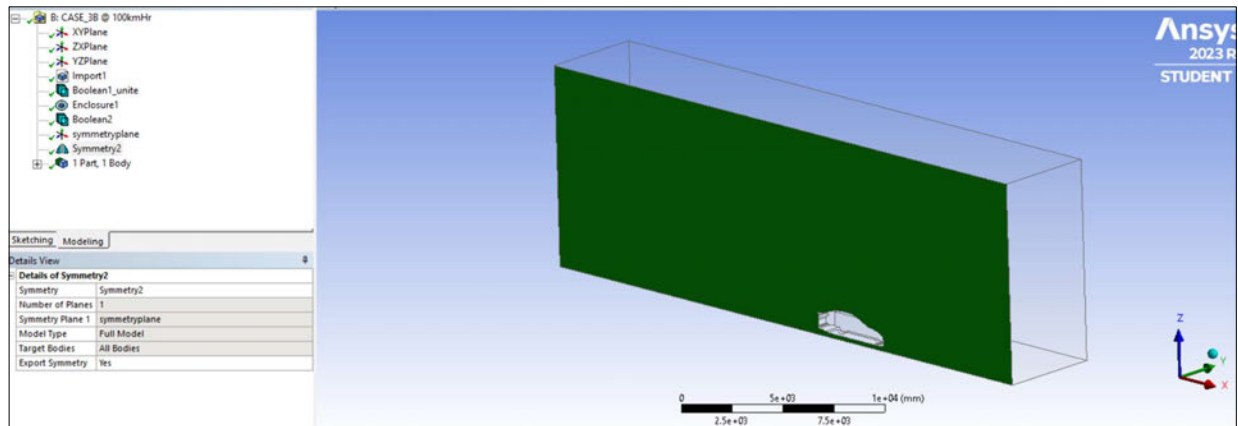


Figure 5-4-Symmetric section_CFD-v01

The domain boundary conditions for this version are defined as shown below.

- Inlet face
- Outlet face
- Symmetry face
- Walls – side walls , top face and ground face
- Car surfaces

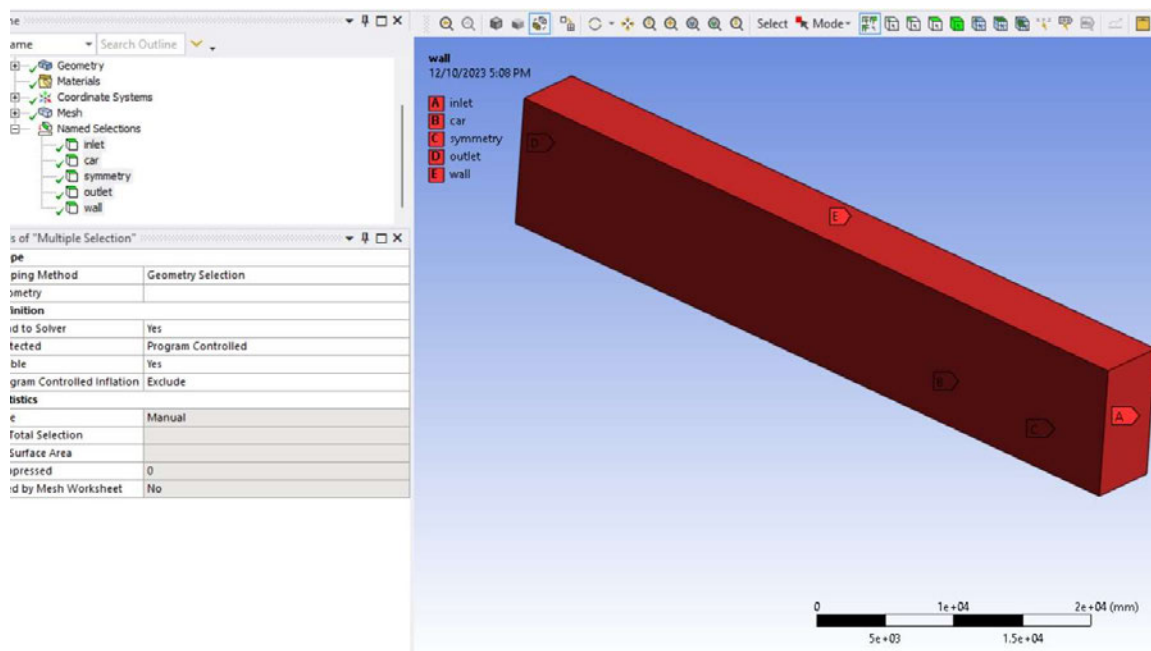


Figure 5-5 - Boundary conditions for CFD-v01

5.2. Mesh setup_CFD-v01



Figure 5-6 - Mesh tab

CFD-v01 was the initial analysis version performed. Student license package of the Ansys Fluent was used with the maximum number of mesh elements allowed for analysis limited to 512,000. All the 3 cases under this version have mesh generated and maintained under this limitation. 250mm size mesh elements were created around the enclosure domain.

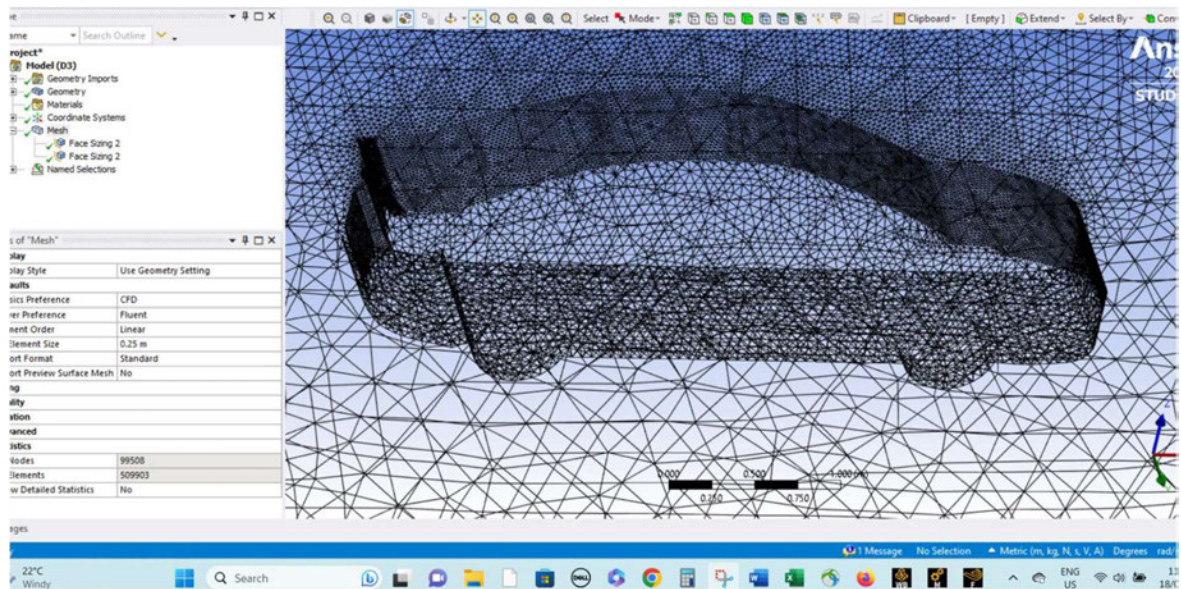


Figure 5-7 - Mesh generation for the whole domain_CFD-v01

Face sizing was used to further refine the mesh size to 25mm around the front, top and rear surface of the car, as well for the whole spoiler surfaces (highlighted in dark blue). Furthermore, for the remaining surfaces of the car, 60mm face sizing was created which is highlighted and shown below.

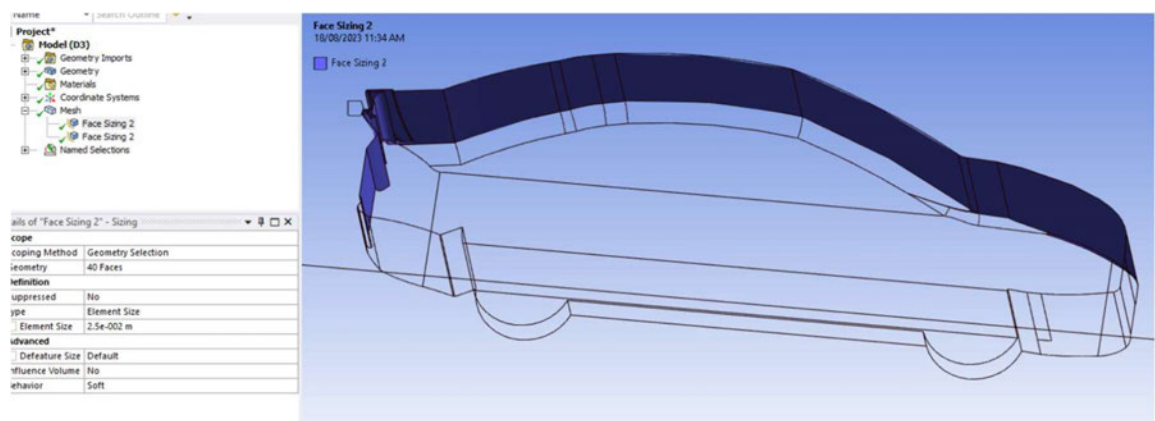


Figure 5-8 - 25mm Mesh face sizing_CFD-v01

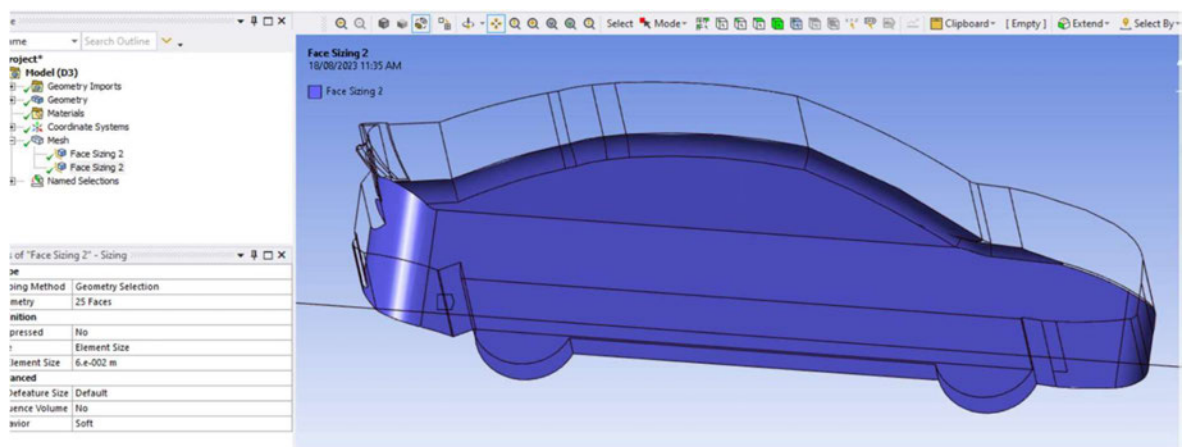


Figure 5-9 - 60mm Face sizing - CFD-v01

Mesh refinement detail as a result of the above process is shown below. Smaller mesh elements around the car and bigger elements for the remaining part of the domain. Since more accurate readings are required from the surface of the car.

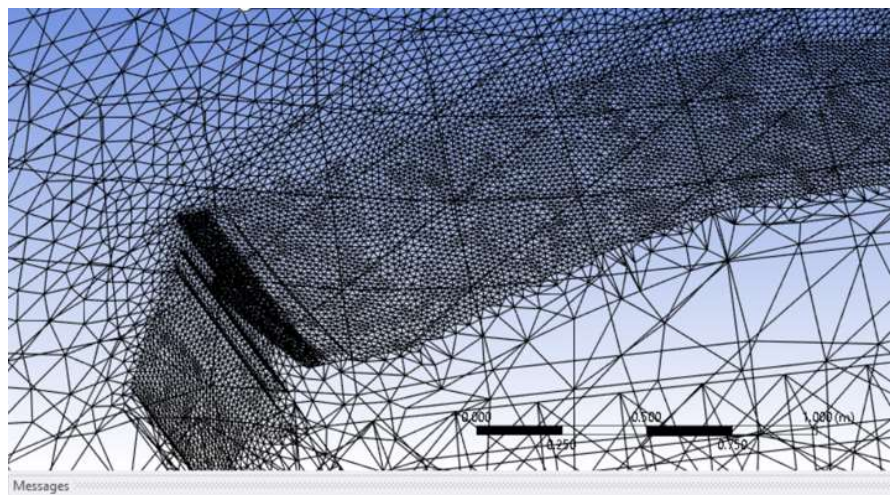


Figure 5-10 - Mesh refinement detail _CFD-v01

5.3. Solver set up process

The next stage of the analysis was to complete the simulation solver set up. This is where selection of viscous model, fluid type, air inlet speed, convergence set up, etc are done. Setup tab is highlighted in the figure of the Ansys fluent.



Figure 5-11 - Setup tab

Two main viscous models are considered in this project, k-epsilon ($k-\epsilon$) and k-omega ($k-\omega$) models. They are two equation models for both velocity and length scale and provide good accuracy results. They use the gradient diffusion hypothesis to relate the Reynolds stresses to the mean velocity gradients and the turbulent viscosity.

In the set-up tab, the viscous model options, k-epsilon viscous model was selected for CFD-v01 analysis.

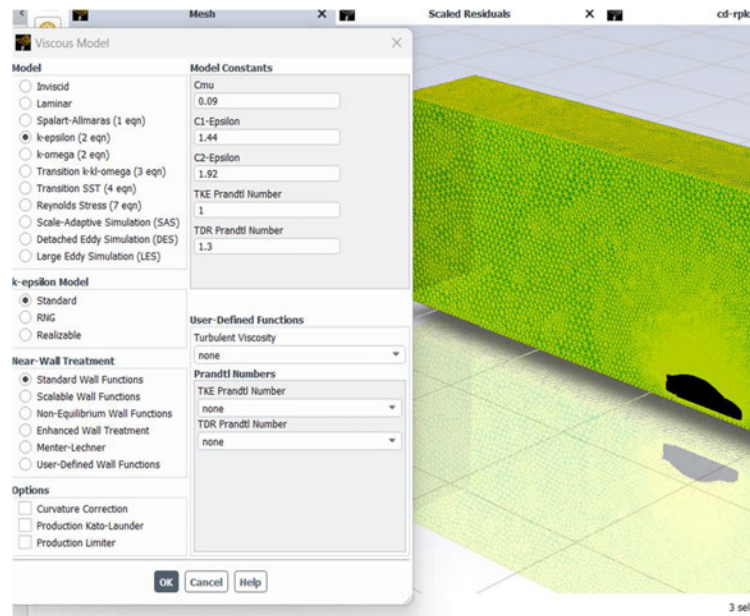


Figure 5-12 -Viscous model_ k-epsilon model_ CFD-v01

Boundary conditions are defined, with air as the fluid material in the inlet flowing at a velocity of 100km/hr. Turbulent intensity is set as default at 5% and turbulent viscosity ratio is at 10. Outlet pressure is set at 0 Pa. In the operating conditions, the operating pressure is set at the atmospheric pressure of 101325 Pa. Density value for the air is set as default.

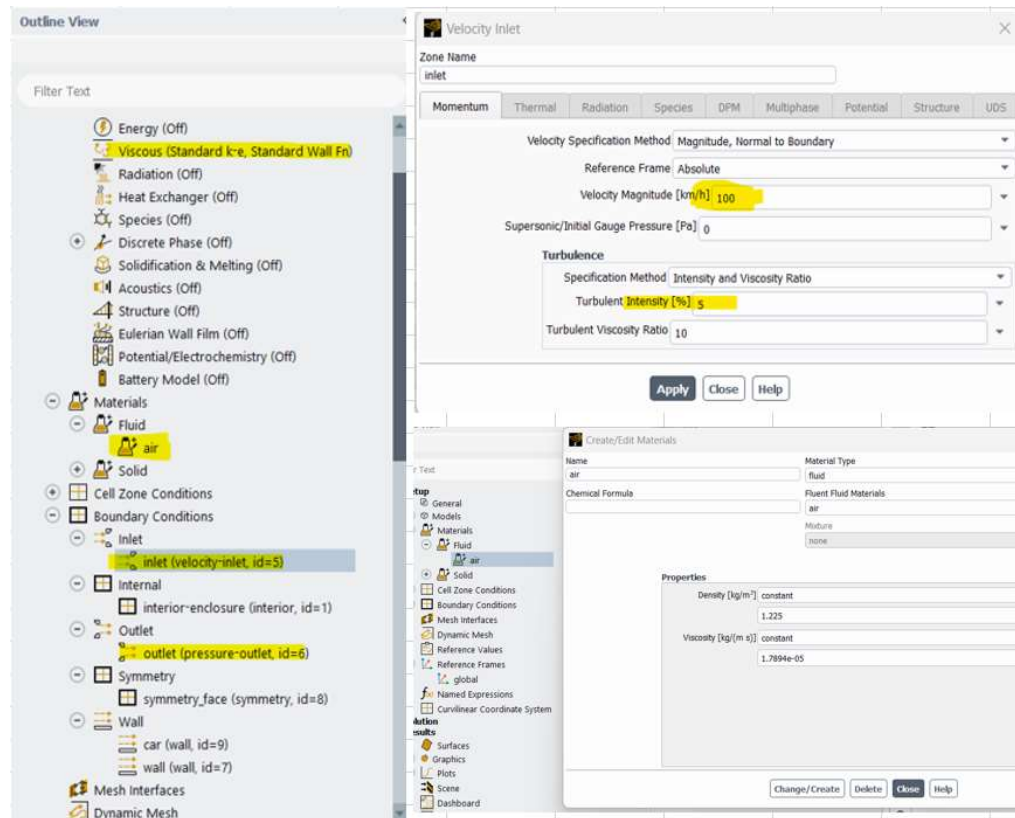


Figure 5-13 - Boundary conditions and parameters defined_CFD-v01

In the reference value section needs to be updated to calculate the pressure coefficients. The velocity value is given as 100km/hr. In the case of external aerodynamics of the cars the reference area corresponds to the area facing the flow, which is the frontal area. This value is derived from the projected area option and entered here the area tab. Rest of the values are set as default.

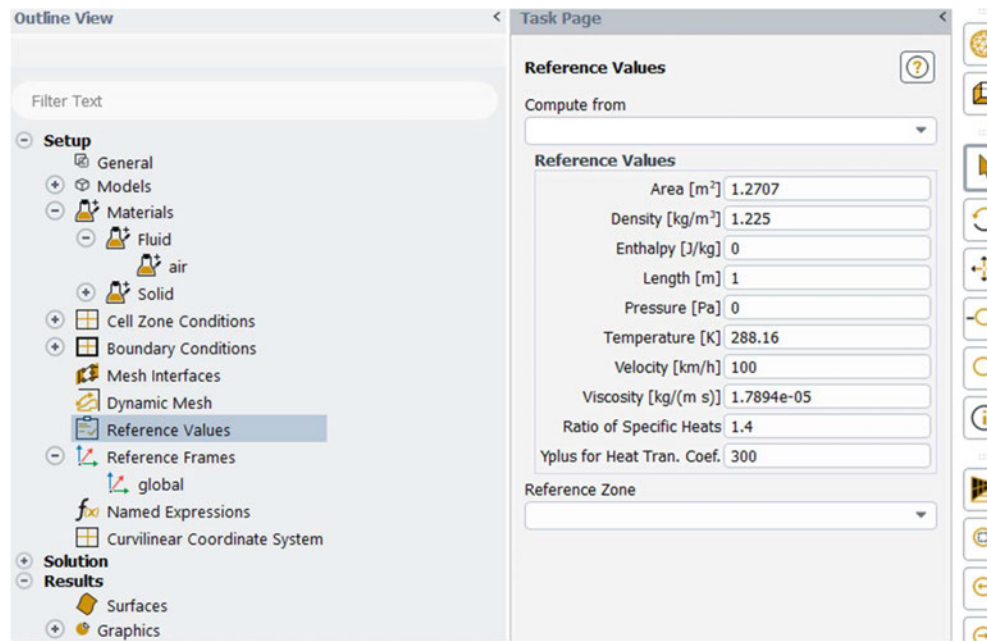


Figure 5-14 - Reference values defined_CFD-v01

Solution method is set as Coupled with default values. Standard initialization was carried out and the simulation was set to run for 1000 iterations, with an expectation that the solution would converge before.

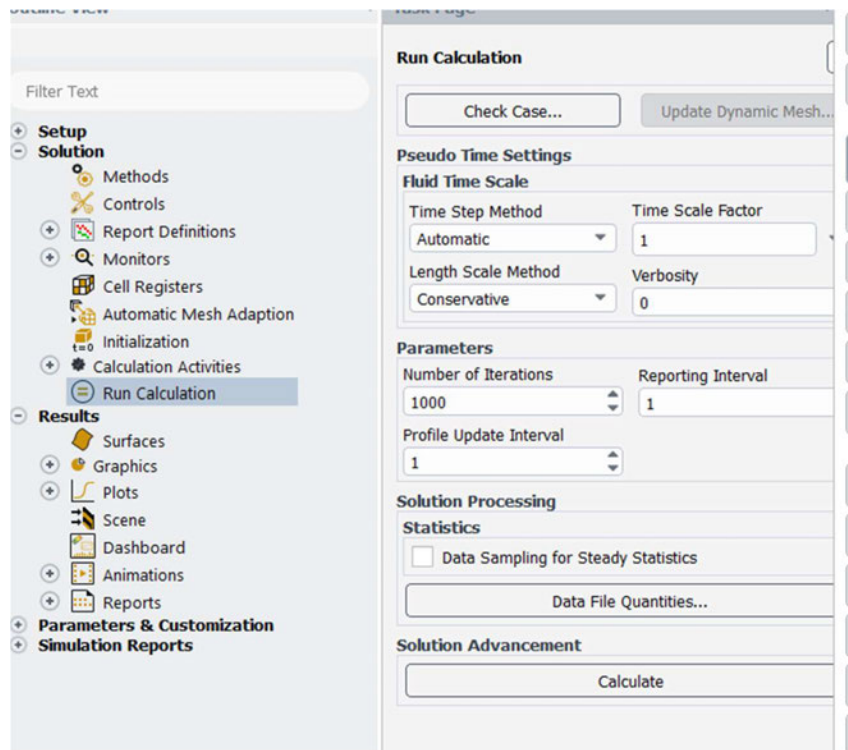


Figure 5-15 - Calculation run_CFD-v01

5.4. Convergence

In order to ensure that the results are accurate it is important that the calculation run is converged. Once the number of iterations is set to run the analysis process will check for convergence on the governing equations and will automatically complete the calculation once the calculation is complete.

For CFD-v01, being the first analysis, the convergence conditions was set at default values to understand the nature of convergence and how the results are derived. However, for version 03 and 04 of the simulation these are set at 10^6 for better accuracy.

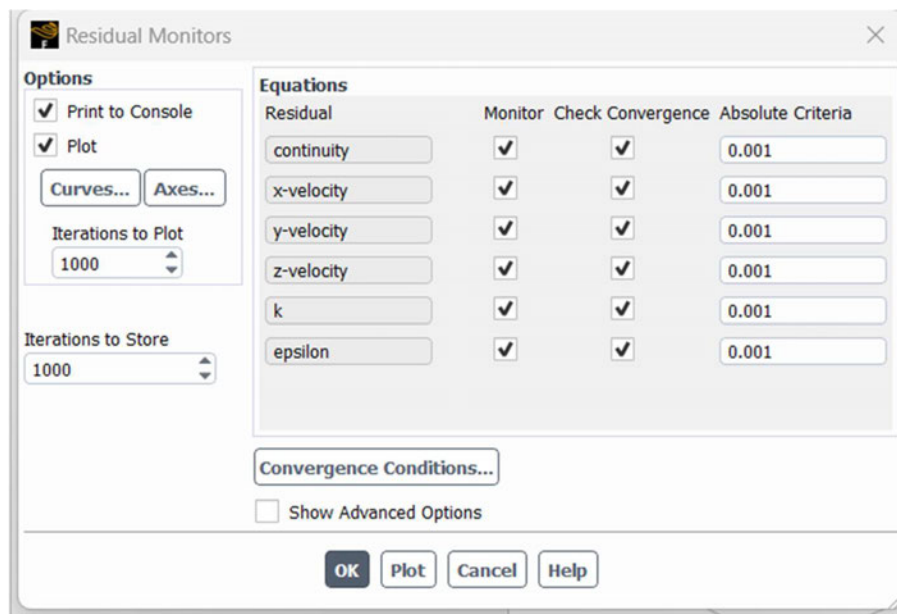


Figure 5-16 - Convergence conditions-CFD-v01

Below given are the residuals plots for all the three cases. In case 1 which is the base car only, the result did not converge and has been in a slightly wavy pattern after 100 iterations. When investigated on how to approach in such cases, it was found in the ANSYS learning website that in such cases the average of the results are taken as a final result. There is a learning video in ANSYS learning where they show the analysis on a FSEA car and the result were quite worse than the above, but they suggest that this wavy result is due to the vortex shedding caused due to the interaction of the car and the air. Being an inherently unsteady problem, this behaviour is expected. The plots of c_d and c_l are stabilised and oscillate around an average value. Based on the average values taken from the results the simulation can be concluded to have reached an acceptable convergence for steady state analysis (Ansys.com).

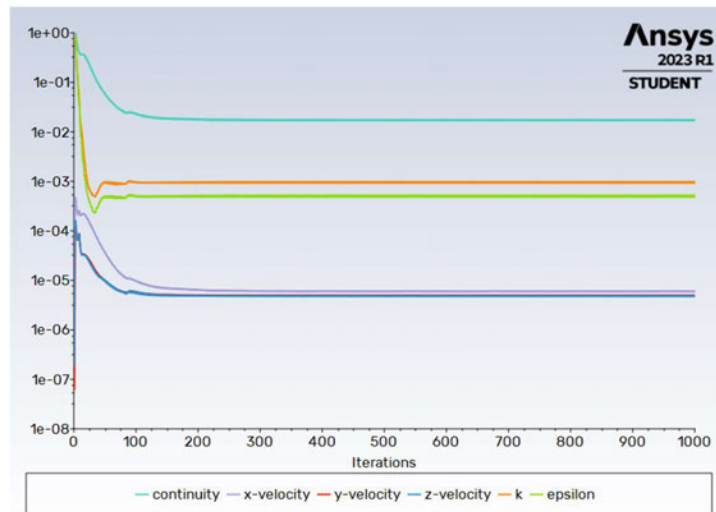


Figure 5-17-Case 1 residual plot_CFD-v01

For case 2 the solution converged at 433 iterations.

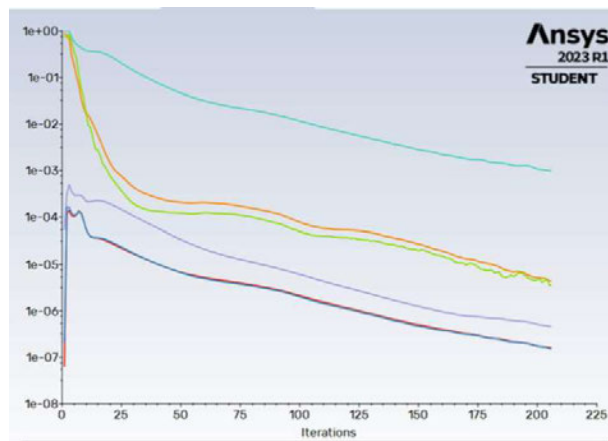


Figure 5-18-Case 2 residual plot_CFD-v01

For case 3 the solution converged at 547 iterations.

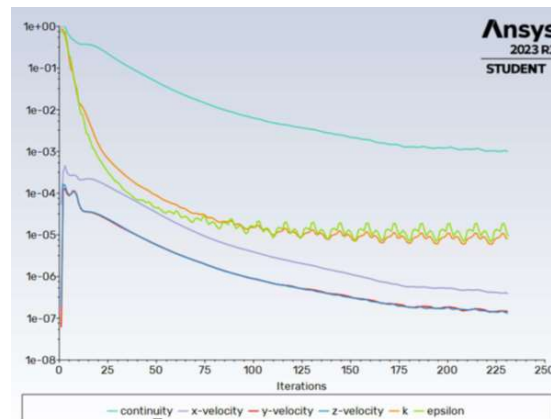


Figure 5-19- Case 3 residual plot_CFD-v01

Table below is the summary of the drag and lift coefficients as well as the drag and lift forces derived from the simulations. The values shows that in Case 3 the lift force is -21.7 N. The negative value indicates that downforce is generated in this case. For Case 1 and 2 have 41.5 N and 130.7N lift force respectively. Case 1 lift force is larger compared to case 2.

Table 5-1-Drag and lift coefficients_CFD-v01

CFD_v01	cd	cl	Drag force (N)	Lift force (N)
Case 1	-0.27	0.22	-158.9	130.7
Case 2	-0.280	0.070	-170.5	41.5
Case 3	-0.260	-0.040	-154.6	-21.7

5.5. Analysing results

The pressure distribution, an overview for all three cases is shown below. The images in the first row is from the plan passing through the centre of the car. The bottom row is the pressure distribution from plane located between the centre lane and one side of the car. For case 3 this is passing through one of the spoiler flanges.

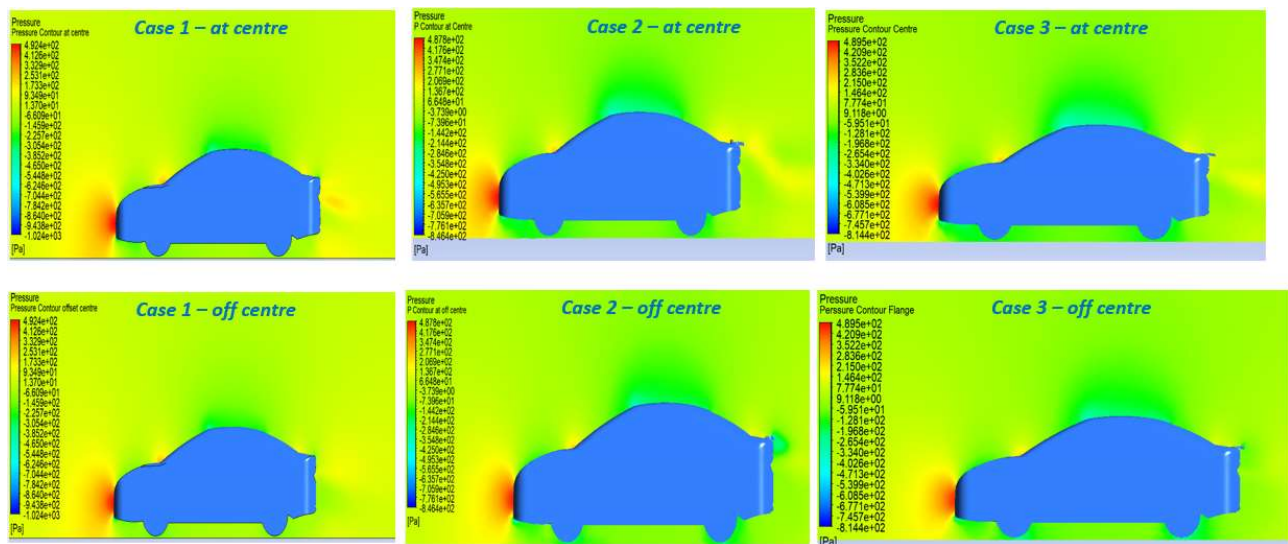


Figure 5-20 - Pressure distribution overview -CFD-v01

Below given are the 3D images of the pressure distribution for all three cases. These images are suggesting the pressure generated values at the rear deck area

- Case 1 is between -90 to -209 Pa
- Case 2 is between 70 to 112 Pa
- Case 3 is between 90 to 120 Pa

This is indicating that the higher pressure is generated (especially around the spoiler) for case3 spoiler flanges are higher than the other two cases.

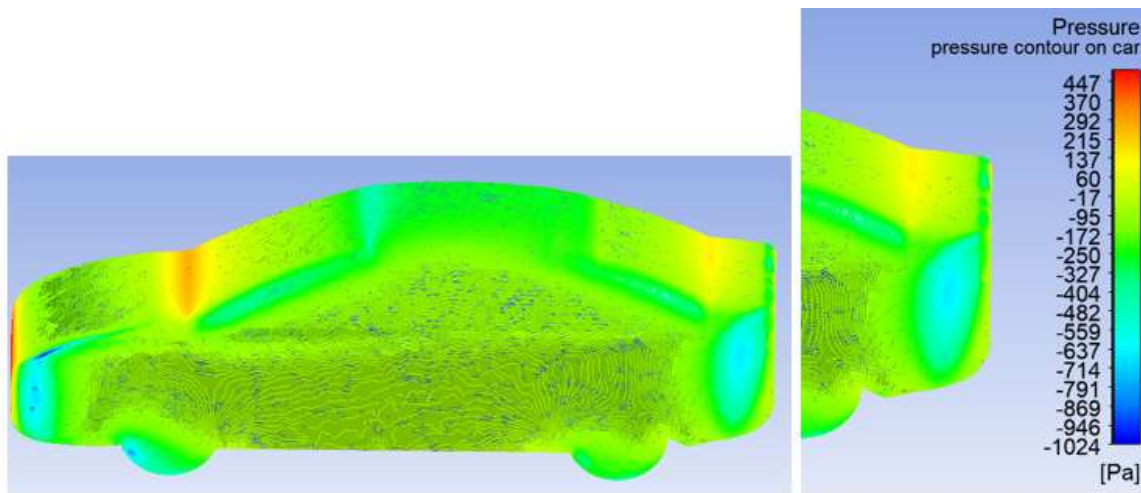


Figure 5-22 - Pressure distribution-Case1_CFD-v01

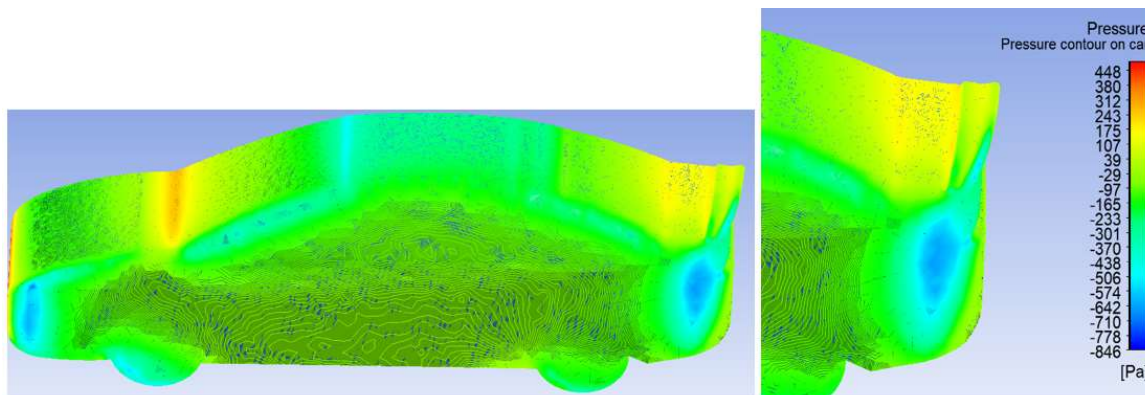


Figure 5-21-Pressure distribution-Case2_CFD-v01

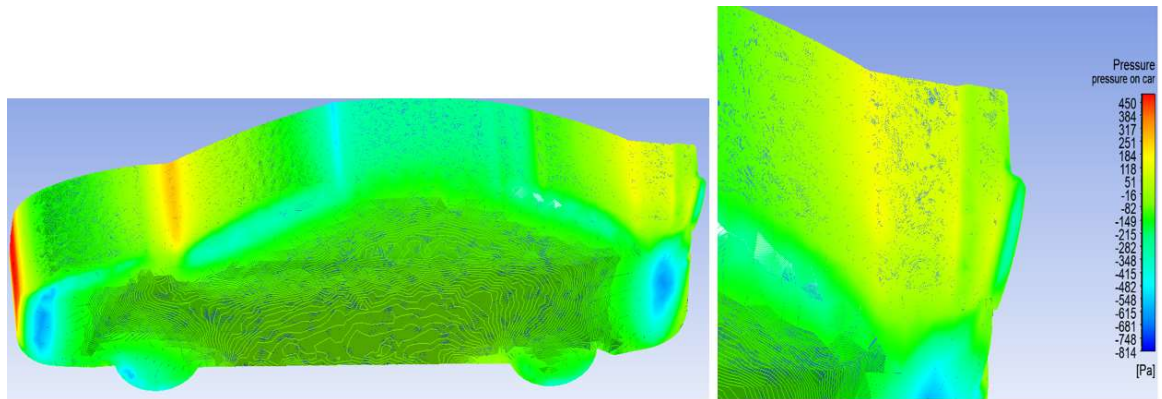


Figure 5-23-Pressure distribution-Case3_CFD-v01

Velocity contours for all the three cases are given below. For Case 3 the wake region is quite less compared to the other two cases as well as the flow separation at off-centre location.

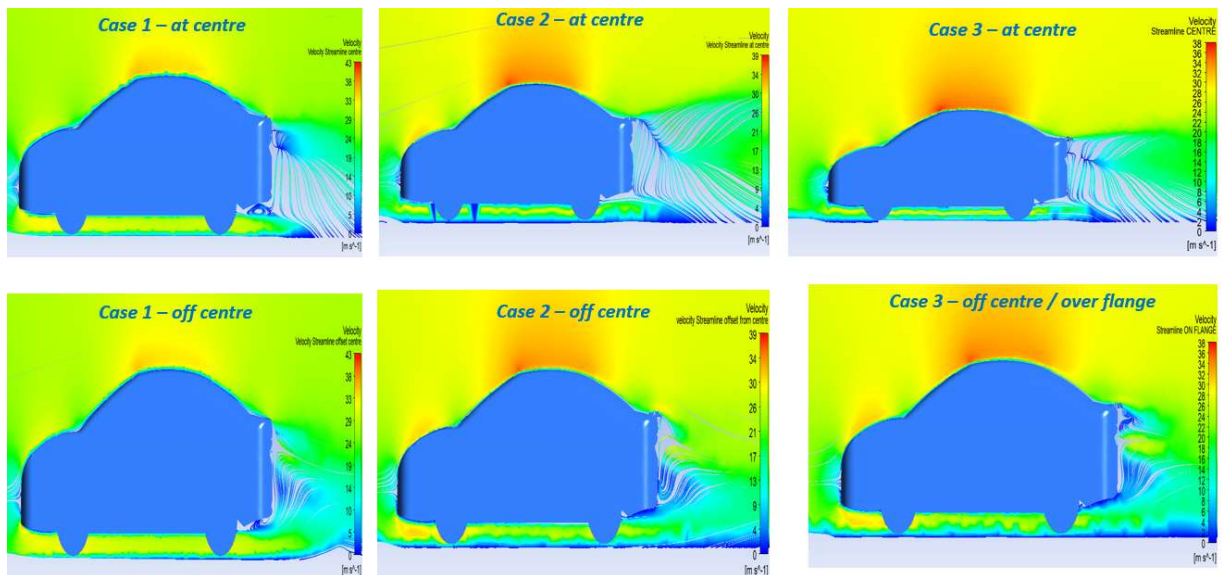


Figure 5-24 - Velocity contour - for all three cases_CFD-v01

5.6. Verdict on CFD-v01

This initial simulation results (CFD-v01) gave a positive hope. However, since the mesh setting with coarse elements and the simulation is performed in a student license package, it was expected that the software's limitations would not provide accurate results. Hence these results were only considered as suggestive and not conclusive. Hence CFD-v03 and CFD-v04 simulations were performed in ANSYS Academic package with refined mesh and two domain sizes with the intention to improve the accuracy and consistency of the results. The results from this analysis are considered to be the conclusive findings in this research project.

A final comparison of findings between these three analysis versions will be discussed at the conclusion section towards the end of this report.

The next few sections will be discussing the simulation procedures and analysis results performed on CFD-v03 and CFD-v04 simulation versions. CFD-v02 version was only progressed till its set up stage for HPC run, but the simulation was not performed due to HPC related technical issues and hence are not discussed in these sections.

6. Final CFD simulation

CFD-v03, CFD-v04 and CFD-v05 are the final simulation versions for the project. The basic methods in these simulations are quite similar to that mentioned in the initial simulation sections. However, any differences in the methods used are specified in the relevant sections. It has to be noted that, since these analyses were performed in the later part of the project, more and more exposure to the Ansys software improved the approach adopted, which are reflected in these sections. As mentioned earlier the 3D CAD model preparation is same for all simulation versions which has been already mentioned in the earlier section.

Differences between the CFD-v03 and CFD-v04 simulation versions are:

- CFD-v03 – Bigger domain size, medium mesh elements
- CFD-v04 – Smaller domain size, medium to fine mesh elements
- CFD-v05 – Smaller domain size, fine mesh elements_Case3 only

Specific dimensional details and parameter changes are mentioned in the relevant sections.

6.1. Geometry preparation in Ansys

Unlike the previous simulation, geometry preparations for these versions are done in Ansys SpaceClaim. The Repair tool in SpaceClaim can be used to improve the imported 3D CAD model, by merging multiple smaller surfaces into one to make a bigger and smoother surface. This enables most of the small surface patches to be merged. This would help in simplifying mesh generation. Below image shows updated surfaces in SpaceClaim.

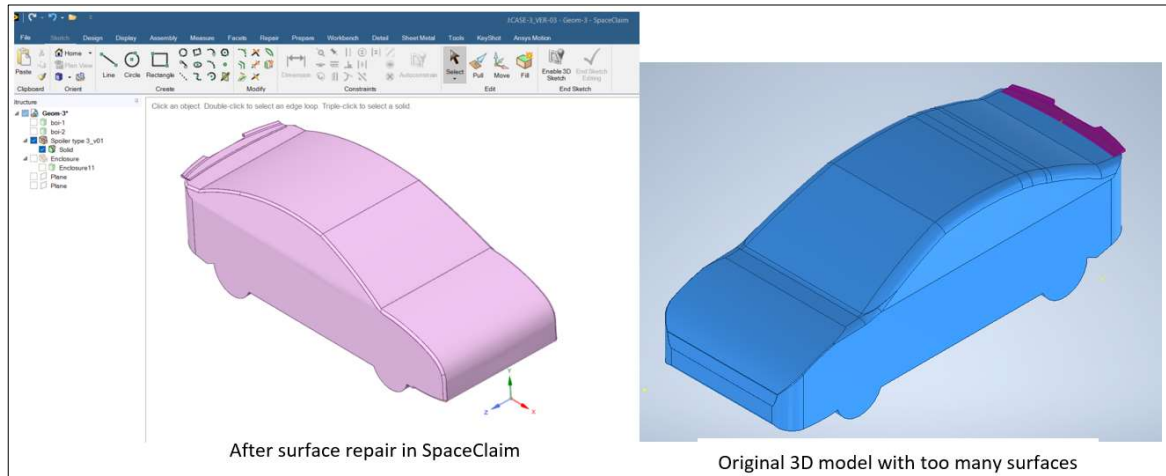


Figure 6-1-Surface preparation comparison

Once the surfaces are improved the next step was to create Body of influence bodies around the car model.

6.1.1. Body of Influence (BOI)

BOI is a geometry resembling an enclosure, created around the car model to define denser mesh elements within that volume. In other words, within each BOI exclusive mesh refinement can be allocated to achieve accurate simulation results. BOI is not a part of the model geometry or enclosure and neither this geometry surfaces can be meshed. This gives the flexibility to do mesh refinement in specific areas. Multiple BOIs can be constructed according to the need.

In this simulations, two BOIs are generated, initially named as boi-1 and boi-2. The first is created just around the car model. The second one is created 500mm away from boi-1 surfaces on the five sides, and its rear face is elongated to flush with the rear face of the enclosure. Please note that the process for BOI creation is same for both CFD-v03 and CFD-v04 versions and only the boi-2 geometrical size varies with the enclosure size at the rear face.

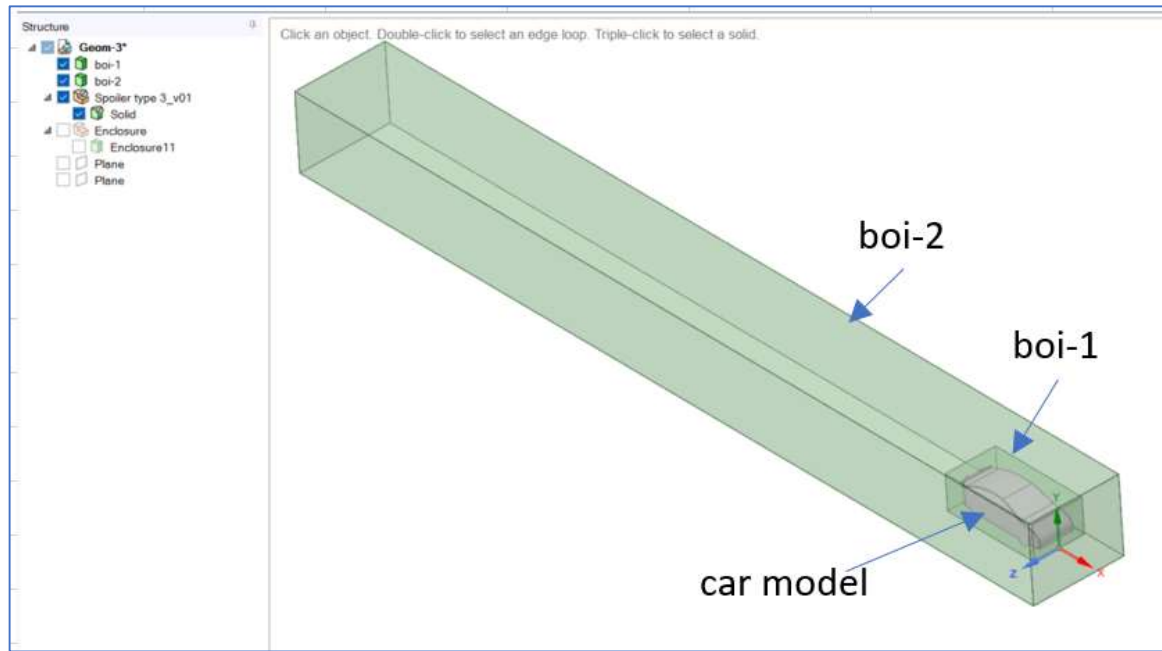


Figure 6-2 - boi-1 and boi-2 geometry

6.1.2. Enclosure – Domain size preparation

Enclosure defines domain for simulation. As mentioned earlier an enclosure is created to resemble a wind tunnel which defines the domain of the simulation. The size of the domain is very important as it significantly influence the behaviour of the air flow within the domain. To derive the domain size the length of the car is used as a reference length and a relative increment is made to this length.

6.1.2.1. Domain size for CFD_v03 cases

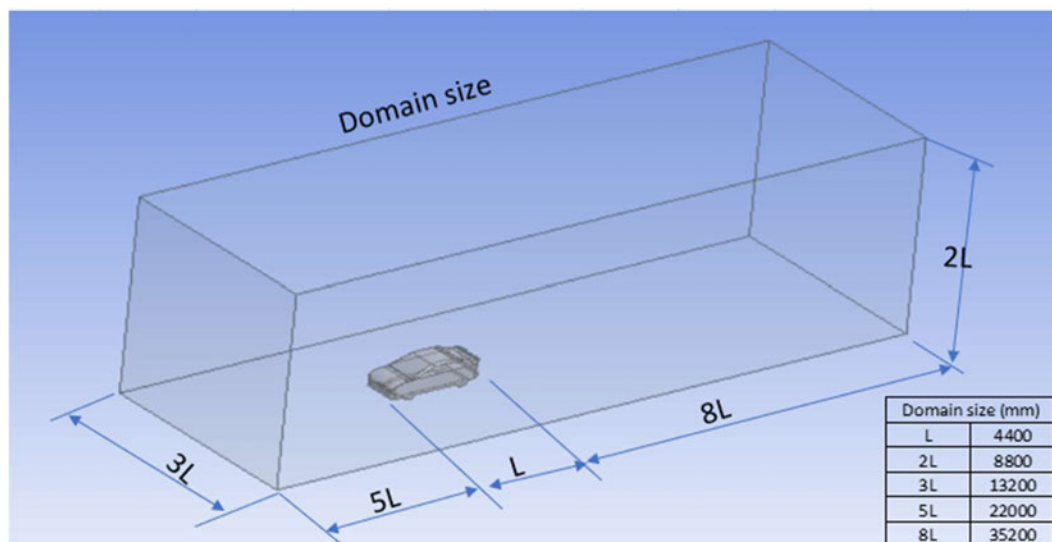


Figure 6-3 – Domain size_CFD-v03

6.1.2.2. Domain size for CFD_v04 & v05 cases

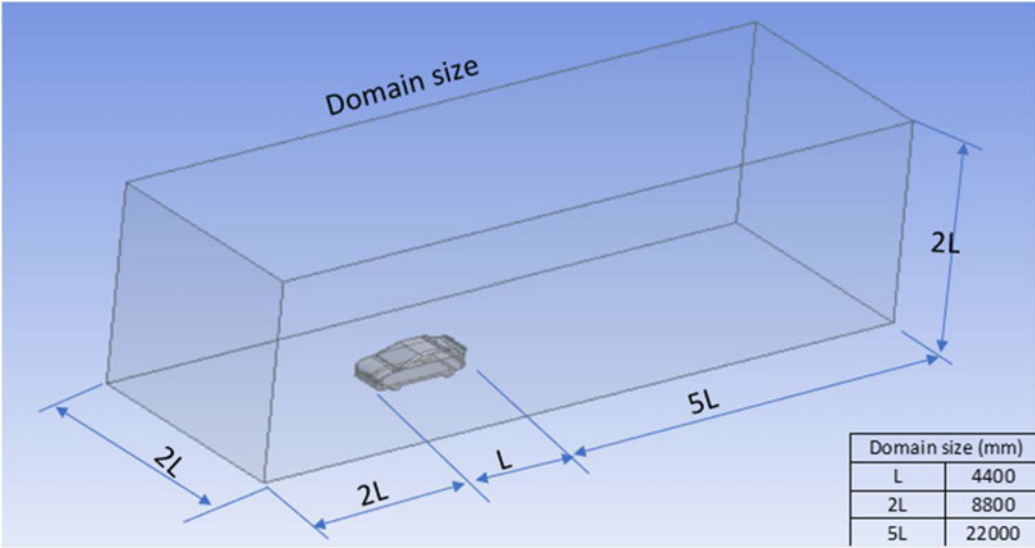


Figure 6-4-Domain size_CFD-v04 & v05

Since the car has symmetric feature, only one symmetric half section of the car ad enclosure is enough to perform the CFD analysis. The section is created, and the enclosure is constructed as shown below.

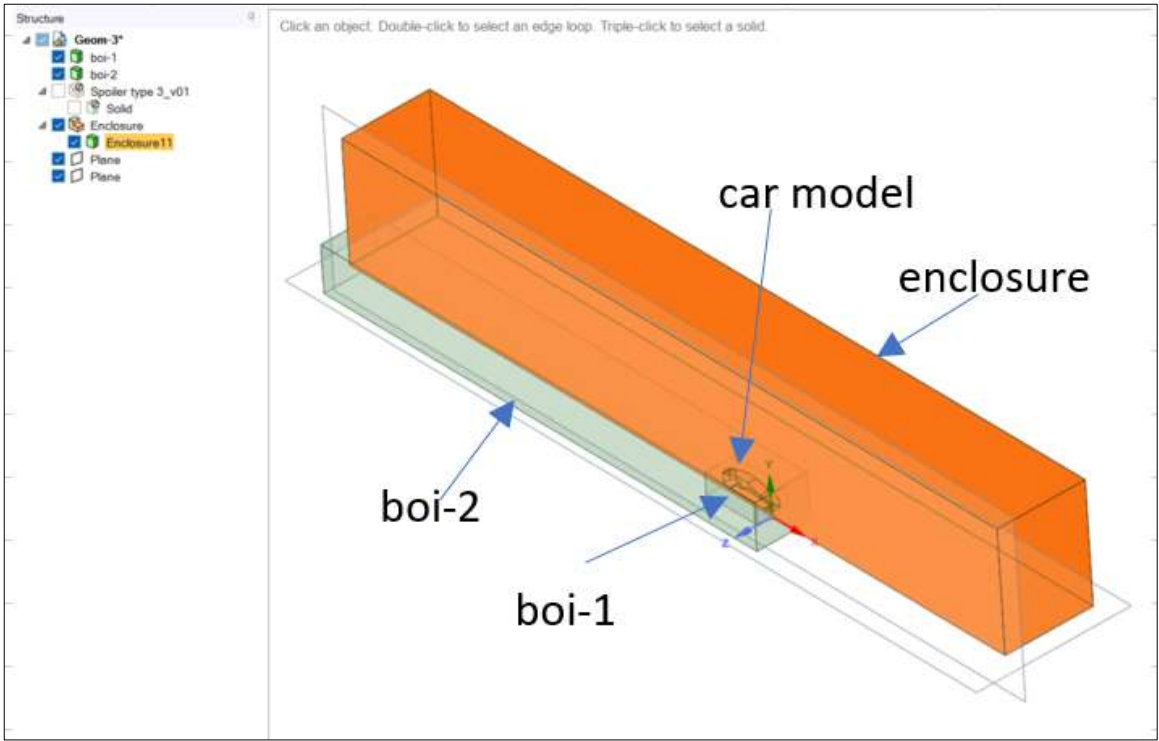


Figure 6-5 - Symmetric form of enclosure and car_CFD-v03

6.1.3. Boundary conditions

Once the enclosure constructed, the boundary conditions are defined as listed. Please note that the boundary conditions defined for CFD-v03 and CFD-v04 are the same and hence this is not detailed again in the next simulation (CFD-v04) section.

- Inlet face
- Outlet face
- Symmetry face
- Walls – side face and top face
- Ground (as wall) – bottom face
- Car – car surfaces

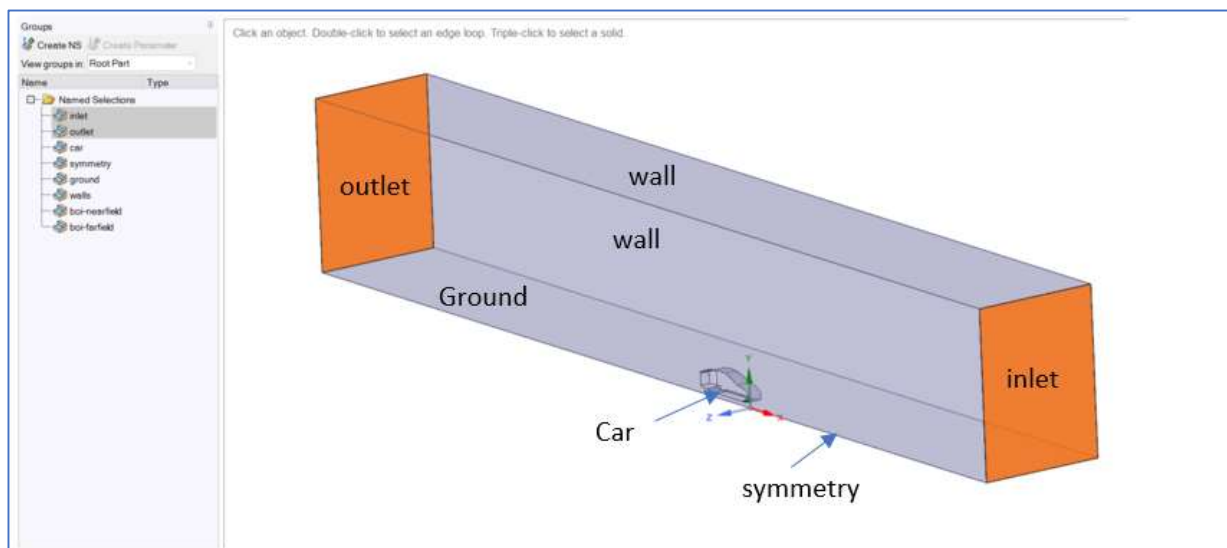


Figure 6-6 - Boundary conditions

The above process completes the geometry preparation and ready for the mesh set up.

6.2. Mesh setup – Watertight meshing

For the final two simulations the mesh elements are generated using Watertight Geometry Meshing workflow in Ansys Fluent. As mentioned in the earlier section, this type of meshing offers flexibility by enabling a customised workflow template which can be used for different geometries.

This session will be demonstrating the step-by-step process in process in this meshing type. Please note that steps are common for all the final simulation versions. Hence during the next simulation versions, these processes are not discussed again. Instead, the surface and volume mesh elements generated for the specific version will be specified.

6.2.1. Local sizing

. The image below is showing a fully generated meshing with poly-hexacore mesh type generated on CFD_v03 version. The first step is to import the geometry into meshing session. Then local sizing option is used to assign specific localised mesh region. Two body of Influence (BOI) geometry constructed in the geometry was first assigned with the mesh elements.

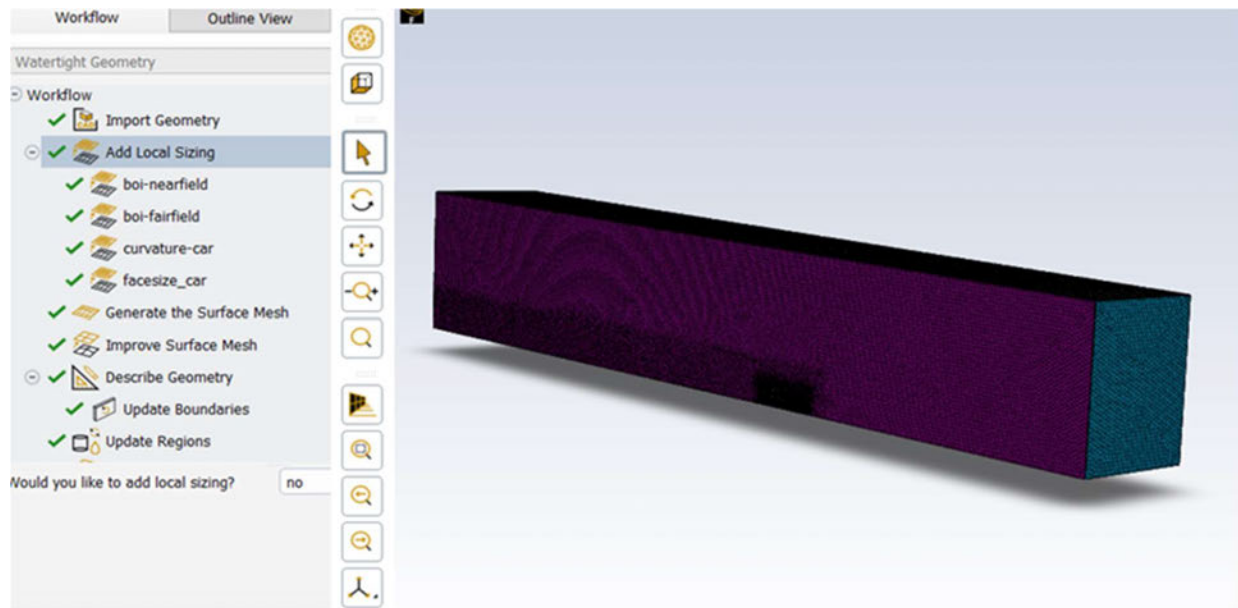


Figure 6-7 - Fully generated meshing

Among the two Body of Influence geometry, boi-1 and boi-2, the smaller one, which covers just around the car profile is boi-1. In the local sizing menu, the boi-1 has been renamed as “boi-nearfield”, size control type is selected as Body of Influence and a target mesh size is set at 50mm with a growth rate of 1.2. The mesh profile can be seen in the red box in the image below. This mesh refinement round the car model improves the accuracy of the simulation around the area of interest.

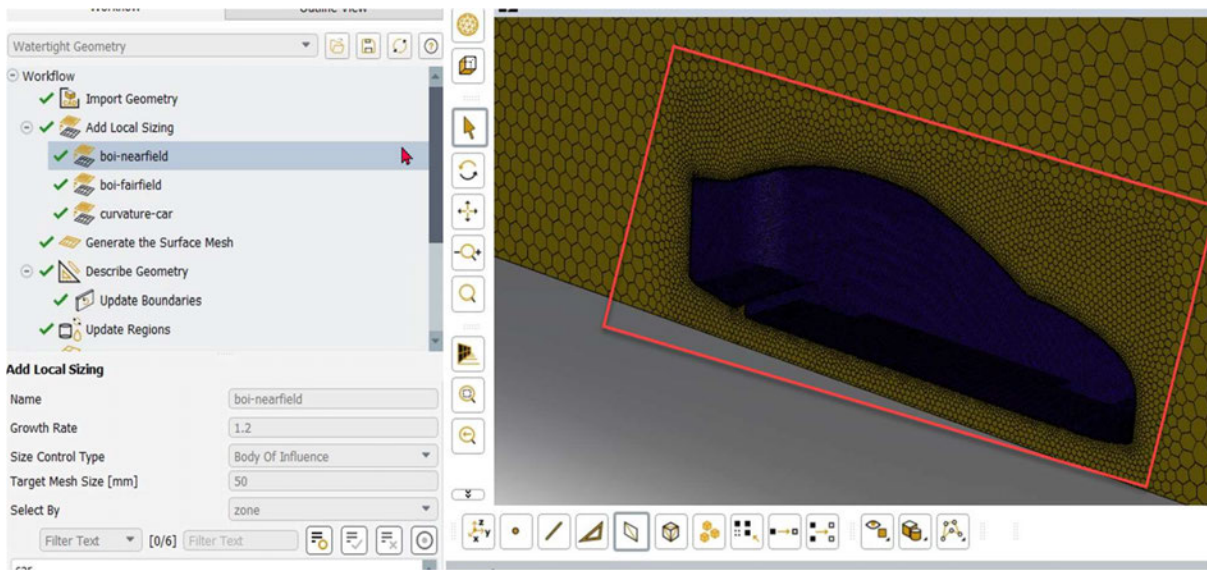


Figure 6-8-Body of influence-nearfield

In the local sizing menu, the boi-2 has been renamed as “boi-fairfield”, size control type is selected as Body of Influence and a target mesh size is set at 150mm with a growth rate of 1.2. The mesh profile can be seen in the green box in the image below. The mesh refinement around this region will allow to capture better understanding around the rear end of the car, to capture the air flow behaviour, vortex generation, more accurate details around the wake region, the turbulence generated, etc.

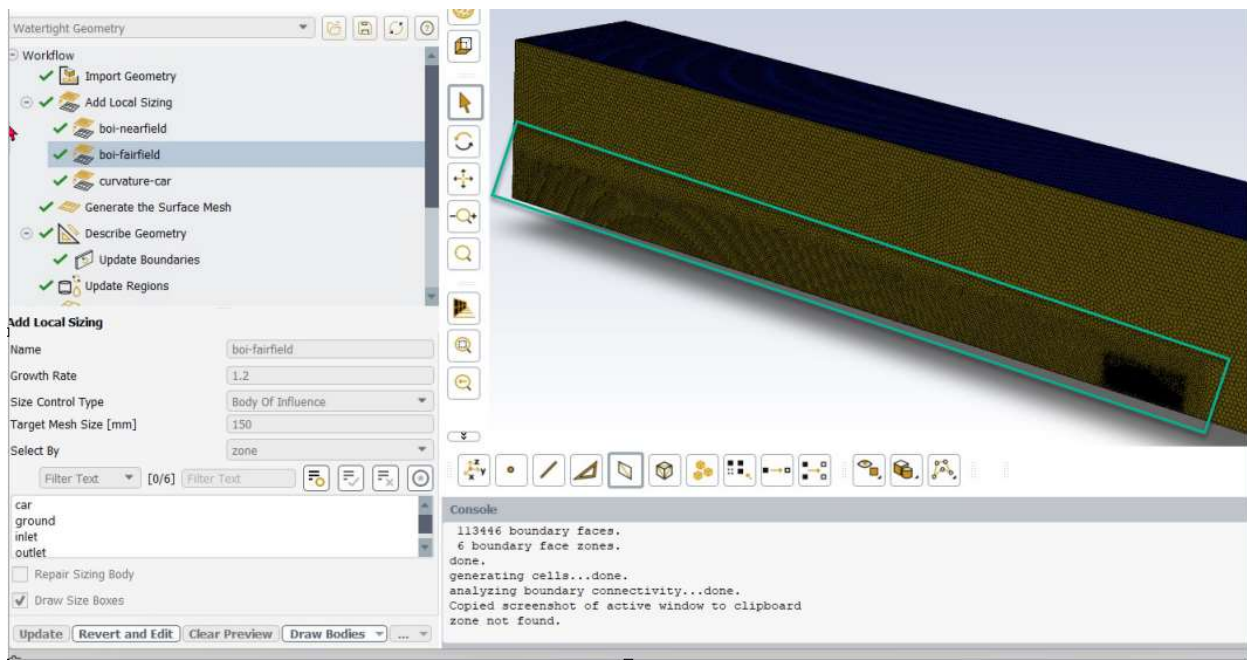


Figure 6-9 - Body of influence - farfield

In the same local sizing menu, the curvature sizing was assigned to the whole car profile for improved meshing around the intricate profile regions. A local minimum size of 5mm and a maximum size of 20mm has been assigned with a growth rate of 1.2.

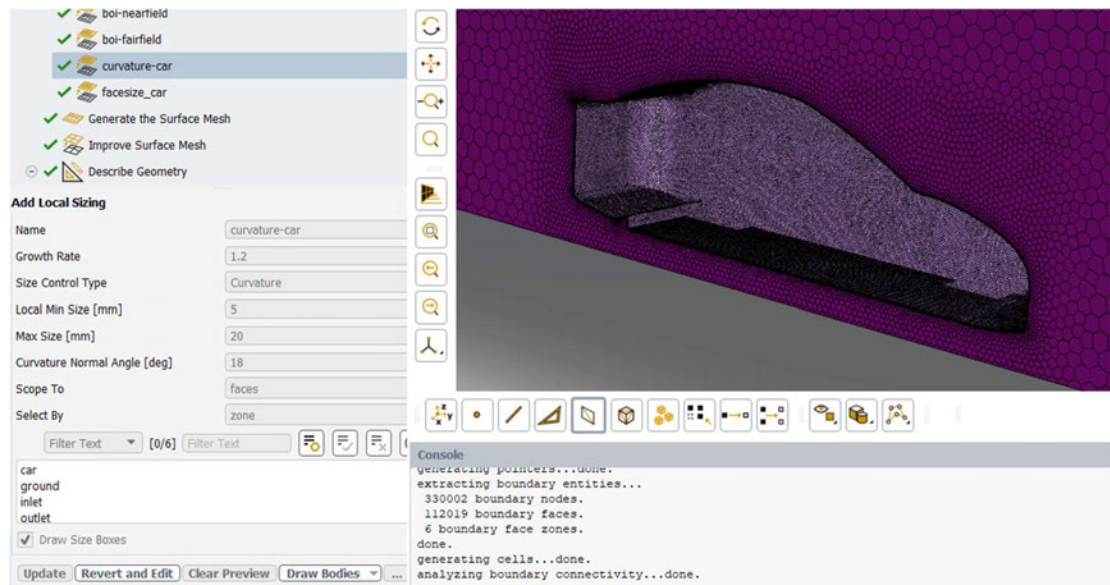


Figure 6-10 - Body of curvature – car profile

6.2.2. Surface meshing - CFD_v03 - coarse mesh

The next stage is to define the surface meshing. Version 03 has a large domain size. A minimum size of 30mm and a maximum size of 250mm was assigned with a growth rate of 1.2. Boundary conditions are assigned corresponding to the allocated faces during geometry preparation.

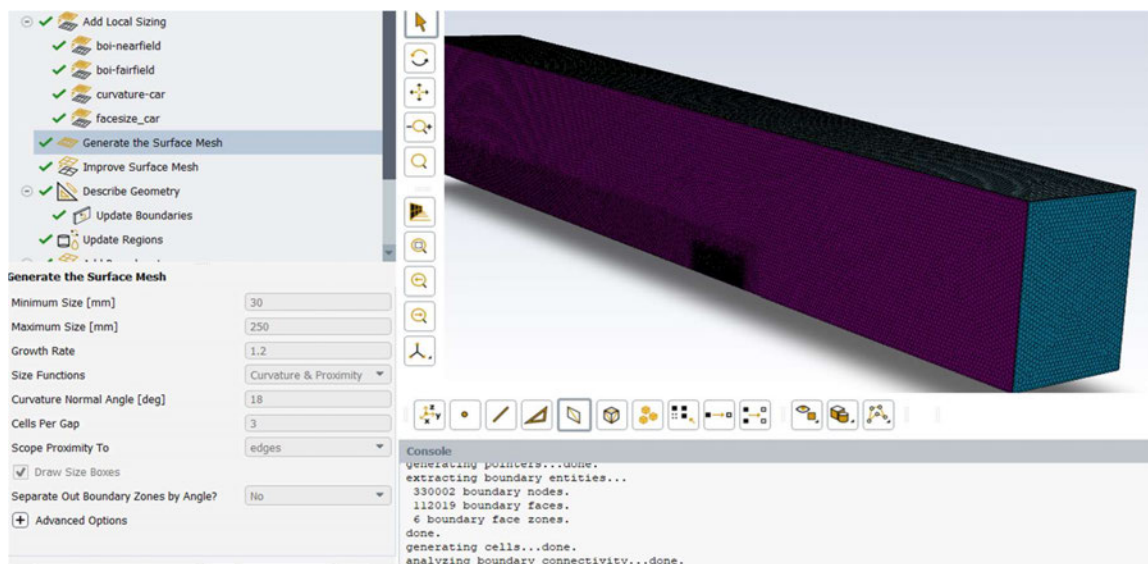


Figure 6-11 -Surface mesh generation_CFD_v03

6.2.3. Surface meshing-CFD_v04 - medium mesh

Version 04 has a smaller domain size as specified in the domain size section. Here a minimum size of 5mm and a maximum size of 100mm was assigned with a growth rate of 1.5.

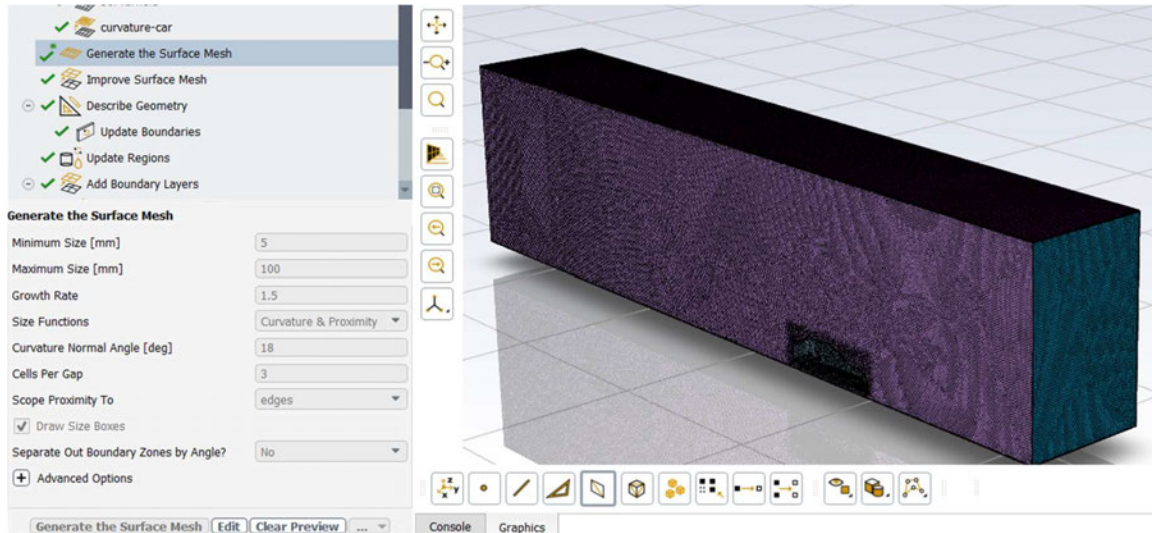


Figure 6-12-Surface mesh generation_CFD_v04

6.2.4. Surface meshing - CFD_v05 - fine mesh

Version 05 has the same domain size as v04 as specified in the domain size section. Here finer mesh size of a minimum of 3mm and a maximum size of 100mm was assigned with a growth rate of 1.2.

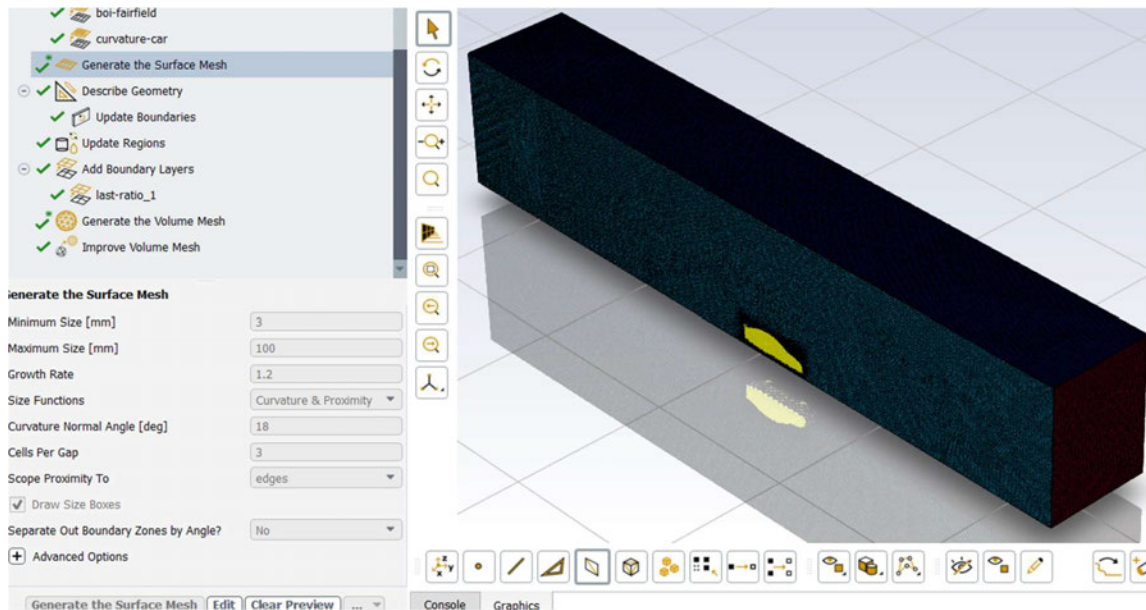


Figure 6-13-Surface mesh generation_CFD_v05

6.2.5. Boundary layer mesh setting

While modelling a viscous flow around the car, the near wall region should have good mesh to capture the effect of boundary layers that forms along these walls. Boundary layer thickness is often very small relative to the characteristic dimensions of the car and hence, it is important to have refined mesh to accurately capture the flow physics in these thin regions. The boundary layer is set as shown in the image below.

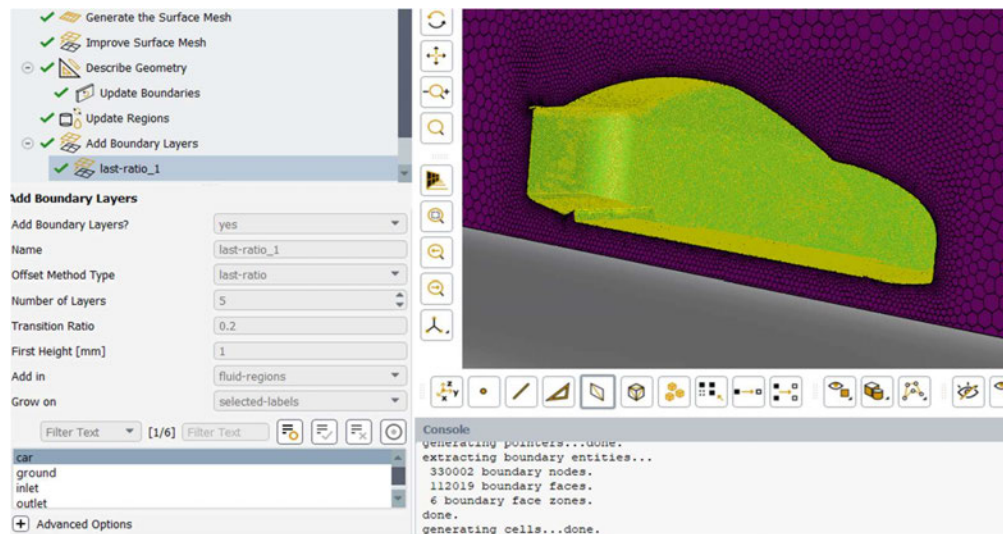


Figure 6-14 - Boundary layer mesh setting

6.2.6. Volume meshing

Volume meshing is generated as shown below. Poly-Hexcore mesh type is used in volume meshing. As detailed in the earlier section, this is a combination of Hexahedral mesh elements, which are good with their accuracy and efficiency, and of polyhedral elements, which are well-suited for complex geometries and offer greater efficiency.

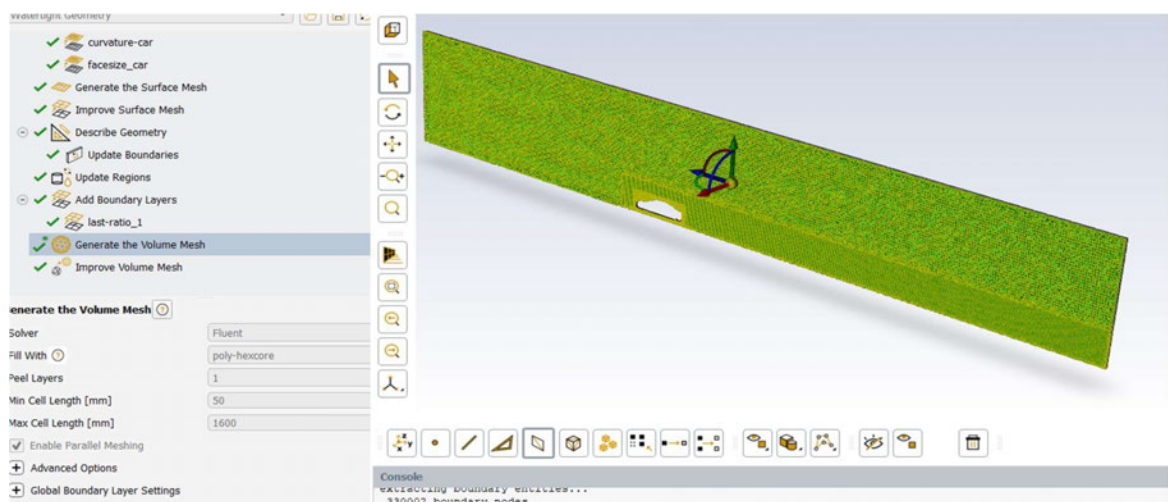


Figure 6-15 - Volume mesh generation

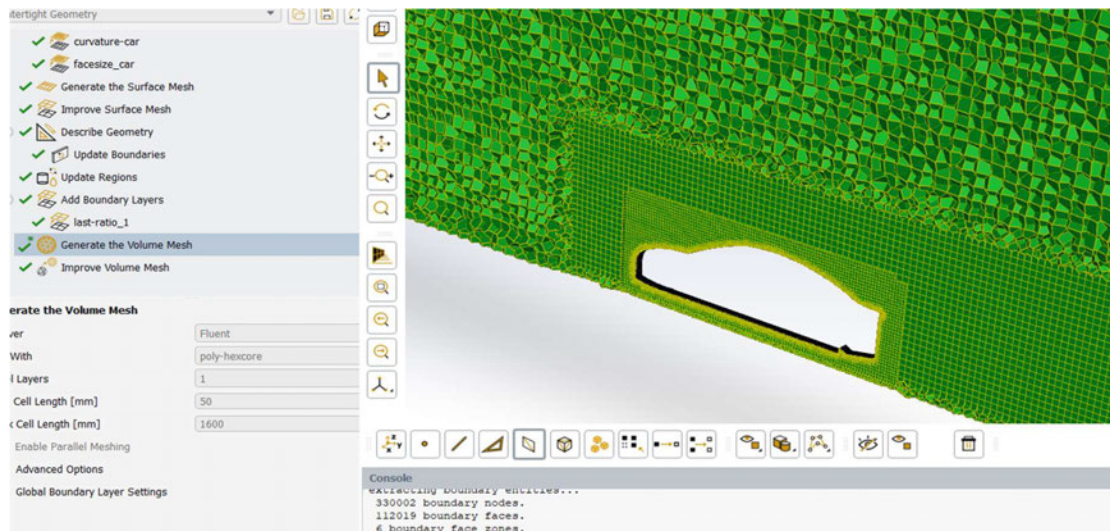


Figure 6-16 - Volume mesh generation fine details

The meshing process performed this step is common for all CFD_v03, CFD_v04 and CFD_v05. After generating the volume meshing, the mesh diagnostics summary was taken for all the cases in all the final simulation versions. Since the difference in the mesh elements details are reasonably small between the 3 cases, but different in each version, mesh summary for case 3 in each version is shown below.

6.2.7. Mesh diagnostics - CFD_v03

The difference in the number of mesh elements for all three cases are reasonably small and hence the mesh diagnostics for Case3 is shown here to represent all three cases here to minimise data repetition shown in the below mesh diagnostics is quite similar across all the three cases in version v03. Similarly, mesh diagnostics for versions v04 and v05 are also shown.

Diagnostics Scope : 1 Objects, 6 Face Zones, 1 Cell Zones	
Objects : (enclosure-enclosure1)	
Surface Diagnostics :	
Total Number of Faces	= 112019
Maximum Skewness	= 0.7093
Maximum Aspect Ratio	= 43.18
Number of Free Faces	= 0
Number of Multi Faces	= 0
Number of Self Intersections	= 0
Number of Self Proximity	= 0
Number of Point Contacts	= 0
Number of Invalid Normals	= 0
Volume Diagnostics :	
Total Number of Cells	= 927638
Minimum Orthogonal Quality	= 0.1
Maximum Aspect Ratio	= 134.54
Number of Stair-Step Locations	= 1
Number of Isolated Cells	= 0

Figure 6-17 - Mesh diagnostics_CFD_v03_Case 3

6.2.8. Mesh diagnostics - CFD_v04

```

Diagnostics Scope : 1 Objects, 6 Face Zones, 1 Cell Zones
Objects          : (enclosure-enclosure1)
-----
Surface Diagnostics :

Total Number of Faces      = 162408
Maximum Skewness          = 0.8831
Maximum Aspect Ratio       = 68.64
Number of Free Faces       = 0
Number of Multi Faces      = 0
Number of Self Intersections = 0
Number of Self Proximity   = 0
Number of Point Contacts   = 0
Number of Invalid Normals  = 0
-----
Volume Diagnostics :

Total Number of Cells      = 1280851
Minimum Orthogonal Quality = 0.1003
Maximum Aspect Ratio       = 78.21
Number of Stair-Step Locations = 1
Number of Isolated Cells   = 0
-----

```

Figure 6-18-Mesh diagnostics_CFD_v04_Case 3

6.2.9. Mesh diagnostics - CFD_v05

```

Diagnostics Scope : 1 Objects, 6 Face Zones, 1 Cell Zones
Objects          : (enclosure-enclosure1)
-----
Surface Diagnostics :

Total Number of Faces      = 242855
Maximum Skewness          = 0.7782
Maximum Aspect Ratio       = 37.88
Number of Free Faces       = 0
Number of Multi Faces      = 0
Number of Self Intersections = 0
Number of Self Proximity   = 0
Number of Point Contacts   = 0
Number of Invalid Normals  = 0
-----
Volume Diagnostics :

Total Number of Cells      = 1428515
Minimum Orthogonal Quality = 0.118
Maximum Aspect Ratio       = 60.14
Number of Stair-Step Locations = 2
Number of Isolated Cells   = 0
-----

```

Figure 6-19-Mesh diagnostics_CFD_v05_Case 3

From the above mesh diagnostics data, the total number of cells can be seen for each version.

- CFD_v03 – 927,638 cells (course mesh)
- CFD_v04 – 1,280,851 cells (medium mesh)
- CFD_v05 – 1,428,515 cells (fine mesh)

6.3. Solver set up for Final simulation.

In solver set up for versions 03 to 05 the main differences compared to that detailed in Initial simulation are detailed here.

6.3.1. Viscous model selection

k- ω GEKO method is selected as viscous model.

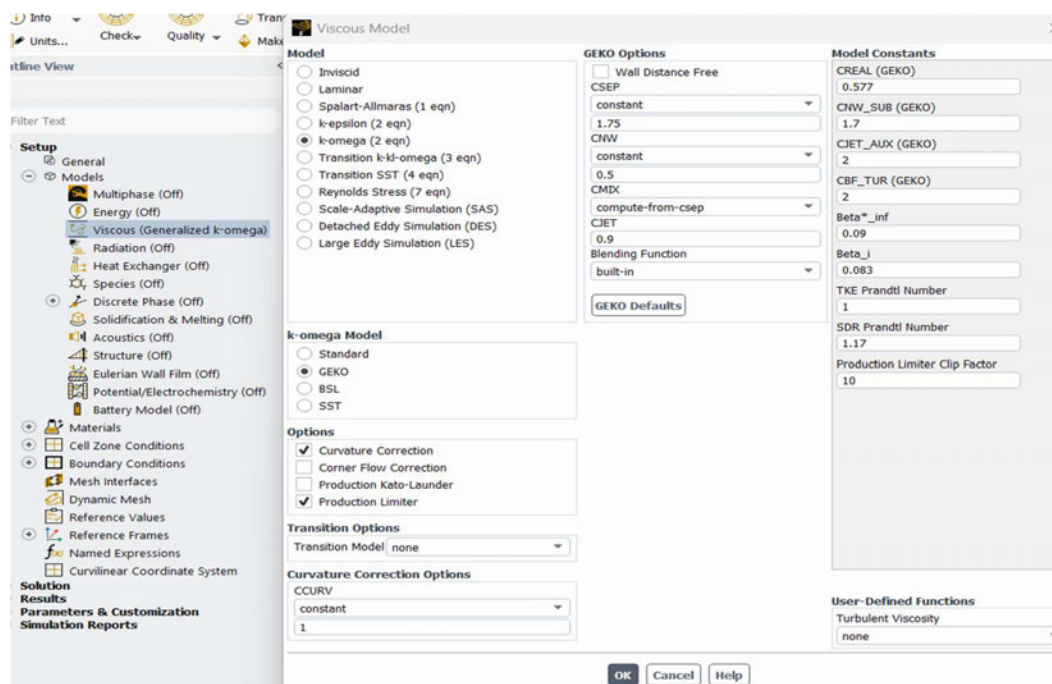


Figure 6-20-Viscous model

6.3.2. Boundary condition - Inlet

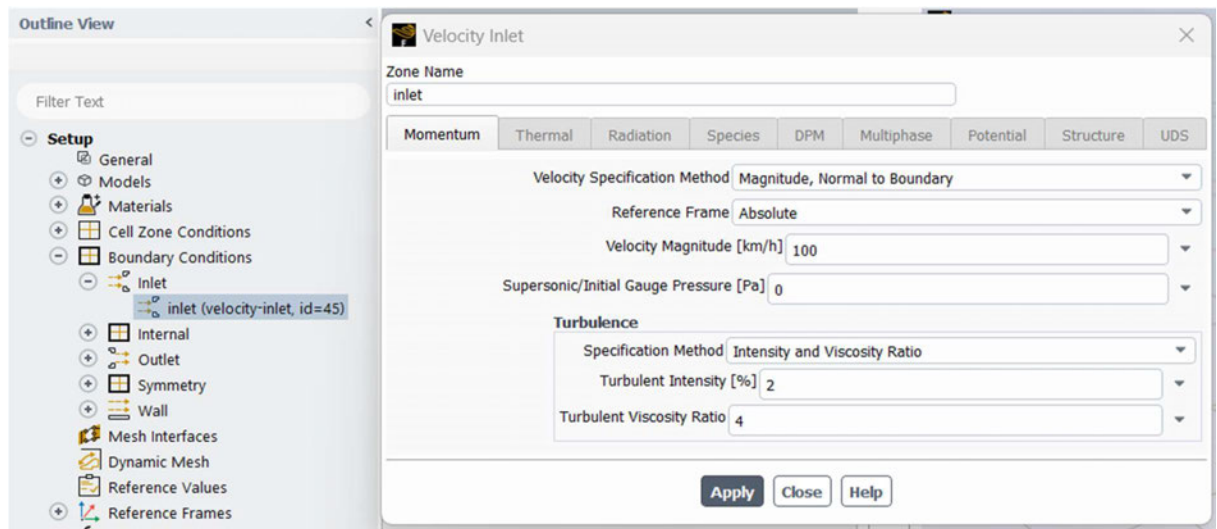


Figure 6-21-Inlet boundary parameters

6.3.3. Boundary condition - Outlet

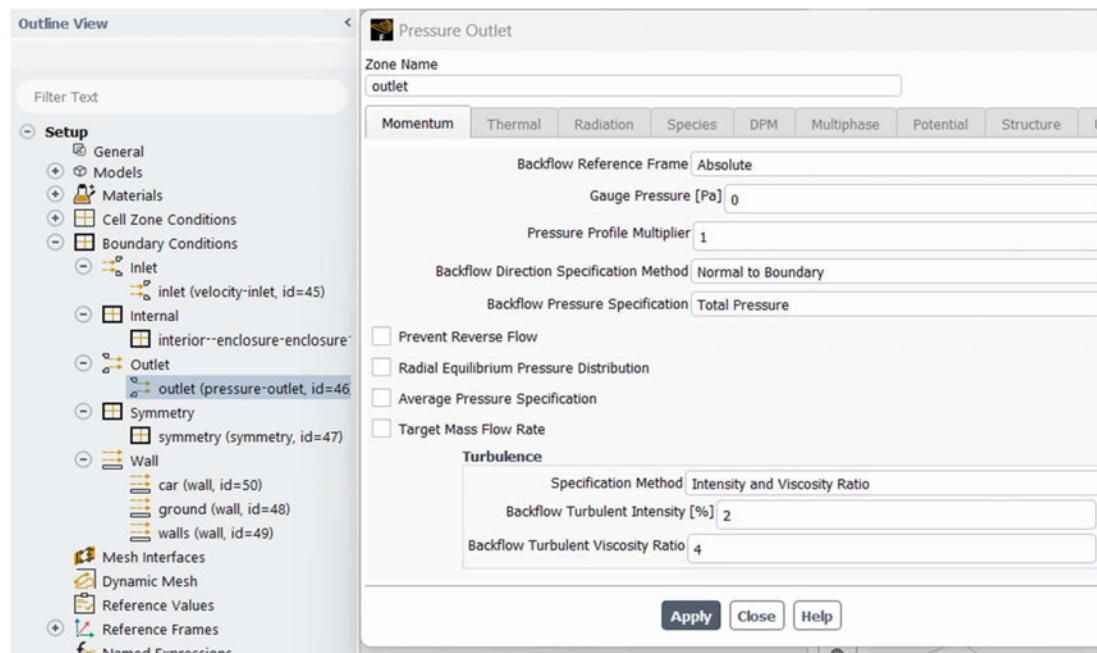


Figure 6-22-Outlet boundary conditions for Final simulations

6.3.4. Boundary condition - Walls

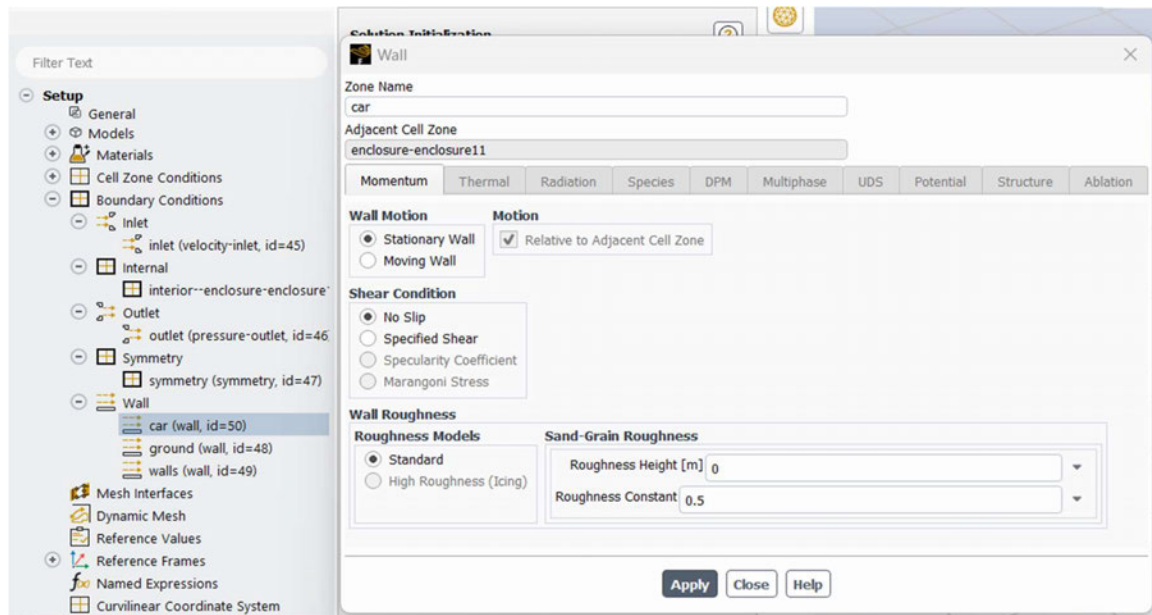


Figure 6-23 - Boundary condition - Car

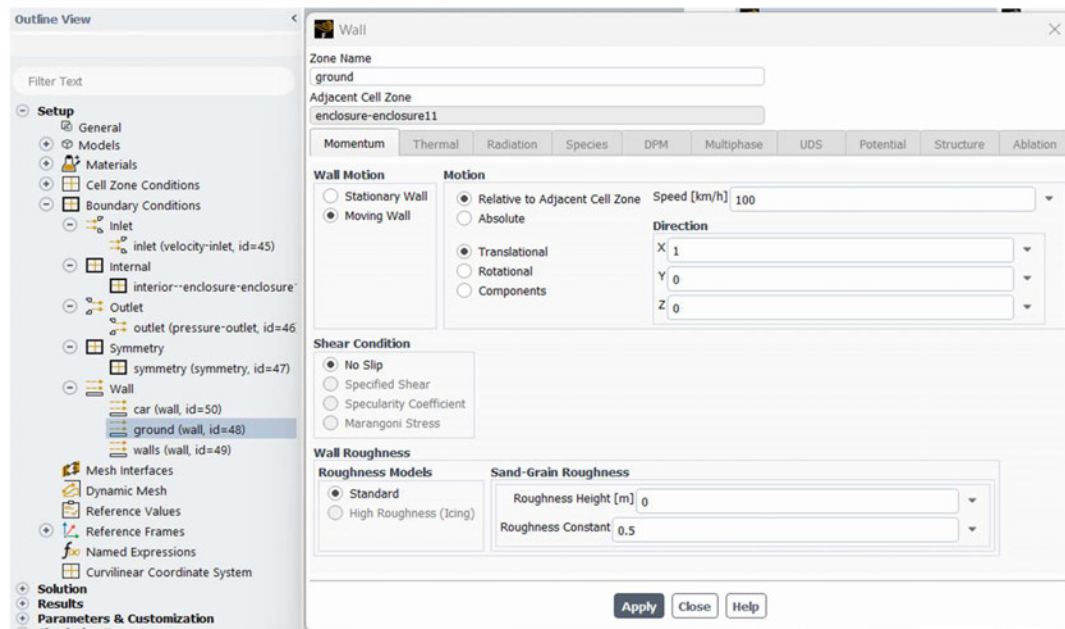


Figure 6-24-Boundary condition – Ground

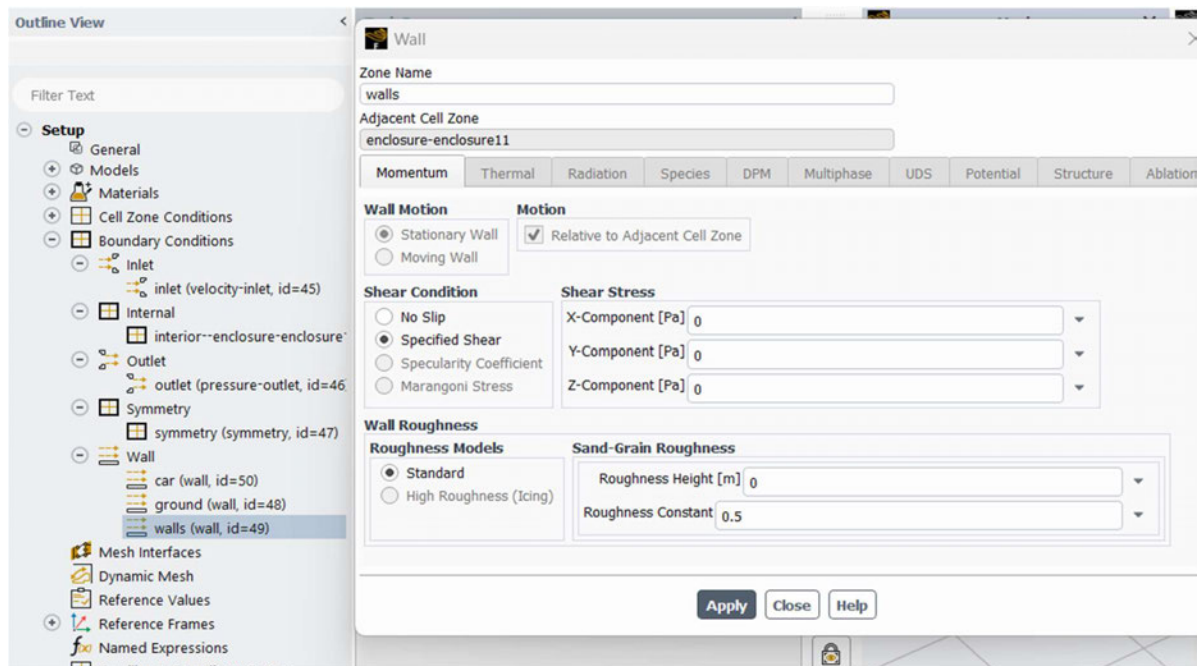


Figure 6-25-Boundary condition - Top and side walls

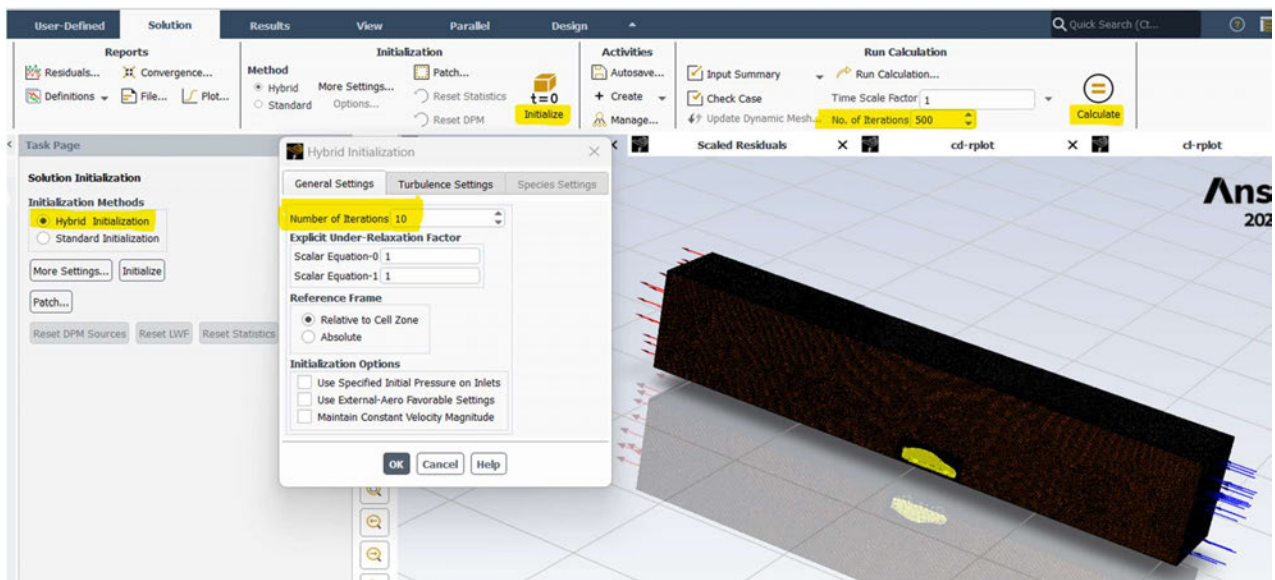


Figure 6-26 - Initialization and calculation run

7. Results

This section is showing the simulation results from version 03 to version 05. The analysis on these results is discussed in the next section, Section 8 – Analysis on Results. It has to be noted that the residual plots for all the simulations showed a common behaviour, which is that they demonstrated oscillating patterns past 150 to 200 iterations and did not converge, though 1000 iterations were run. Due to the steady oscillating pattern the number of iterations for some of the analysis was reduced 500 or less instead of 1000. Being a steady oscillating pattern, I can be confirmed that reducing the number of iterations would not affect convergence.

7.1. Residuals_CFD_v03

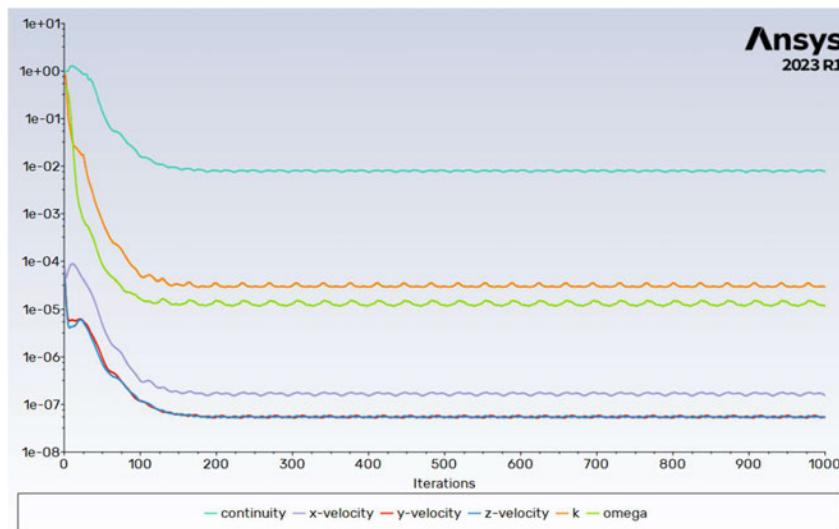


Figure 7-1 - Residuals-Case 1_CFD_v03

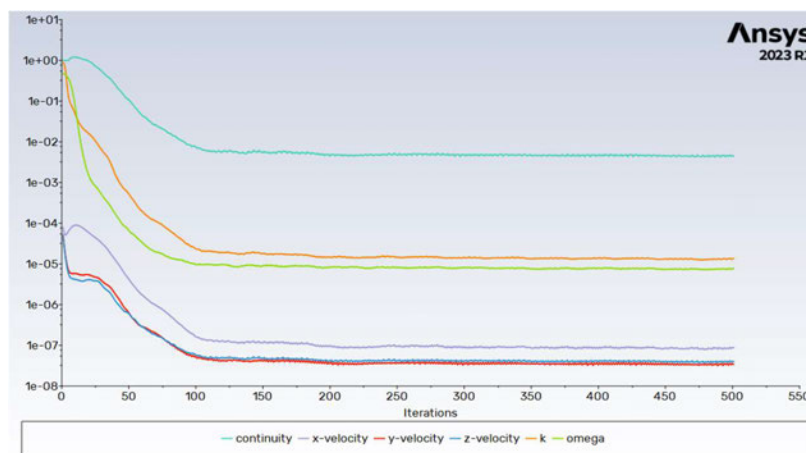


Figure 7-2-Residuals-Case 2_CFD_v03

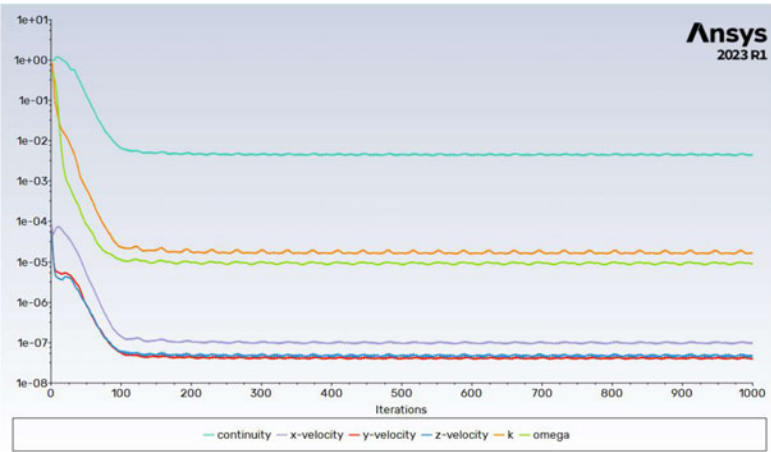


Figure 7-3-Residuals-Case 3_CFD_v03

7.2. Residuals_CFD_v04

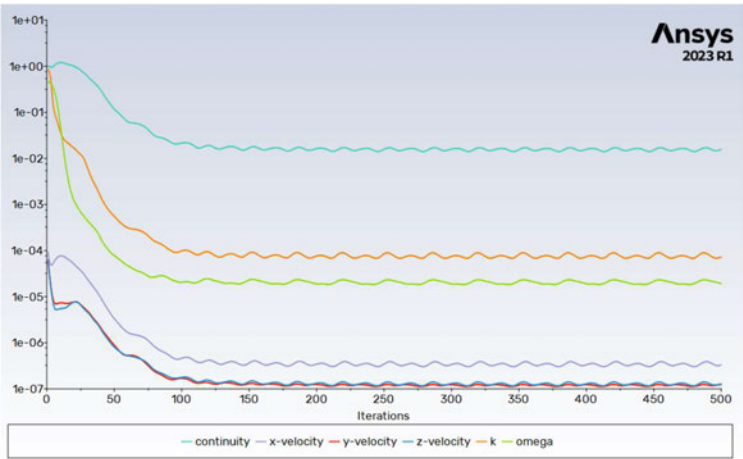


Figure 7-4-Residuals-Case1_CFD_v04

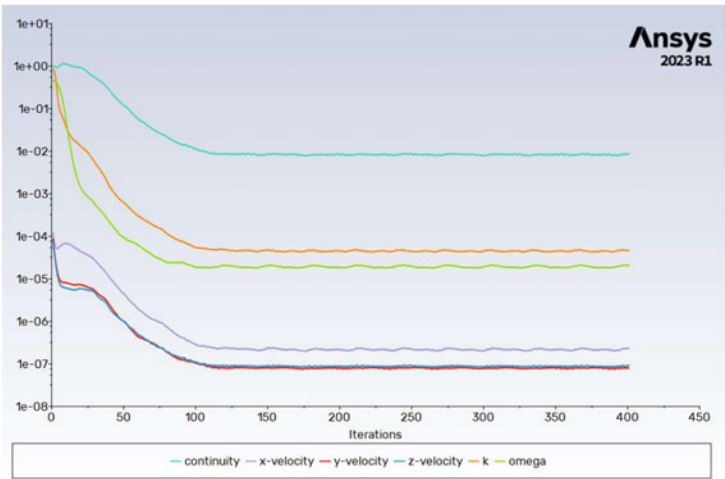


Figure 7-5-Residuals-Case2_CFD_v04

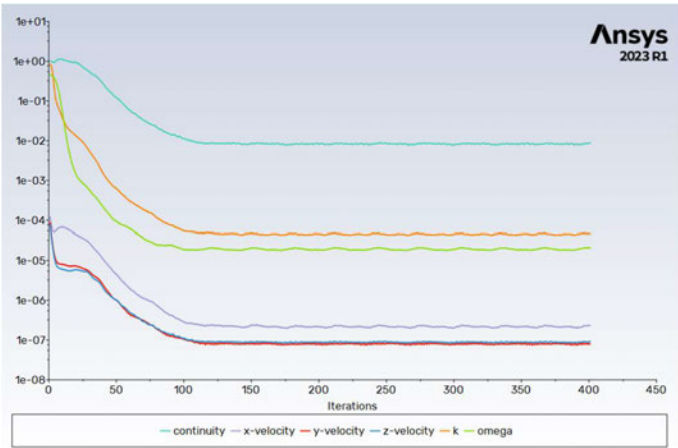


Figure 7-6-Residuals-Case3_CFD_v04

7.3. Residuals_CFD_v05

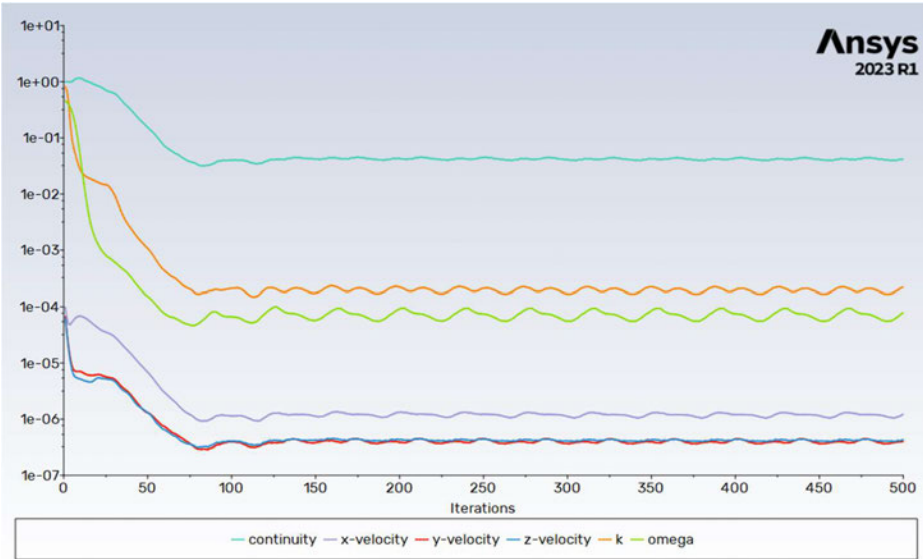


Figure 7-7-Residuals-Case3_CFD_v04

7.5. Pressure contours

In this section 3D visualisation of the pressure distribution around the car in each case is shown for a comprehensive understanding of the air pressure behaviour.

7.5.1. Pressure contours – Case1-v03

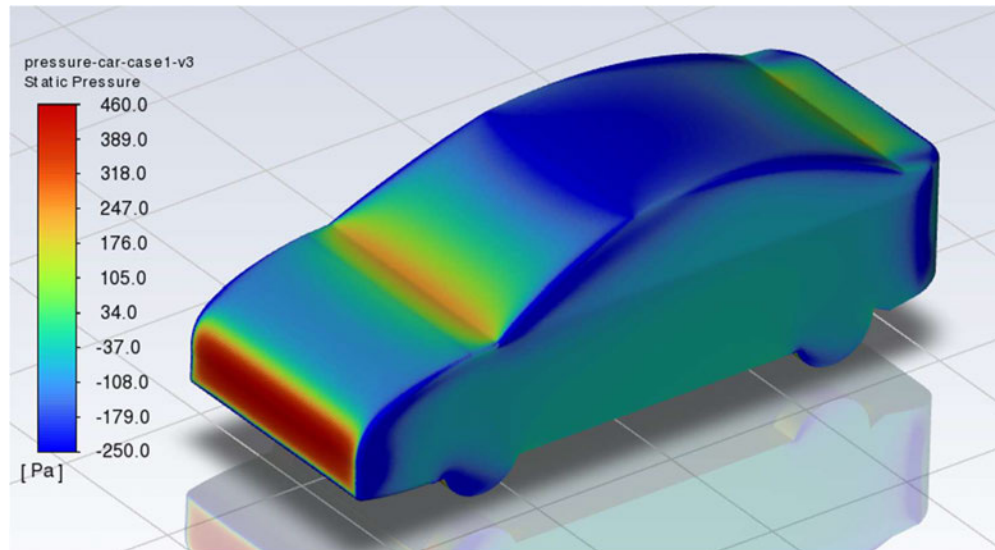


Figure 7-8 - Pressure contours – Case1-v03

7.5.2. Pressure contours – Case2-v03

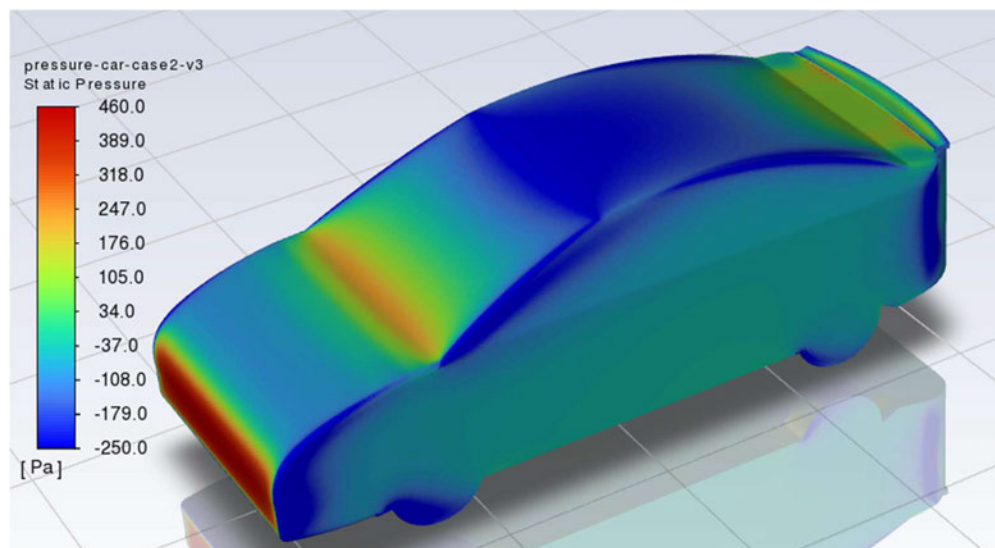


Figure 7-9-Pressure contours – Case 2-v03

7.5.3. Pressure contours – Case3-v03

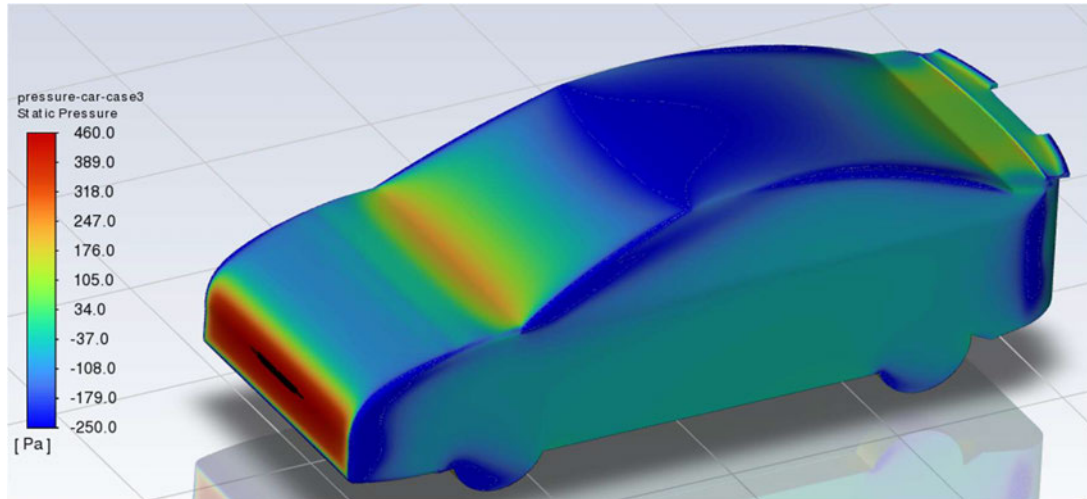


Figure 7-10-Pressure contours – Case 3-v03

7.5.4. Pressure contours – Case1-v04

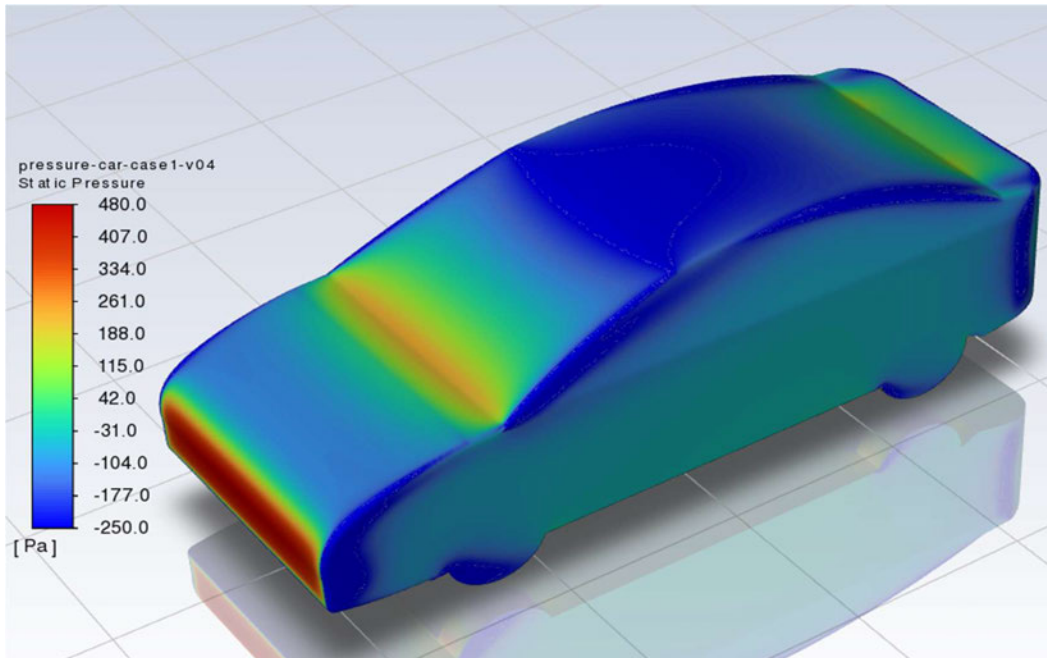


Figure 7-11-Pressure contours – Case 1-v04

7.5.5. Pressure contours – Case2-v04

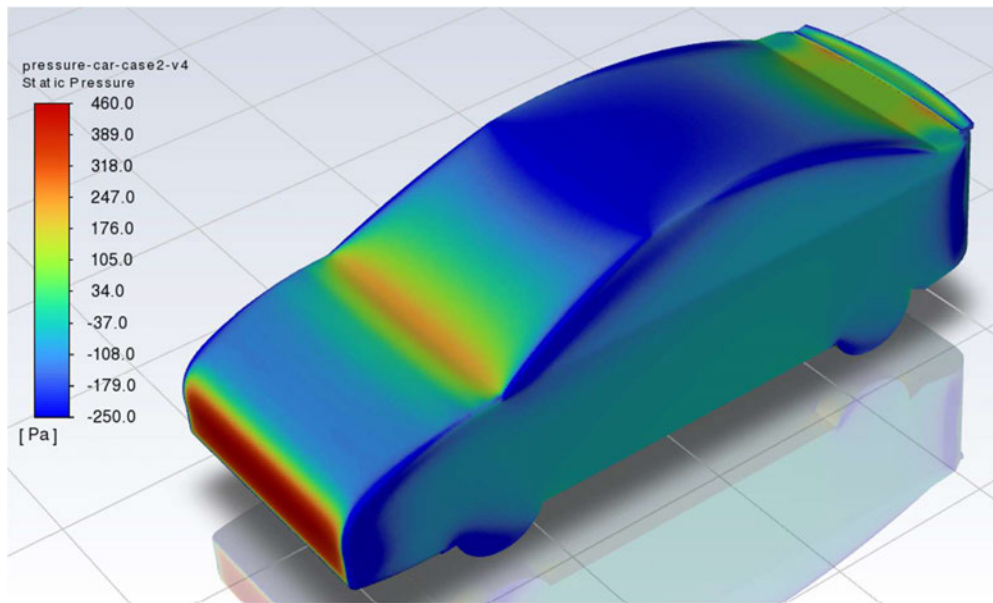


Figure 7-12-Pressure contours – Case 2-v04

7.5.6. Pressure contours – Case3-v04

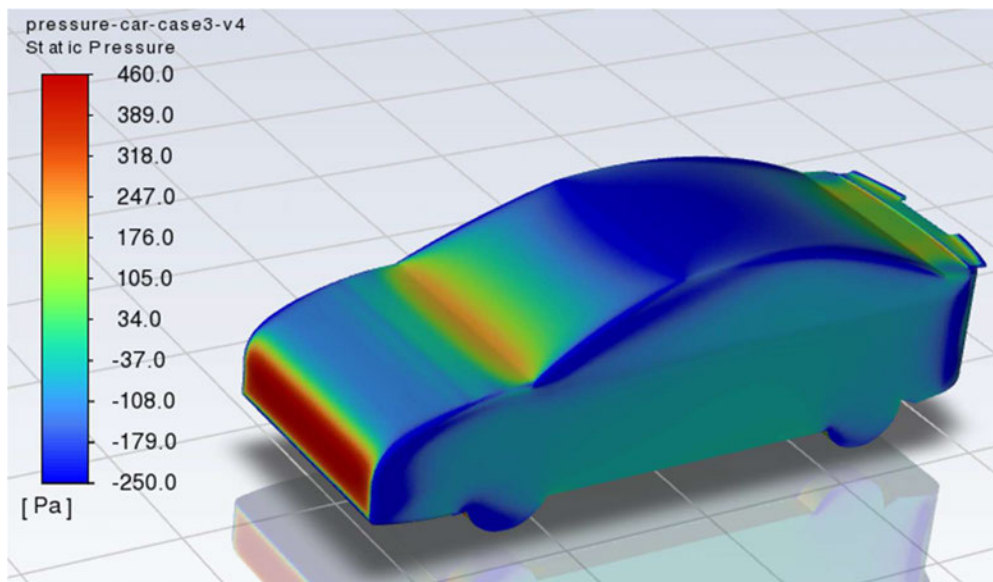


Figure 7-13-Pressure contours – Case3-v04

7.5.7. Pressure contours – Case3-v05

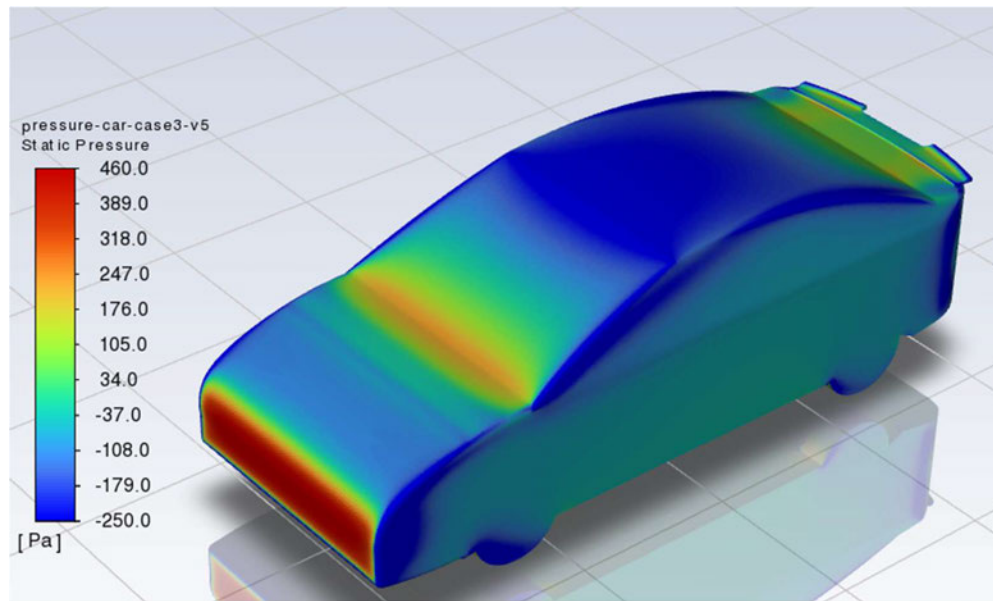


Figure 7-14-Pressure contours – Case3-v05

7.6. Velocity contours

In this section 3D visualisation of the velocity flow around the car in each case is shown for a comprehensive understanding of the velocity behaviour, when the air is flowing at a speed 100km/hr.

7.6.1. Velocity contours – Case1-v03

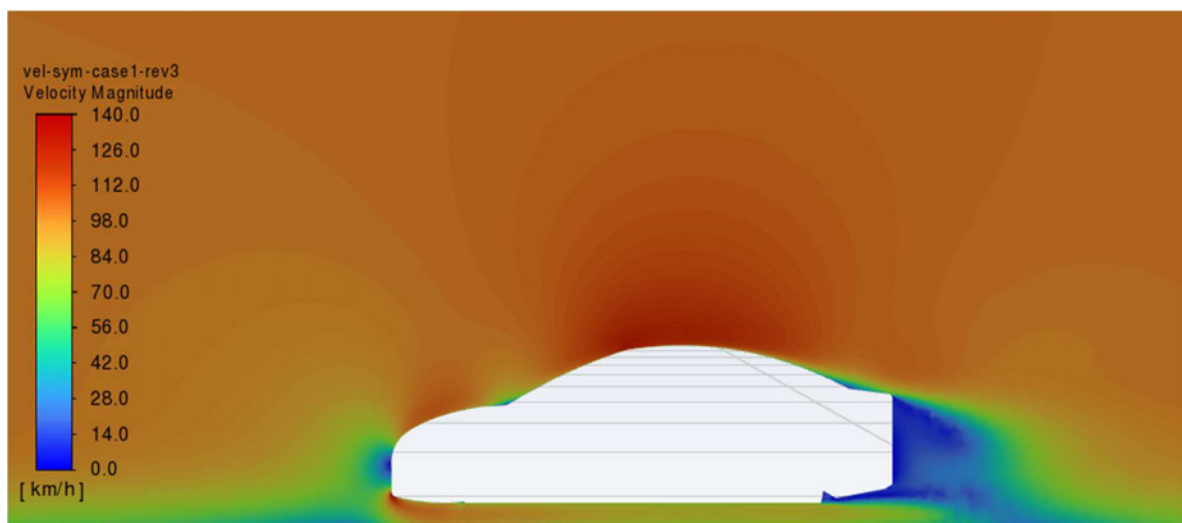


Figure 7-15-Velocity contour at midplane – Case1-v03

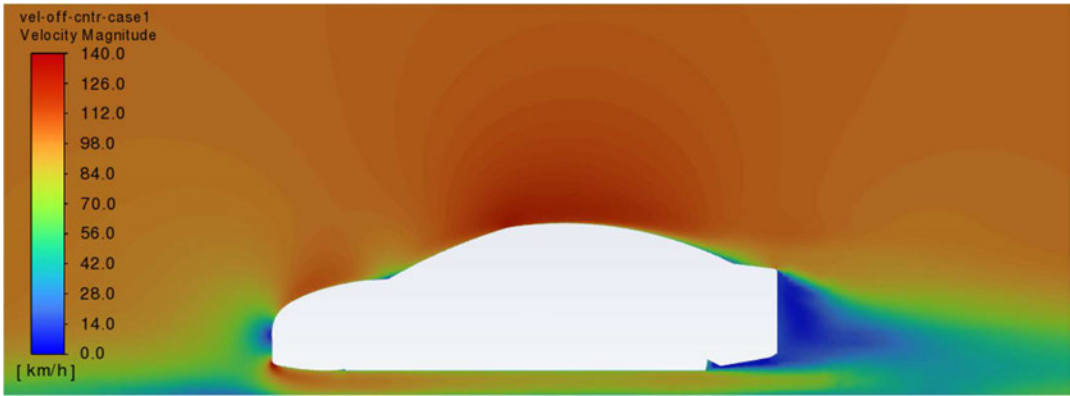


Figure 7-16-Velocity contour off centre – Case1-v03

7.6.2. Velocity contours – Case2-v03

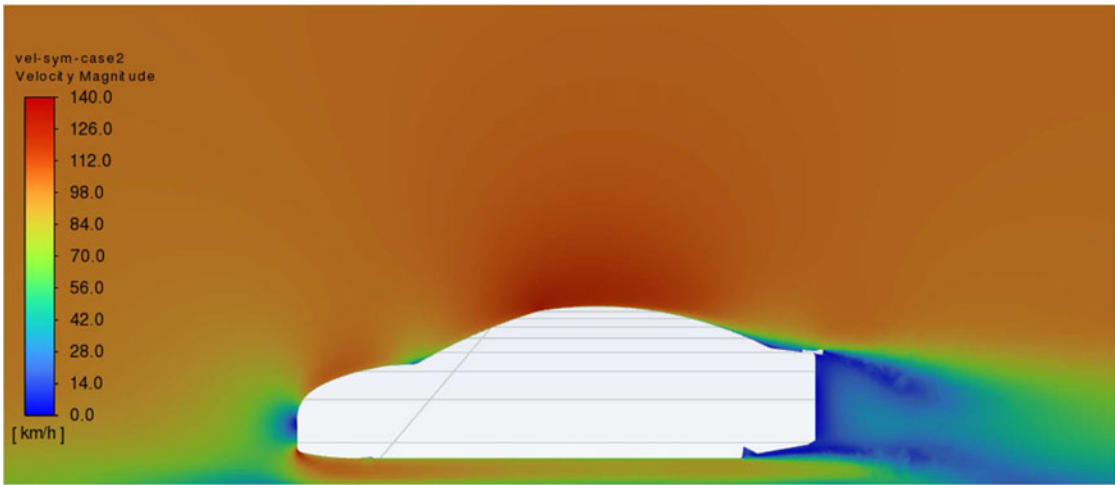


Figure 7-17-Velocity contours at midplane– Case2-v03

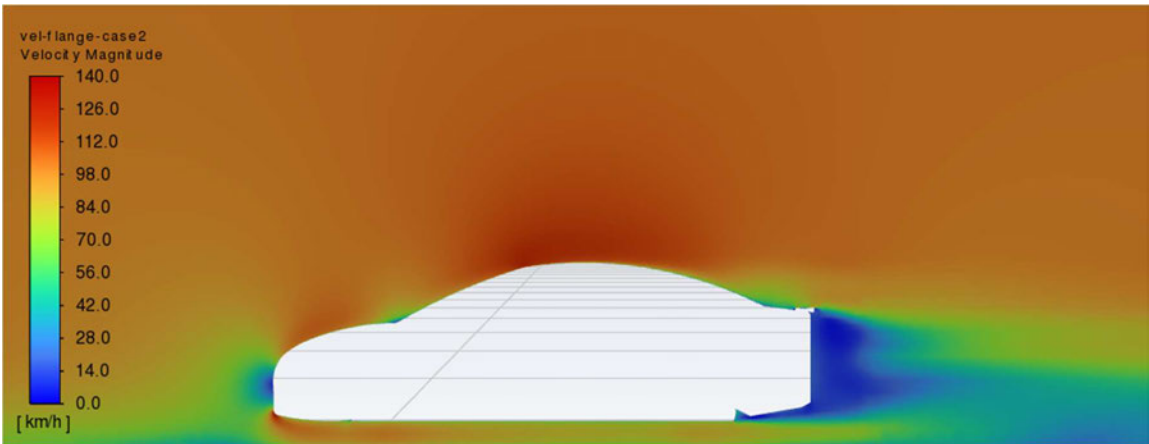


Figure 7-18-Velocity contours at off centre– Case2-v03

7.6.3. Velocity contours – Case3-v03

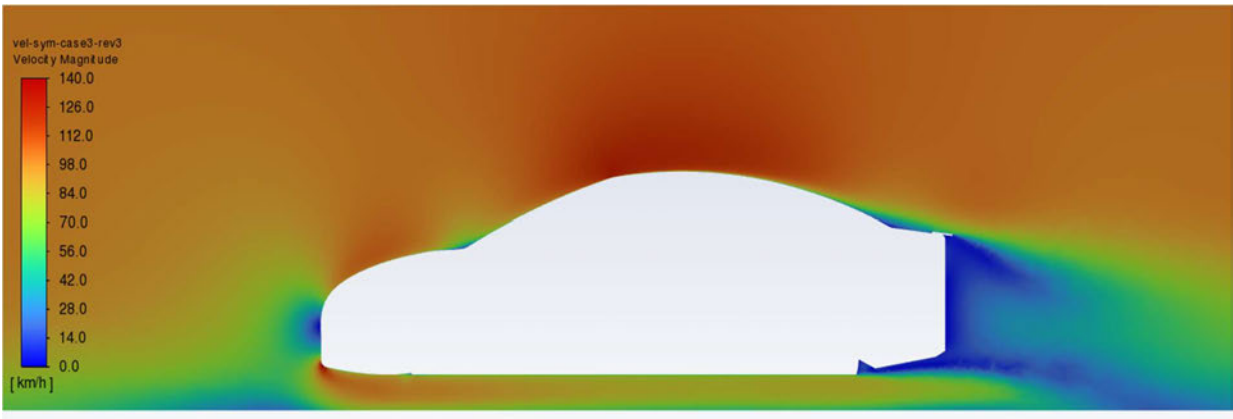


Figure 7-19-Velocity contours midplane– Case3-v03

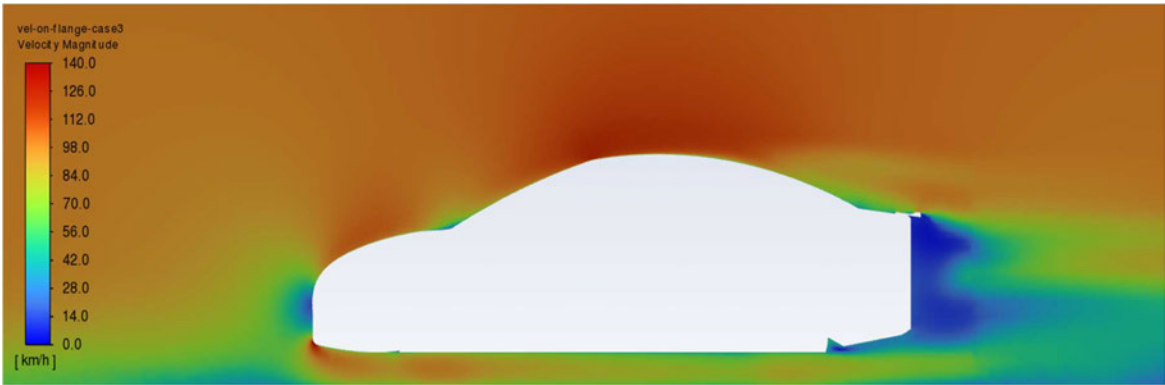


Figure 7-20-Velocity contours on flange– Case3-v03

7.6.4. Velocity contours – Case2-v04

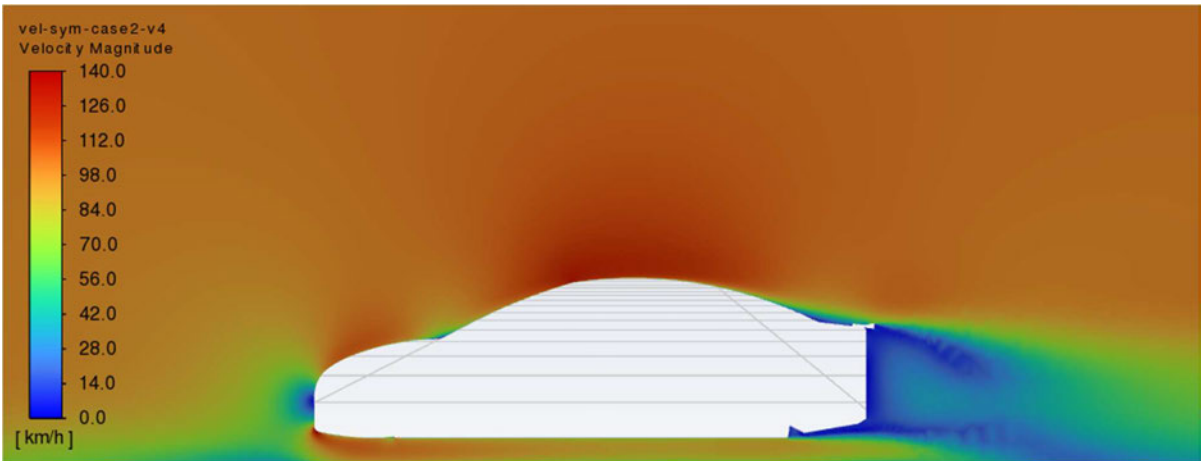


Figure 7-21-Velocity contours midplane – Case2-v04

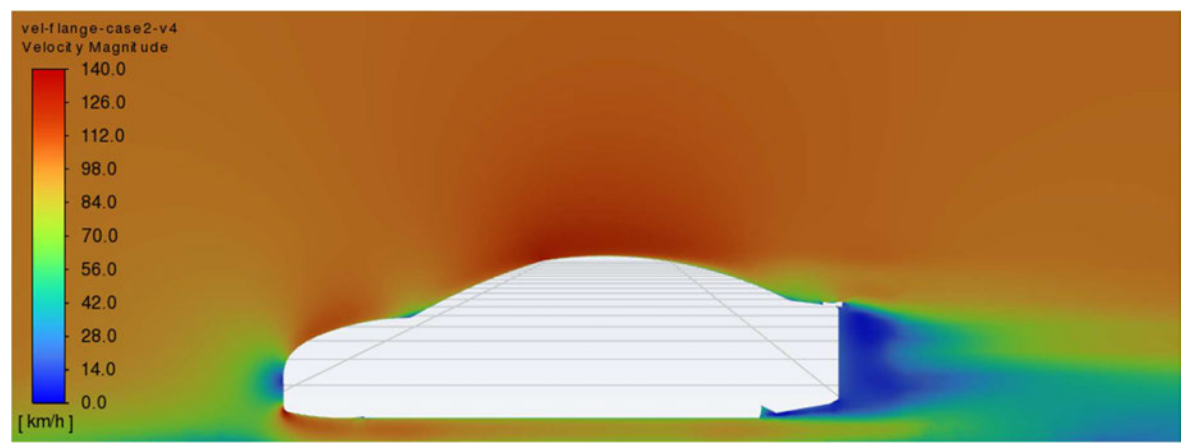


Figure 7-22-Velocity contours off centre – Case2-v04

7.6.5. Velocity contours – Case3-v04

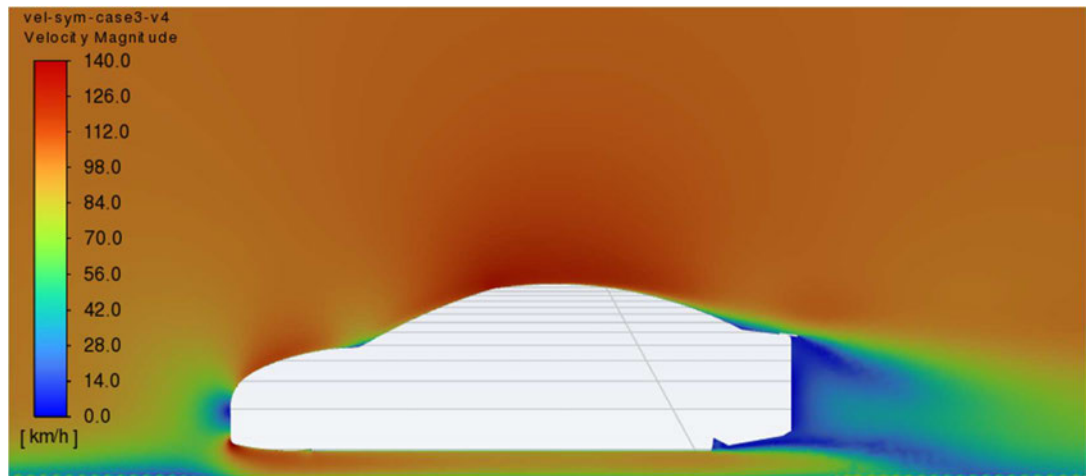


Figure 7-23-Velocity contours midplane – Case3-v04

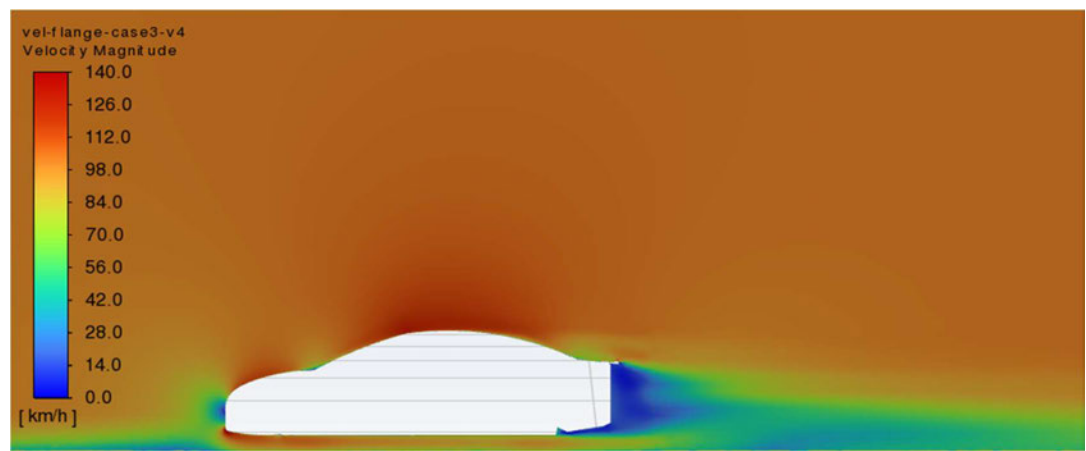


Figure 7-24-Velocity contours off centre– Case3-v04

7.6.6. Velocity contours – Case3-v05

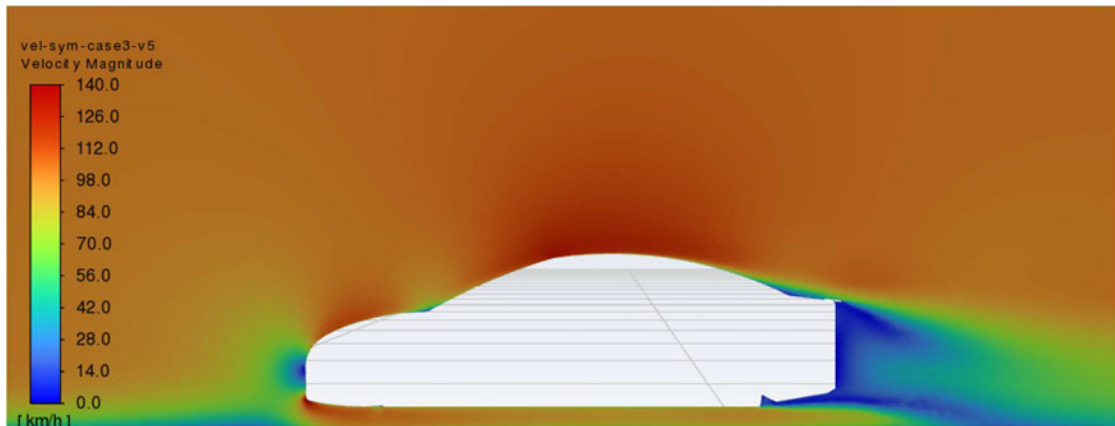


Figure 7-25-Velocity contours midplane – Case3-v05

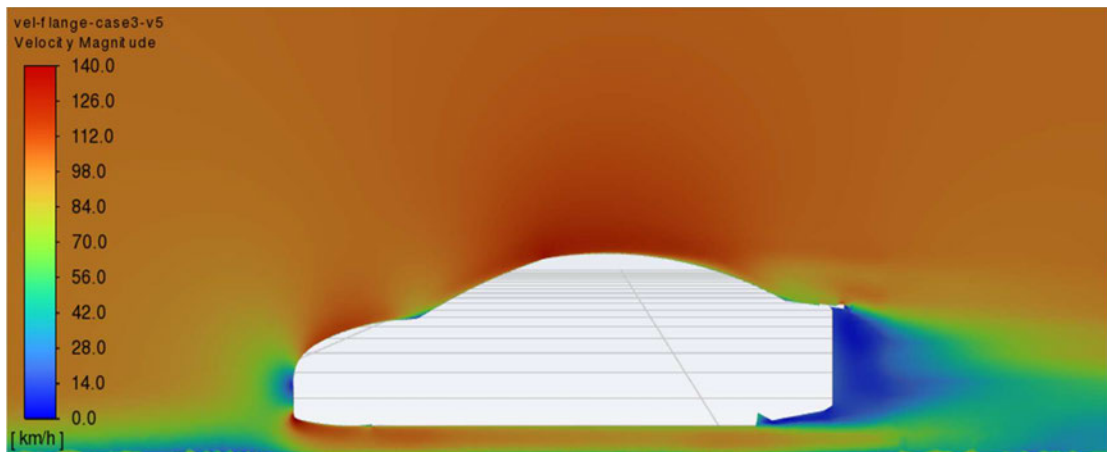


Figure 7-26-Velocity contours off centre – Case3-v05

7.7. y^+ (y plus) analysis

y^+ is a dimensionless parameter which represents the wall distance from the first grid cell to the surface wall. For a standard wall function, the y^+ values should be between 30 and 300 (Ansys.com, 2017). Below given y^+ values shows that all the cases are under 94 and hence this can be deemed as within the acceptable range.

7.7.1. Y-plus_case1-v03

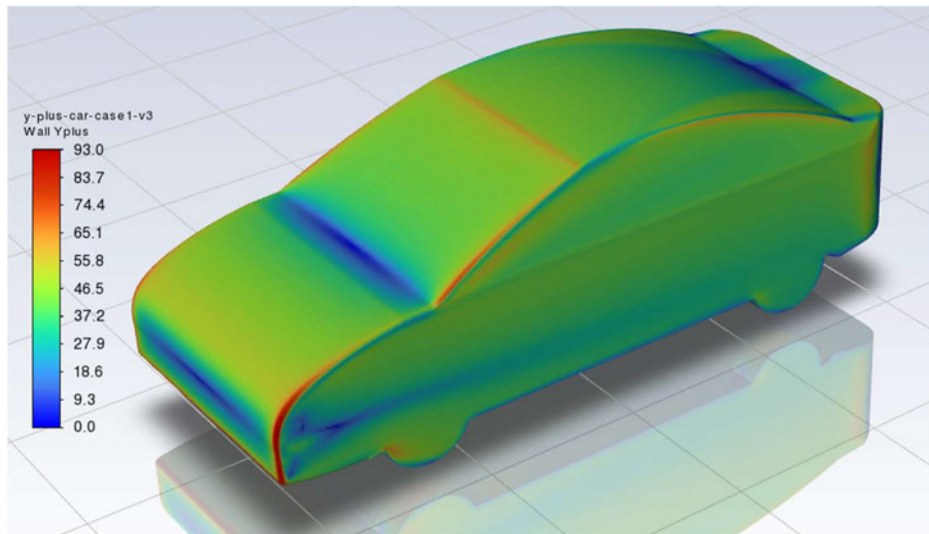


Figure 7-28--Y-plus_case1-v03

7.7.2. Y-plus_case2-v03

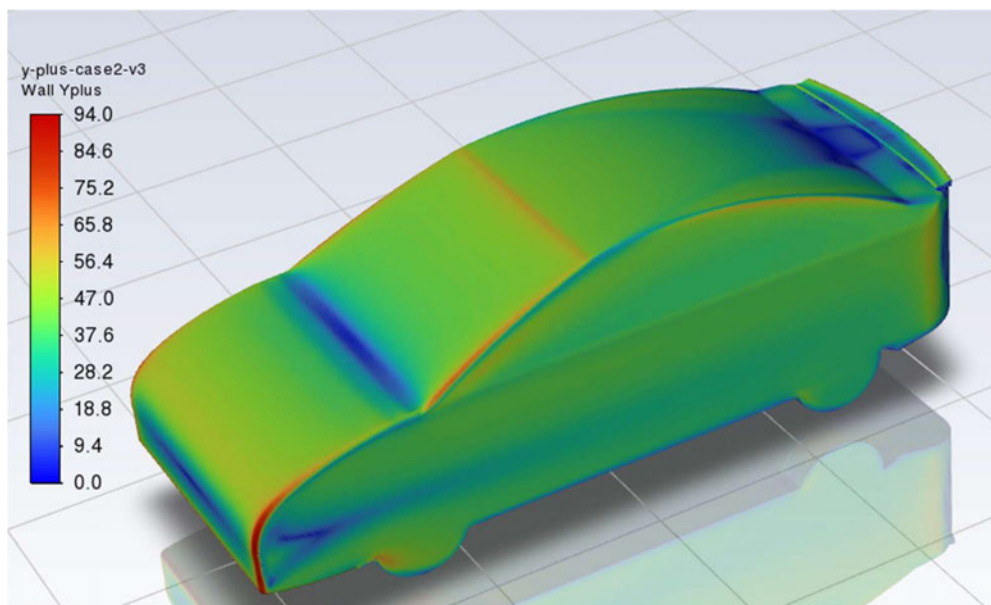


Figure 7-29-Y-plus_case2-v03

7.7.3. Y-plus_case3-v03

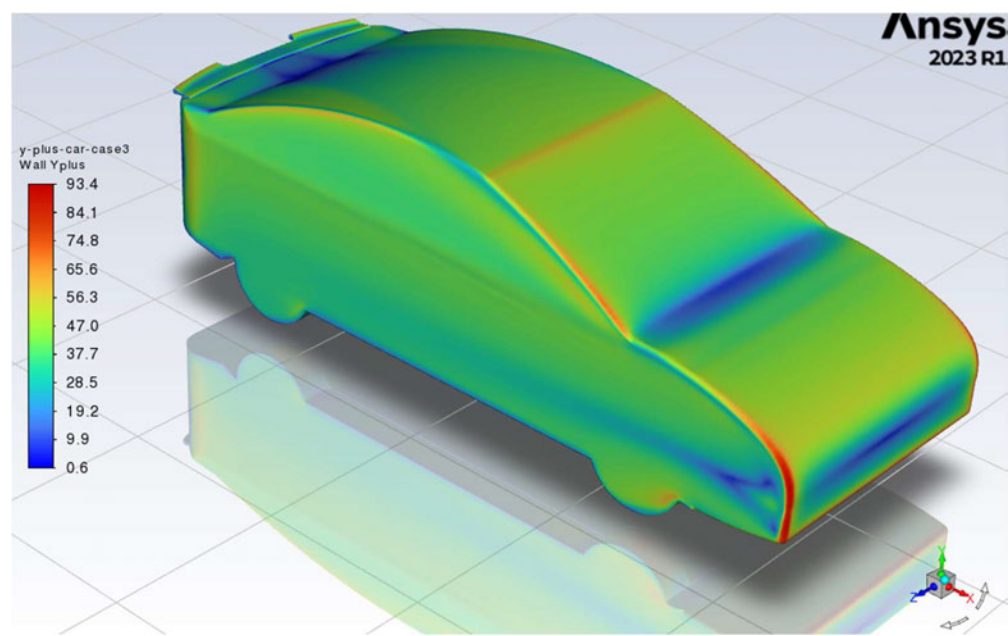


Figure 7-30-Y-plus_case3-v03

7.7.4. Y-plus_case1-v04

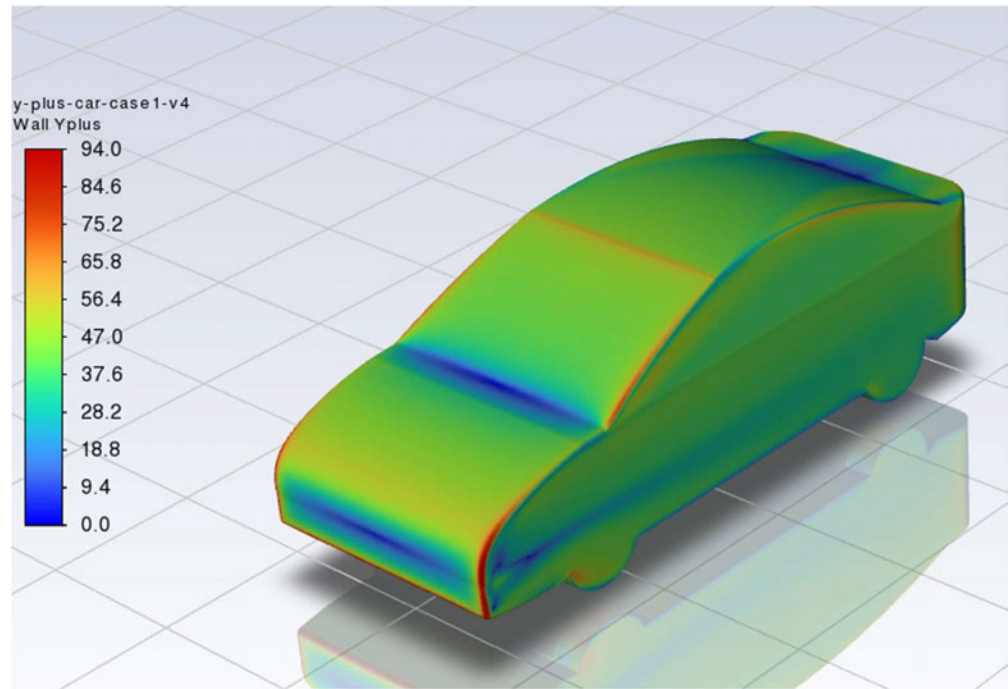
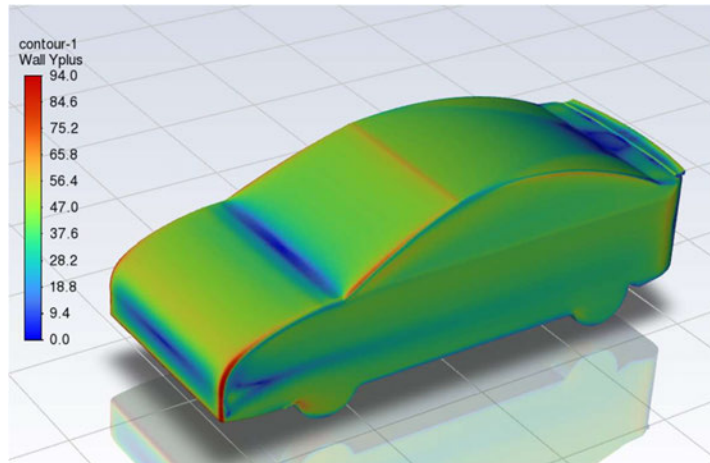
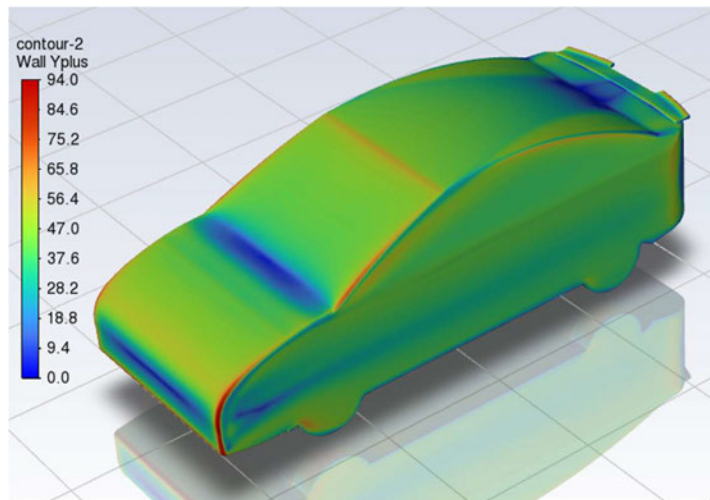


Figure 7-31-Y-plus_case1-v04

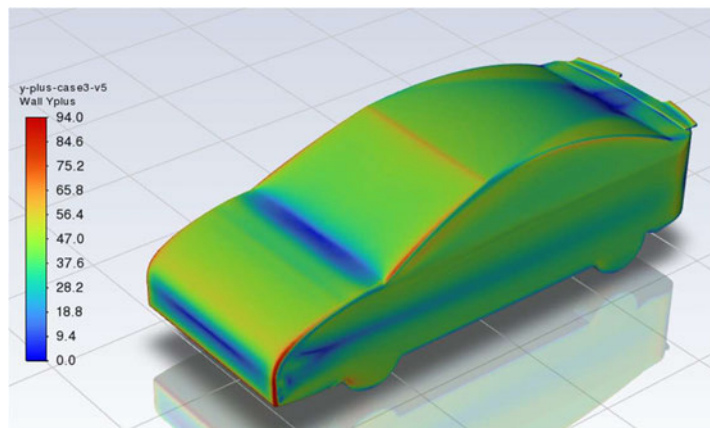
7.7.5. Y-plus_case2-v04

*Figure 7-32-Y-plus_case2-v04*

7.7.6. Y-plus_case3-v04

*Figure 7-33-Y-plus_case3-v04*

7.7.7. Y-plus_case3-v05

*Figure 7-34-Y-plus_case3-v05*

8. Analysis on Results

8.1. Residual plots analysis

From the plots generated, it is noted that the residual plots from all the final simulations showed a common behaviour, that they demonstrated steady oscillating patterns past 150 to 200 iterations and did not converge at 1000 iterations. Such steady oscillating behaviour is due to the vortex shedding caused due to the interaction of the car and the air (Ansys.com, 2023). Some of the cd and cl plots are shown below which confirms the above statement.

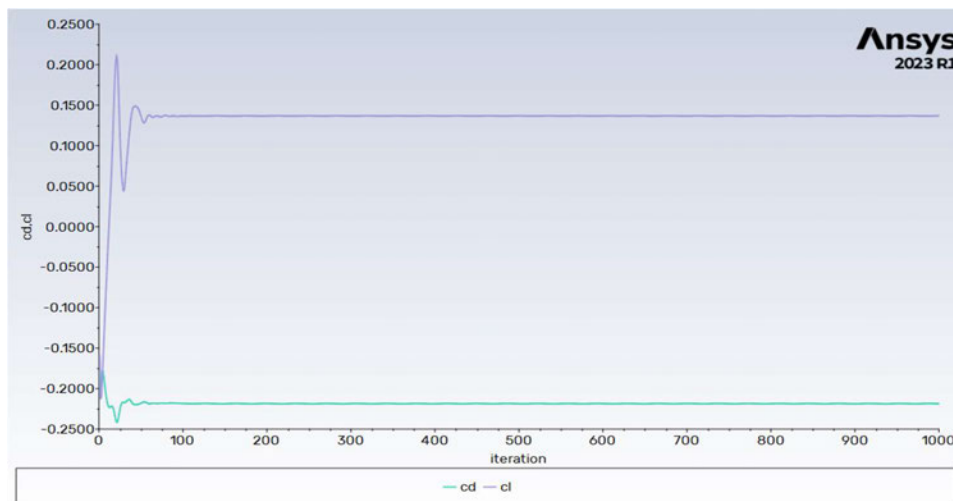


Figure 8-1-cd and cl plot-Case3_CFD-v03

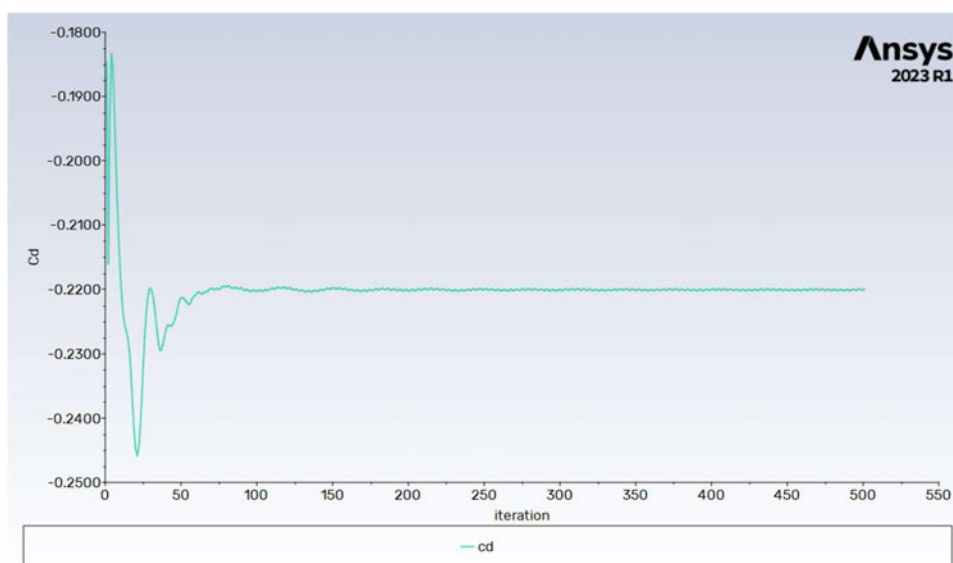


Figure 8-2-Figure 8 2-cd plot- Case2_CFD-v03

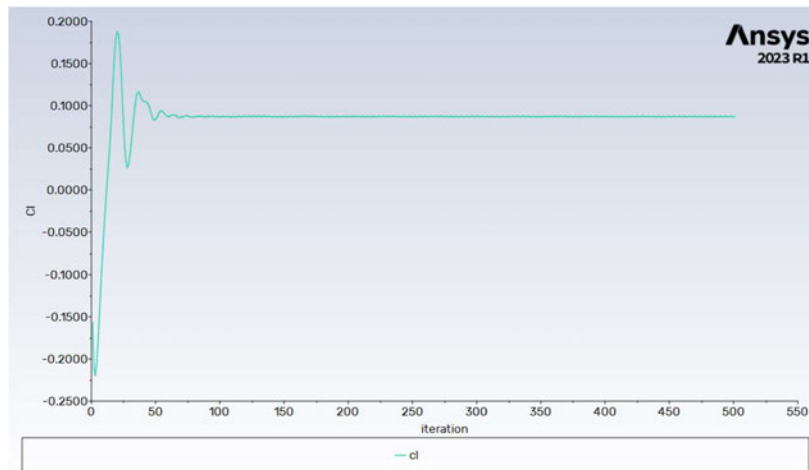


Figure 8-3-Figure 8 2-cl plot- Case2_CFD-v03

8.2. Pressure contour analysis

In terms of pressure contour, the region of static pressure is high at the frontal region in all cases and that is very much expected. This is obviously due to air flow is interrupted by the frontal face of the car and subsequent air build up in the region generates the high pressure.

The area of interest in this project is the rear deck region of the car where the air flow is influenced by the spoiler profile. For case 1 (both v03 and v04) without a rear spoiler, the pressure build-up behind the car is very less. From the image below it can be understood that only in the region in yellow shade has positive pressure values and the remaining part of the rear deck has negative pressure values. Pressure values are negative pressure at the rear end of the deck. These values confirm the lift force generated in those regions.

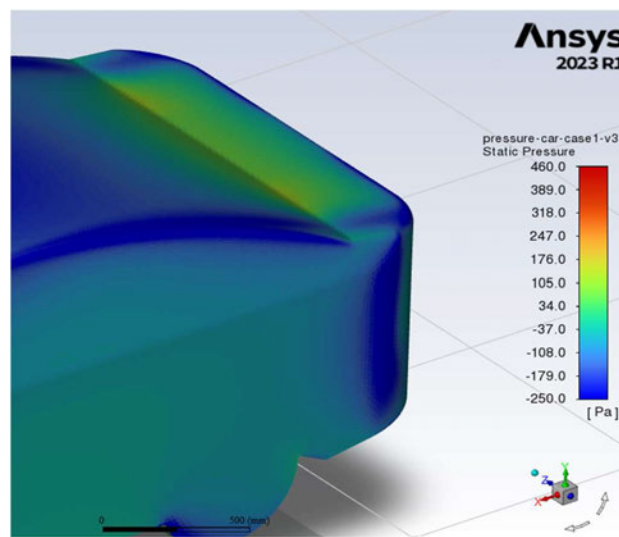


Figure 8-4 - Case 1- pressure contour at rear deck region

Reviewing case 2, looking at the image below, the pressure build-up is fairly spread over the rear deck and on the spoiler profile with increased pressure build up near the front edge of the spoiler. The pressure values in those region range between 175 to 300pa. The lift force values derived from the analysis confirms that higher pressure values in those region is the reason for reduced lift force generated compared to case 1 and case 3 in the final versions.

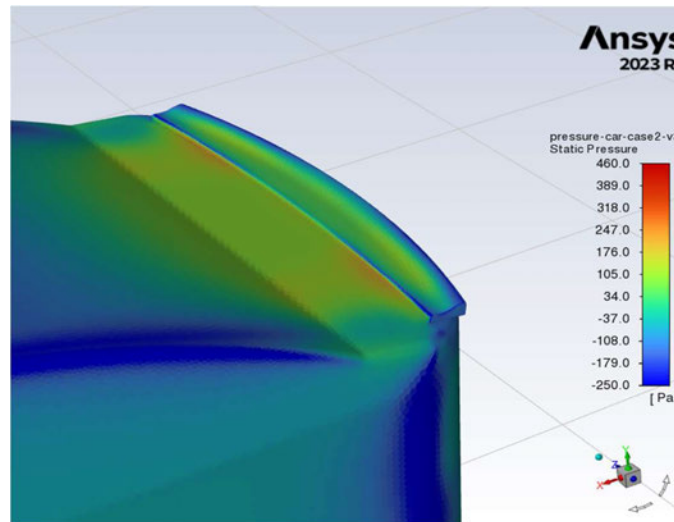


Figure 8-5-Case 2- pressure contour at rear deck region

Reviewing case 3, the image below, the pressure build-up is fairly spread over the rear deck like in case 2 however the pressure intensity is lesser. Due to this reason the lift force generated are larger than case 2 but quite lesser than case 1.

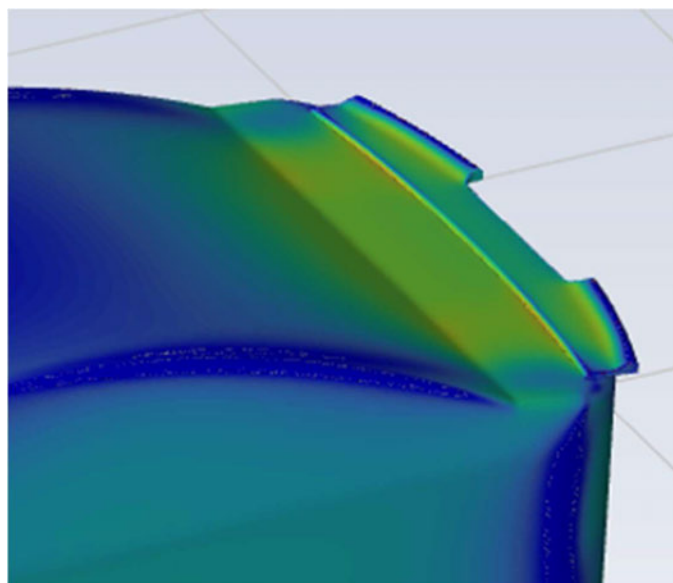


Figure 8-6-Case 3- pressure contour at rear deck region

8.3. Velocity contour analysis

Below given are two set of comparison images for velocity contours. The first set is the velocity contour passing through the midplane of the car. The second set of comparison is on a plane located midway between the midplane and a side face of the car. This is to capture the air flow behaviour on the flanges for case 3 as well as for case 2.

The velocity contour at the midplane indicates that for case 1 due to the flow separation at the rear end of the deck the vortex generated is resulting in low velocity region behind the car, in other words, higher pressure values are generated. In case of case 2 the spoiler has larger profile in the central region and hence this has delayed the flow separation. And for case 3 the central part of the spoiler has extended flange with flat profile. Indeed the flow separation was extended but to a lesser degree compared to case 2 which has a wedged profile.

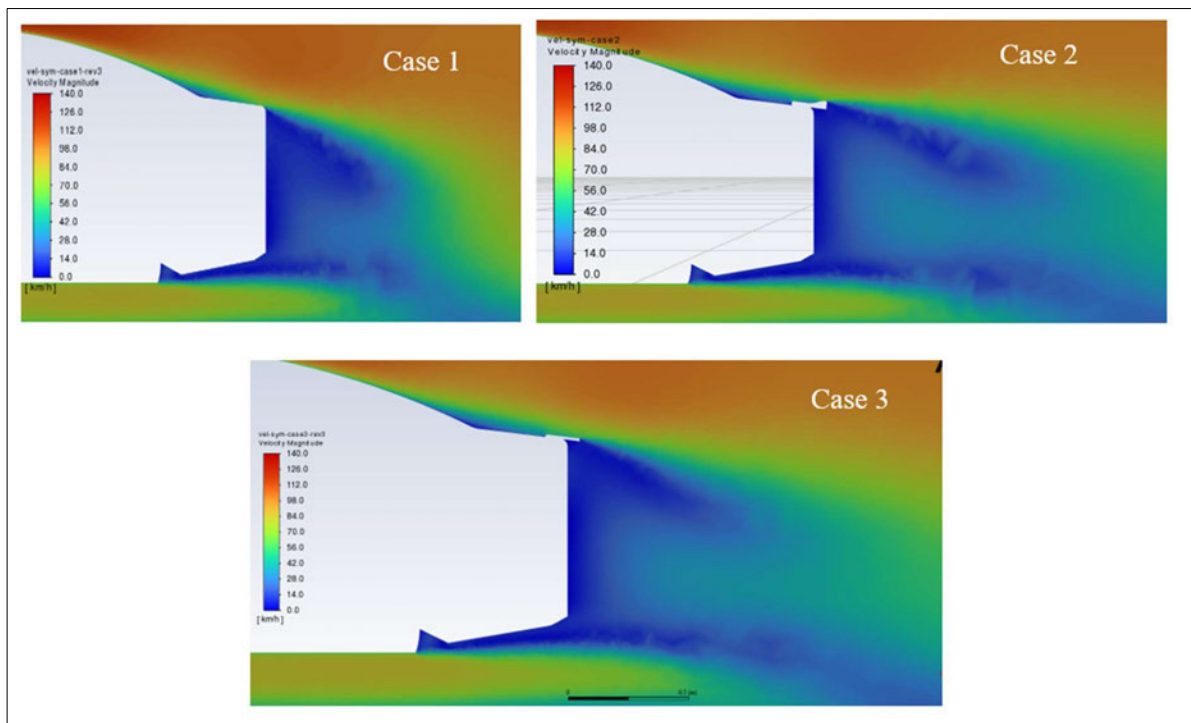


Figure 8-7-Velocity contour at midplane- case comparison

In the case of the velocity contour at the off-centre plane, case 1 has very similar behaviour as discussed above. For case 2 and case 3, since the behaviour is slightly opposite compare to the midplane behaviour. Since case 3 has extended flange on the side the air separation is delayed better than case 2. This seems to be not significant enough when looking at the values in terms of lift force generated. This however is suggesting that the idea of new profile can be made more effective with further design modification of the new spoiler profile

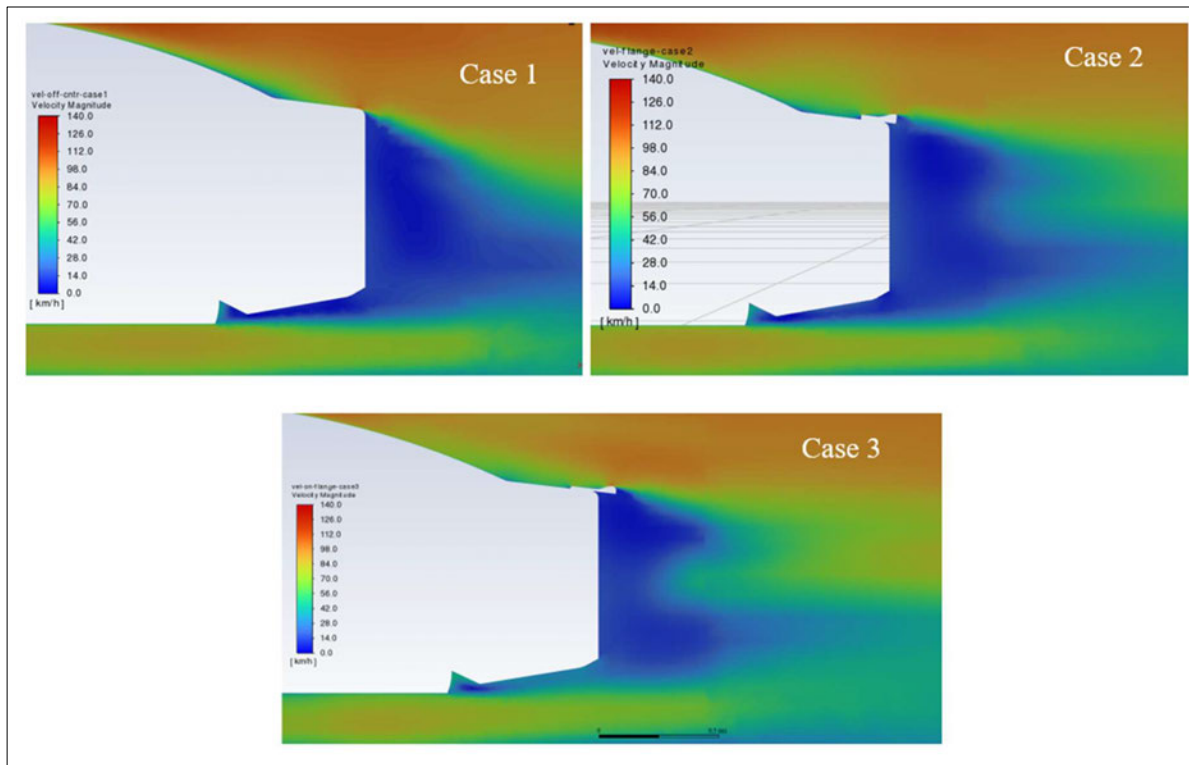


Figure 8-8-Velocity contour off centre- case comparison

8.4. Drag and lift force analysis

The plots of c_d and c_l are stabilised and oscillate around an average value. Based on the average values taken from the results the simulation can be concluded to have reached an acceptable convergence for steady state analysis.

The drag and lift values from the simulation indicate that the variation in drag force values is relatively small between the cases in all versions and hence can be ignored. Lift force generated can be seen highest in Case 1 and lowest in Case 2. Case 3 did not achieve the expected reduction in the lift force compared to Case 2. As per the data below, Case 3 spoiler has 18% to 23% (between versions) increased lift force generated compared to Case 2. It is understood that this increase could be the result of the geometric profile of the new spoiler. The geometric profile analysis is discussed in the next section.

Table 8-1- Drag and Lift force comparison

CFD Versions	Cases	Drag (CD)	Lift (CL)	Drag Force (N)	Lift force (N)	% change	up/down
v04	Case 1	-0.2223	0.197	-133.56	118.06	-	-
	Case 2	-0.2214	0.084	-133.00	50.14	58%	-18%
	Case 3	-0.2219	0.120	-133.26	71.83	39%	
v03	Case 1	-0.2216	0.217	-133.09	130.03	-	-
	Case 2	-0.2199	0.087	-132.12	52.26	60%	-23%
	Case 3	-0.2187	0.137	-131.38	82.18	37%	

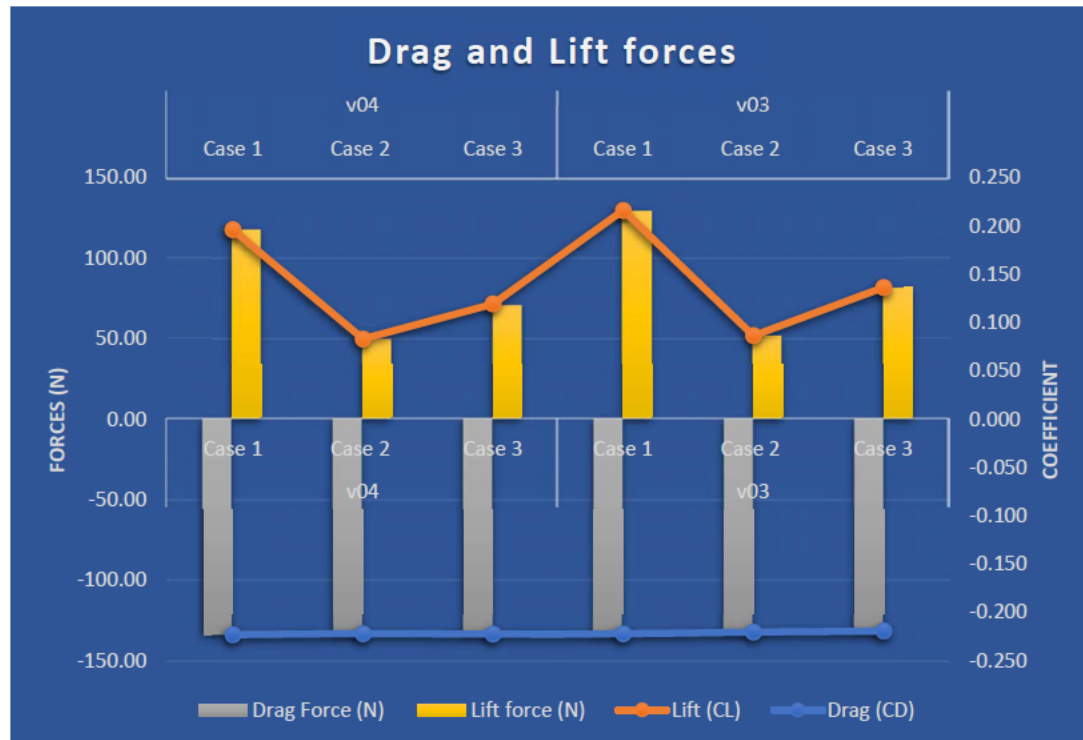


Figure 8-9 - Drag and Lift force comparison

8.5. Geometry analysis of the new spoiler

Based on the values obtained for lift forces and reviewing the pressure distribution and velocity contours, a potential design modification to the new spoiler profile seems to be very reasonable to consider. From the analysis it is understood that the larger curved profile on the spoiler web has caused an increased velocity over the curved profile. This can be seen in the image shown below. By changing the profile less curved and improving the ridge feature on the spoiler to retain more air over the flange areas would have resulted in an increased pressure build-up and this would have reduced the lift force.

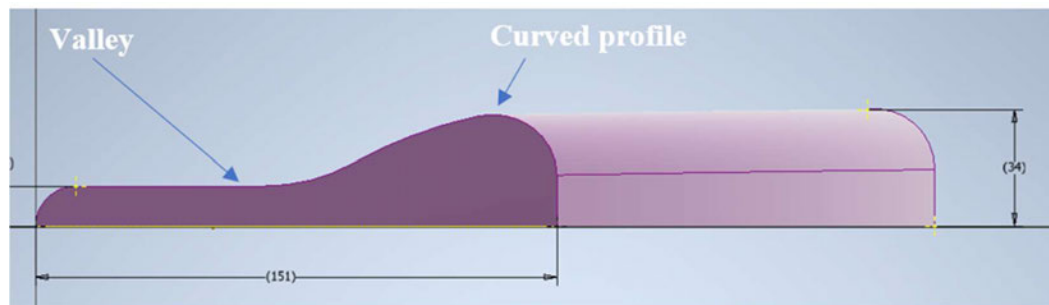


Figure 8-10 - Curved profile of the new spoiler

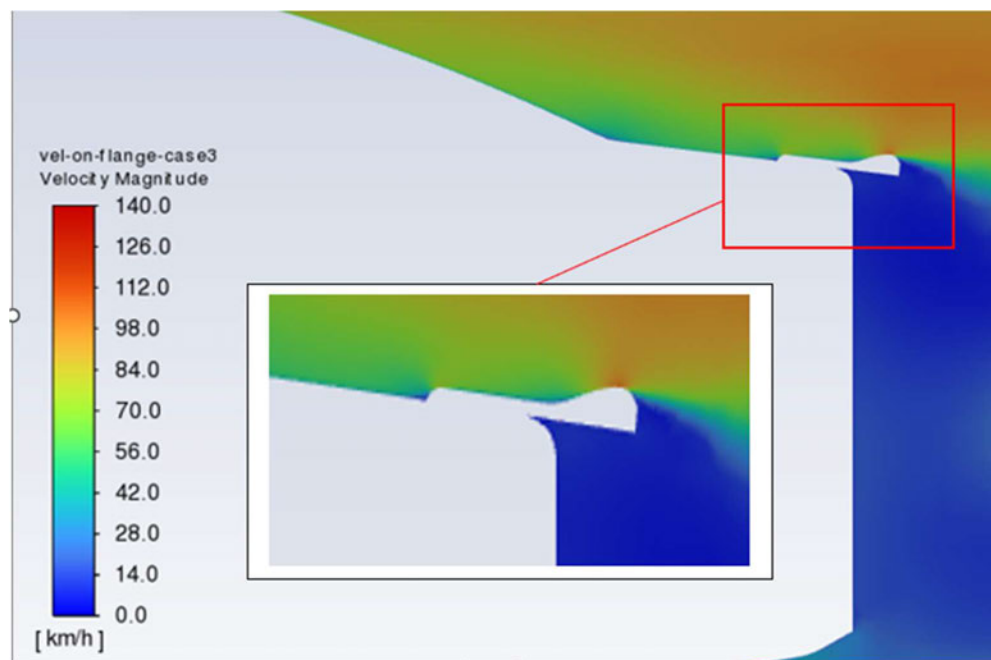


Figure 8-11 - Velocity increase over the spoiler flange curve- case 3

8.6. Domain size change analysis

The domain size change analysis is important to understand if this is influencing the consistency of the results. The details of the domain size change is specified in section 6.1. Based on the simulation done following are the observations:

- Domain size change shows changes in the cd & cl values.
- Values of cd are small and can be negligible.
- Values of cl is reasonably improved with the smaller domain size (CFD_v04)

Table 8-2-Figure 8 11-Domain size change analysis

Domain size change analysis					
Cases	CFD Versions	Drag (cd)	cd % change	Lift (cl)	cl % change
Case3	v04	-0.2219	1.46%	0.120	-14.38%
	v03	-0.2187		0.137	
Csse2	v04	-0.2214	0.68%	0.084	-4.19%
	v03	-0.2199		0.087	
Case1	v04	-0.2223	0.31%	0.197	-10.12%
	v03	-0.2216		0.217	

8.7. Mesh sensitivity analysis

Mesh sensitivity analysis is done for Case3 in version 4 and version 5 which has same domain size and smaller compared to v03.

Mesh elements details for Case 3 in these versions are:

- CFD_v04 – 1,280,851 cells (medium mesh)
- CFD_v05 – 1,428,515 cells (fine mesh)
- 11.5% mesh refinement done in v05.

Table 8-3-Mesh sensitivity analysis

Mesh sensitivity analysis					
CFD Versions	Cases	Drag (CD)	cd % change	cl % change	Lift force (N)
Case3	v05	-0.2274	2.42%	0.126	4.78%
	v04	-0.2219		0.120	

As per the values in the table it is indicating that the difference in c_d value is small and negligible. The c_l value is also not significant, however, the trend is indicating that the mesh refinement is resulting in a slight increase c_l values. This could be due to the more detailed analysis that is possible with the improved mesh. This may need an extensive study on all the analysis including domain change in conjunction with the mesh refinement to comprehensively understand this behaviour. Due to the limited time and resources available for this project such extended activities are beyond the scope of this project,

9. Conclusion

This research project has conducted the CFD analysis with limited time frame, capacity and resources. Without prior knowledge to the CFD area, the journey through the learning curve and research has been quite interesting. There have been many challenges faced during the course of the project and has now come to a conclusion.

The conclusions made are:

- 1) The expected improvement in lift force with the proposed rear spoiler design concept is not achieved as intended,
- 2) It is understood that the profile of the spoiler flanges needs potential modification by reducing the curved profile along the flange webs.
- 3) Increasing the ridge height to effectively capture more flowing air around the flange area would also be beneficial.
- 4) This research is however confirming the fact that the presence of a rear deck lid spoiler is improving the lift force compared to the base car without a rear spoiler.
- 5) This understanding reinforces the scope of possible improvement that can be achieved in the rear deck spoiler design through further investigation and analysis.
- 6) Domain size change simulation has very shown narrow influence on the accuracy of the results. However scope of refined mesh at multiple domain size is worth explorable.
- 7) Changing the domain size was worth investigating. This has provided an insight into the matters that needs to be considered for CFD analyses.
- 8) Mesh sensitivity analysis is indicating that mesh refinement has reasonable influence to the accuracy of the result.
- 9) It is understood that further mesh refinement could potentially improve the simulation behaviour and would result in more reliable outcome.

- 10) The simulations indicate that the convergence conditions can be considered complete in cases where the residuals are demonstrating steady oscillating behaviour.
- 11) Similarly, for drag and lift forces, solution can be considered converged if the pattern is demonstrating steady oscillating behaviour.
- 12) The accuracy of the results from this analysis shall be considered reasonable ideally within the limited scope of the project.

10. Future Scope

This project is limited by time and resources and hence concluded in the previous chapter. However this topic carried a huge potential to explore and refine this rear deck spoiler. It is interesting to note that a minor design change in the spoiler profile has a potential to significantly improve the functionality of the spoiler. The challenge is to investigate and refine the ideas and concepts by extensive research analysis and trials.

- Rear deck spoiler design can be further improved by refining the profile.
- Analysis with highly refined mesh has a huge potential to improve the results.
- Multiple air velocity application would suggest the air behaviour more broadly.
- The length of the flange in the concept design may be altered to have wider are sideways, by reducing the cut-out width.
- This design change in conjunction with the profile curve update as mentioned earlier could potentially reduce the lift force.

11. References

1. Active Aero. (2023). Retrieved from <https://www.motioncontrols.com/product-segments/active-aero>
2. Aktas, U., & Abdallah, K. (2017). *Aerodynamics Concept Study of Electric Vehicles-Drag Reduction and Range Increase*. (Master's Thesis in Automotive Engineering). CHALMERS UNIVERSITY OF TECHNOLOGY, Sweden.
3. Ansari, A. R., & Rana, P. K. (2017). CFD analysis of aerodynamic design of maruti alto car. *International Journal of Mechanical Engineering and Technology*, 8(3).
4. ANSYS. (2022). Ansys Fluid simulation. *ANSYS CFD Simulation*. Retrieved from <https://www.ansys.com/products/fluids/ansys-fluent>
5. Ansys.com. (2017). Select appropriate wall function for turbulence modeling and what is the requirement for y plus. *Ansys forum-Fluids*. Retrieved from <https://forum.ansys.com/forums/topic/select-appropriate-wall-function-for-turbulence-modeling-and-what-is-the-requirement-for-y-plus/>
6. Ansys.com. (2023). Solver Setup in Ansys Fluent — Lesson 3. *Aerodynamics of an FSAE Car*. Retrieved from <https://courses.ansys.com/index.php/courses/aerodynamics-of-an-fsae-car/>
7. Cakir, M. (2012). CFD study on aerodynamic effects of a rear wing/spoiler on a passenger vehicle. *MECHANICAL ENGINEERING MASTER'S THESES*, 1. Retrieved from https://scholarcommons.scu.edu/mech_mstr/1
8. Chaurasiya, V. V., Kushwaha, D. B., & Raees, M. (2017). Aerodynamic analysis of vehicle using CFD. *International Journal of Recent Trends in Engineering & Research*, 3(3), 131-137.
9. Das, R. C., & Riyad, M. (2017). CFD Analysis of Passenger Vehicle at Various Angle of Rear End Spoiler. *Procedia Engineering*, 194, 160-165. doi:<https://doi.org/10.1016/j.proeng.2017.08.130>
10. How a car works. (2023). *Car Anatomy*. Retrieved from <https://www.newkidscar.com/automotive-engineering/what-is-car-aerodynamics/>
11. Ipilakyaa, T. D., Tuleun, L. T., & Kekung, M. O. (2018). Computational fluid dynamics modelling of an aerodynamic rear spoiler on cars. *Nigerian Journal of Technology*.
12. Kazi, A. D., Acharya, P., Patil, A., & Noraje, A. (2016). Effect of spoiler design on hatchback car. *International Journal of Modern Trends in Engineering and Research (IJMTER) Volume*, 3.
13. Krzysztof Kurec, M. R., Tobiasz Mayer, Sylwester Tudruj, Janusz Piechna. (2019). Flow control for a car-mounted rear wing. *International Journal of Mechanical Sciences*, 152, 384-399. doi:<https://doi.org/10.1016/j.ijmecsci.2018.12.034>.

14. Laha, D. (2015). Computational aerodynamic analysis of a rear spoiler on a car in two dimensions Retrieved from https://www.academia.edu/25504634/Computational_aerodynamic_analysis_of_a_rear_spoiler_on_a_car_in_two_dimensions
15. Li, R. (2017). *Aerodynamic Drag Reduction of a Square-Back Car Model Using Linear Genetic Programming and Physic-Based Control*.
16. Li, Y., & Zhu, H. (2019). *A research on electric car styling design and low aerodynamic drag*. Paper presented at the IOP Conference Series: Materials Science and Engineering.
17. Nabil, T., Omar, A. H., & Mansour, T. M. (2020). Experimental approach and CFD simulation of battery electric vehicle body. *International Journal of Fluid Mechanics & Thermal Sciences*, 6(2), 36.
18. Qi-Liang, W., Zheng, W., Xian-Liang, Z., Li-Li, L., & Zhang, Y.-C. (2017). *Analysis of Aerodynamic Performance of Tesla Model S by CFD*. Paper presented at the 3rd Annual International Conference on Electronics, Electrical Engineering and Information Science (EEEIS 2017).
19. R.Varun, D. S. S., Rajiv Varma, Sreejith K.V. (2018). CFD Analysis of Aerodynamics of Car *International Journal of Innovative Research in Science, Engineering and Technology*, 7(5), 4689-4693. doi:10.15680/IJIRSET.2018.0705037
20. Ramasamy, D., Mohanesan, K., Kadirgama, K., Noor, M., & Rahman, M. (2017). Hybrid electric vehicle car body drag analysis using computational fluid dynamics. *International Journal of Automotive and Mechanical Engineering*, 14, 4496-4507.
21. SIMSCALE. (2022). Computational Fluid Dynamics. Retrieved from <https://www.simscale.com/docs/simwiki/cfd-computational-fluid-dynamics/what-is-cfd-computational-fluid-dynamics/>
22. Singh, J., & Randhawa, J. S. (2014). CFD analysis of aerodynamic drag reduction of automobile car-a review. *International Journal of Science and Research*, 3(6), 213-215.
23. Yuan Cheng, S., Mansor, S., Abdullah, M. A., & Zakaria, M. S. (2020). Numerical Study of Aerodynamic Performance of Hatchback Vehicle Fitted with a Strip Spoiler: Effect of Yaw Angle. *Journal of Advanced Research in Fluid Mechanics and Thermal Sciences*, 47(1), 108-118. Retrieved from <https://akademiabaru.com/submit/index.php/arfmts/article/view/2237>

Appendix A - Project specification

For: Shamith Puthalath

Title: **Design of rear spoiler on a car model – Computational simulation approaches**

Major: Mechanical Engineering

Supervisors: Ahmad Sharifian

Enrollment: ENG4111 – EXT S1, 2023

ENG4112 – EXT S2, 2023

Project Aim: This project is aiming to perform aerodynamic simulations on rear spoiler design of a car model aiming to achieve a reduced drag force without compromising much on the down force.

Programme: Version 02, 10th May 2023


Planning Specifications:

1. Perform initial background research on aerodynamic study of cars.
2. Conduct literature reviews, specifically on car rear spoiler aerodynamics.
3. Identify current methods, systems and technology available to perform studies.
4. Develop design specifications and constraints for concept developments.
5. Develop concepts on various spoiler design configurations.
6. Identify technical requirements, including software to perform computational simulations.
7. Develop time plan and resource requirements.
8. Identify any costs involved to conduct the research project and develop a budget plan.
9. Develop concepts models in 3D modelling and perform specification checks.
10. Perform aerodynamic simulation analysis using 3D models as per specifications.
11. Perform analysis at HPC (High Power Computing Facility)UniSQ.
12. Analyze the results and document the findings.
13. Develop a research project report based on the analysis.

If time and resource permit:

14. Based on the achieved results, improve the design for better results.

Appendix B – Risk Assessment

NUMBER	RISK DESCRIPTION	TREND	CURRENT	RESIDUAL
2508	Research project - CFD simulation of rear spoiler of a car		Not Assessed	Not Assessed
DOCUMENTS REFERENCED				
RISK OWNER	RISK IDENTIFIED ON	LAST REVIEWED ON	NEXT SCHEDULED REVIEW	
Shamith Puthalath	27/05/2023			
RISK FACTOR(S)	EXISTING CONTROL(S)	PROPOSED CONTROL(S)	OWNER	DUE DATE
Computational Fluid Dynamics (CFD) analysis conducted at my residence for research project. No risk involved	Control: N/a	Control: N/a		31/10/2023

Appendix C – Project schedule

Weekly schedule		ENG4111 Semester 1- 2023					Mid Sem- break	ENG4111 Semester 1- 2023							Exams & Semester break					ENG4112 Semester 2- 2023										Mid Sem- break	ENG4112 Semester 2- 2023					
		February		March			April			May				June				July				August				September				October						
Phases	Activity	1	2	3	4	5	6	7	8	9	10	11	12	13	14	15	16	17	18	19	20	21	22	23	24	25	26	27	28	29	30	31	32	33	34	35
Phase 1	Preparation phase																																			
1A	Project commencement																																			
1B	Discuss with the supervisor																																			
1C	Background research																																			
1D	Update project planning																																			
Phase 2	Resource planning																																			
2A	Request for software																																			
2B	Install software																																			
Phase 3	Litreature review																																			
3A	Collect litreature documents																																			
3B	Prepare litreature reviews																																			
Phase 4	Design phase - 3D modelling																																			
4A	3D modelling																																			
4B	ANSYS simulation training																																			
4C	Discuss with the supervisor																																			
Phase 5	Progress report for semester 1																																			
5A	Prepare progress report																																			
5B	Submit progress report																																			
Phase 6	CFD Simulation phase																																			
6A	ANSYS CFD simulation																																			
6C	Draft the findings																																			
6D	Discuss with the supervisor																																			
Phase 7	Data analysis																																			
7A	More ANSYS simulations																																			
7B	Review the results																																			
7C	Analysis using HPC facility																																			
7D	Discuss with the supervisor																																			
Phase 8	Dissertation																																			
8A	Draft the dissertation																																			
8B	Discuss with the supervisor																																			
8C	Attend the ENG4903 conference																																			
8D	Submit final dissertation																																			

Appendix D - Challenges faced and HPC issues.

The research project has face significant challenges during the course of the project and the major one was the inability to operate the HPC to run CFD simulation with highly refined mesh. Even though the access to HPC was rectified after some initial glitches, following issues hindered the its use and had to abort the plan to use it. A significant amount of time was wasted on trying to work on HPC.

The version 2 of the simulation was prepared with highly refined mesh elements. More than 5 million mesh elements were in each of the case to run in HPC.

- Very slow interface
- Very slow response time and graphics were blurring
- Model movement withing the Ansys fluent was hard top control due to graphics issue.

Due to the above the project file was prepared in ANSYS Academic version from geometry preparation, mesh generation until solution solver setup and then the file was transferred using into strudel by FileZilla app with a hope to only keep the final steps of initialization and run calculation to be execute in HPC. But the file failed to open. The file sections were not interacting to each other in HPC as shown in the image below.

